



Cite this: *Mater. Adv.*, 2024, 5, 846

## Titanium nitride (TiN) as a promising alternative to plasmonic metals: a comprehensive review of synthesis and applications

Ujjwal Mahajan,<sup>a</sup> Mahesh Dhonde,<sup>ID \*a</sup> Kirti Sahu,<sup>ID \*b</sup> Pintu Ghosh<sup>c</sup> and Parasharam M. Shirage<sup>ID \*d</sup>

Titanium nitride (TiN), a prominent transition metal nitride (TMN), has garnered significant attention due to its exceptional characteristics and versatile applications in modern technologies. This comprehensive review highlights TiN's unique properties, positioning it as a promising alternative to traditional plasmonic metals due to its ability to overcome cost limitations and maintain plasmonic behaviour at lower temperatures. The paper presents recent research on TiN, encompassing various synthesis techniques, structural considerations, and its diverse range of applications. By focusing on the synthesis aspect, the review delves into the different methods employed to produce TiN, showcasing the breadth of available strategies. Additionally, the article sheds light on emerging applications where TiN demonstrates its prowess, such as solar energy acquisition, energy storage, photocatalysis, electrochemical sensing, biomedical implants, and protective coatings. Acknowledging the challenges and limitations of TiN, the review addresses potential areas for improvement and research directions. By offering a comprehensive analysis of TiN's capabilities, this review serves as an invaluable resource for researchers and scientists in the dynamic field of materials science and engineering. The synthesis strategies and extensive technological applications discussed here will undoubtedly inspire further exploration and innovation in using TiN for advancing cutting-edge technologies.

Received 4th November 2023,  
Accepted 3rd January 2024

DOI: 10.1039/d3ma00965c

[rsc.li/materials-advances](http://rsc.li/materials-advances)

### 1 Introduction

Transition metal nitrides are a class of compounds that feature nitrogen atoms occupying interstitial sites within the parent metal lattice.<sup>1</sup> Examples of such compounds include vanadium nitride (VN),<sup>2,3</sup> titanium nitride (TiN),<sup>4,5</sup> and chromium nitride (CrN).<sup>6,7</sup> The aforementioned materials have the ability to manifest in three distinct crystal structures (see Fig. 1), namely



Mr Ujjwal Mahajan received his masters degree in Physics from Shree Neelkantheshwar Govt. Post Graduate College, Khandwa, India, in 2021. He is currently a PhD student and University Research Fellow (URF) at Medi-Caps University, Indore. His current research is focused on synthesizing transition metal-doped oxides and nitrides-based nanocomposites for energy related applications.

Ujjwal Mahajan



Mahesh Dhonde

Dr Mahesh Dhonde is presently serving as an Assistant Professor in the Department of Physics at Medi-Caps University located in Indore, India. He earned his PhD degree from Devi Ahilya University, Indore, in 2019. His current research includes nanomaterial synthesis for energy harvesting, dye-sensitized solar cells, photocatalysis and nanomaterials for energy and environmental applications.



face-centered cubic (fcc), hexagonally close-packed (hcp), and simple hexagonal (hex).<sup>8</sup> Transition metal nitrides typically demonstrate greater covalent and metallic properties than their corresponding sulfides and oxides, irrespective of their structural configuration.<sup>9</sup> As a result, they have extraordinary properties such as high melting temperatures, toughness, high Young's modulus, broad band gaps, excellent electrical conductivity (metallic), and outstanding thermal and chemical stabilities.<sup>10–13</sup> The distinctive characteristics exhibited by metal nitrides render them highly advantageous candidates for a diverse range of energy-related applications, encompassing heterogeneous catalysis, photocatalytic elimination of pollutants, and energy storage and conversion.<sup>13–16</sup> Among the transition metal nitrides, TiN is one of the most extensively studied and widely employed materials due to its exceptional mechanical, electrical, and thermal properties (see Fig. 2).

Titanium nitride, with the chemical formula TiN, belongs to the family of refractory compounds known as transition metal



**Kirti Sahu**

*Dr Kirti Sahu received her PhD degree from Devi Ahilya University in 2018. Presently she is working as an Assistant Professor in the Department of Physics, Govt. S. N. G. P. G. College, Khandwa. Her research area includes nano-materials synthesis for energy-harvesting applications, Dye-sensitized solar cells, and photocatalysis.*



**Pintu Ghosh**

*Dr Pintu Ghosh has been serving as an Associate Professor at the College of Optical Science and Engineering, Zhejiang University, China, since 2023. Prior to this role, he held the position of Assistant Professor at the same institution from 2019 to 2021. His academic journey includes a postdoctoral fellowship at Zhejiang University spanning from 2016 to 2018 and an integrated MSc–PhD dual degree at the Indian Institute of Technology Bombay in India from 2007 to 2016.*

nitrides.<sup>18</sup> It is a hard, wear-resistant material with a high melting point and excellent thermal stability, making it suitable for extreme conditions and high-temperature applications.<sup>19,20</sup> TiN is widely recognized for its remarkable mechanical properties.<sup>20–23</sup> These attributes have led to its utilization in various industries, such as cutting tools,<sup>24</sup> wear-resistant coatings,<sup>25</sup> and protective layers for electronic devices.<sup>26,27</sup>

Besides its mechanical prowess, TiN exhibits interesting electrical properties, including metallic conductivity, high electron mobility, and low resistivity.<sup>28,29</sup> These properties have made TiN an attractive material for applications in microelectronics, where it is employed as a diffusion barrier, an adhesion layer, or an ohmic contact in integrated circuits and nanoelectronics. Furthermore, the catalytic properties of TiN have recently received considerable attention.<sup>30</sup> The surface chemistry and unique electronic structure of TiN make it an intriguing material for catalytic reactions, including ammonia synthesis, nitrogen fixation, and oxygen reduction.<sup>31–33</sup> Its potential as a replacement for expensive metal catalysts has sparked interest in developing TiN-based catalysts for sustainable and cost-effective industrial processes.<sup>34</sup>

The synthesis of TMNs can be achieved through a variety of methods, including chemical vapor deposition, reactive sputtering, and arc melting.<sup>35–37</sup> These methods allow for the control of the resulting materials' composition, crystal structure, and morphological features. Furthermore, the characterization of TMNs is essential for understanding their properties and behavior. The crystal structure, morphology, and chemical composition of TMNs can be determined using several structural, microscopic, and spectroscopic approaches. In the past few years, numerous reviews have highlighted the progress made in utilizing metal nitrides for applications such as energy storage and conversion,



**Parasharam M. Shirage**

*Dr Parasharam M. Shirage is currently working as a Professor in the Department of Metallurgy Engineering and Materials Science at the Indian Institute of Technology Indore. He received his master's and doctoral degrees from Shivaji University, Kolhapur (India). He was a Visiting Fellow at the Tata Institute of Fundamental Research (TIFR), Mumbai, and a Senior Scientist at the National Institute of Advanced Industrial Science and Technology (AIST), Tsukuba, Japan. He is a recipient of the highly prestigious Medal from the Materials Research Society of India (MRSI) 2020. His research interests include electrochemistry, thin film growth, high pressure to synthesize novel materials, novel superconductor search, isotope effects, point contact spectroscopy, microwave studies, and nanomaterials for solar cell applications and energy storage, gas sensing, etc.*



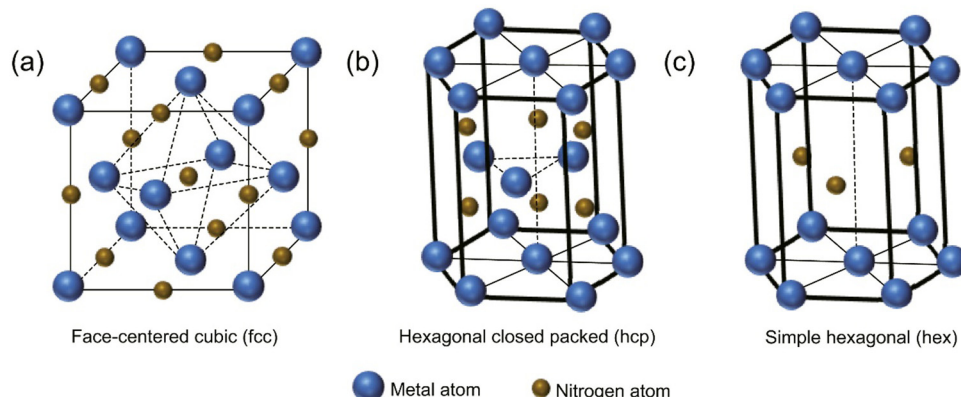


Fig. 1 Typical crystal structures of TMNs; (a) fcc, (b) hcp, and (c) hex (reproduced from ref. 17 with permission).



Fig. 2 Various properties of titanium nitride (TiN).

fuel cells, and electrocatalysis.<sup>38–40</sup> For example, Luo and colleagues provided a comprehensive overview of nanostructured TMNs and their energy-related applications.<sup>17</sup> Meng *et al.* presented a detailed overview of TMNs and their electrocatalytic applications.<sup>41</sup> Lin and co-workers discussed recent advancements in nanostructured TMNs for water electrolysis.<sup>42</sup> Mahadik *et al.* highlighted recent development in the synthesis and electronic structure engineering of nanostructured TMNs for supercapacitor applications.<sup>43</sup> Recently, Yang *et al.* and Zhang *et al.* summarized applications of TMNs for electrochemical nitrogen reduction and as a functional separator for lithium-sulfur batteries.<sup>44,45</sup> More recently, Batool and co-workers highlighted the recent advancements in iron (Fe) and nickel (Ni)-based TMNs for hydrogen evolution.<sup>46</sup>

In addition to TiN, several other metal nitrides such as FeN, CoN, NiN, VN, and MoN have been explored by researchers for various applications.<sup>47,48</sup> Each metal nitride has its own set of

advantages and applications, but TiN's combination of hardness, chemical stability, biocompatibility, optical and electrical properties, and ease of deposition makes it particularly versatile across various industries and applications. TiN research has come a long way in recent years, yet a comprehensive exploration of its synthetic methods and wide-ranging applications remains elusive in the literature. While numerous publications have focused on specific applications of various metal nitrides, a thorough investigation specifically addressing TiN, including its synthesis and diverse range of applications, is conspicuously absent. Recognizing the pressing need to bridge this knowledge gap and considering the rapid advancement of TiN, we present an updated and comprehensive overview of the synthetic strategies employed for producing TiN-based materials. Furthermore, we delve into the extensive array of applications wherein these materials demonstrate their immense potential, encompassing electrodes for energy storage devices, electrocatalysis, photovoltaics, biomedical applications, electrochemical sensing and wear-resistant coatings. By meticulously surveying the existing body of research, we aim to consolidate the current state of knowledge on TiN, shedding light on its synthesis techniques and highlighting the remarkable versatility of this burgeoning field. Our comprehensive review addresses the key challenges and recent advancements, offering valuable insights for researchers and practitioners with useful new perspectives.

## 2 Synthetic methods for TiN nanostructures

The production of TiN nanostructures has attracted considerable interest owing to their distinctive characteristics and possible utilization in diverse domains. Various synthetic techniques have been devised to produce TiN nanostructures, each with unique benefits that allow for accurately manipulating their structure, morphology, and chemical composition. This study presents a comprehensive analysis of various prominent synthetic methodologies utilized in fabricating TiN nanostructures.



## 2.1 Chemical vapor deposition (CVD)

TiN synthesis using the chemical vapor deposition (CVD) technique has emerged as a prominent method for producing TiN films and nanostructures with controlled properties.<sup>49</sup> CVD offers precise control over the deposition parameters, allowing the synthesis of uniform and high-quality TiN coatings on various substrates. The process involves the reaction of titanium precursor, typically titanium tetrachloride ( $TiCl_4$ ) and ammonia ( $NH_3$ ), in a controlled environment at elevated temperatures.<sup>50</sup> During the CVD process, the precursor gases are introduced into a reaction chamber, typically made of quartz, along with a carrier gas that aids in transporting the reactants. The chamber is then heated to high temperatures, typically from 700 to 1000 °C, promoting the decomposition of the precursor gases and the subsequent reaction of  $TiCl_4$  with  $NH_3$ . This chemical reaction facilitates the formation of TiN on the substrate's surface.<sup>51</sup> The growth and control of TiN during CVD are achieved by carefully adjusting the deposition parameters. Factors such as precursor flow rates, chamber pressure, temperature, and deposition time are fine-tuned to achieve the desired film properties. These parameters influence the growth rate, film thickness, uniformity, and crystalline structure of the TiN coating.<sup>35,51,52</sup>

TiN is often deposited in  $H_2$  surplus, allowing for rapid reduction of  $TiCl_4$  to  $TiCl_{4-x}$ . However, CVD in a hydrogen-deficient environment has the potential to alter the  $TiCl_4/TiCl_3$  equilibrium and the decreased reactivity of the Ti-precursor.<sup>49,53</sup> The growth of TiN was investigated by Fieandt *et al.* using CVD with a reaction gas mixture consisting of nitrogen ( $N_2$ ), titanium tetrachloride ( $TiCl_4$ ), and hydrogen ( $H_2$ ). The deposition procedure was conducted on three distinct metal substrates, namely cobalt (Co), iron (Fe), and nickel (Ni), employing a range of temperatures spanning from 850 °C to 950 °C.<sup>51</sup> Gas-phase interactions with metal substrates were studied utilizing computational thermodynamics. This study examines the viability of utilizing Fe and Ni as alternative binder phases in cemented carbides to replace Co. Thermodynamic calculations were employed to analyze the chemical reactions between the gaseous phase and the metallic substrates. According to thermodynamic simulations, Ni substrates are the most resistant to etching in the reaction gas phase. Applying the CVD technique on cobalt (Co) substrates led to the formation of compact and columnar shape coatings composed solely of single-phase TiN. Substrate corrosion was not seen at all deposition temperatures. The authors conclude that TiN must be deposited on a Ni-based binder phase with a low  $H_2$  partial pressure and a significant amount of  $N_2$  to prevent corrosion or undesired phases. Su *et al.* fabricated TiN films using the CVD technique and used titanium chloride, ammonia, and hydrogen as carrier gases.<sup>54</sup> The films were deposited on various substrates (See Fig. 3(a-c)). The researchers proposed a kinetic model for simulating the TiN film growth rate. Crystal orientation in TiN films was found to be supersaturation dependent, with the underlying *c*-plane sapphire dictating the favoured orientation. TiN films with a low growth rate and a low N/Ti ratio in the gas phase are golden in color, while TiN films with a high growth rate are brown.

Das and colleagues studied the effects of  $N_2$  gas flow rates on TiN coating properties.<sup>35</sup> They synthesized TiN coatings on Si substrates at 1000 °C using  $TiO_2$  powder. The coatings had a dense microstructure, increased surface roughness, and a B1  $NaCl$  crystal structure (see Fig. 3(d)). Higher  $N_2$  flow rates decreased corrosion resistance, and the acoustic and optic phonon modes shifted to higher intensities. The mechanical properties showed a maximum hardness of 30.14 GPa and Young's modulus of 471.85 GPa. Ramanuja *et al.* investigated the synthesis of TiN films *via* low-pressure chemical vapor deposition (LPCVD) using  $TiCl_4$  and  $NH_3$ , focusing on these films' growth kinetics, composition, and characteristics.<sup>50</sup> As the temperature increased, the chlorine concentration of the solution decreased, and the growth rate was shown to be stoichiometrically dependent on  $NH_3$  and  $TiCl_4$  partial pressures. The film's density and resistivity changed due to deposition temperature and flow rate ratios. The deposits had conformal step coverage up to a 4:1 aspect ratio. Recently, Feng *et al.* recently incorporated plasma-enhanced CVD to *in situ* nitride titanium plates to improve conductivity and corrosion resistance.<sup>55</sup> They examined surface shape, hydrophobicity, interfacial conductivity, and corrosion resistance after synthesizing TiN coatings at varied temperatures and intervals. Lower temperatures slowed surface reactions, while higher temperatures accelerated TiN particle development. Longer nitriding time accumulated TiN nanoparticles continuously, creating a uniform coating but lowering flatness. TiN coating prepared by nitriding at 650 °C for 90 min (TiN-650-90) is compact, smooth, and fuel cell water-resistant. Titanium's corrosion potential is lower than TiN-650-90's 0.56  $\mu A\ cm^{-2}$  corrosion current density. Titanium bipolar plates have low deposition temperature, fast deposition speed, high hydrophobicity, conductivity, and corrosion resistance, enabling effective surface modification.

TiN production through CVD allows for conformal coating on complicated and three-dimensional substrates, which is a significant advantage. Because of this, CVD can be used in many different fields, such as microelectronics, wear-resistant coatings, catalysis, and energy storage devices. CVD is also interesting for high-throughput industrial applications since it enables mass production. However, there are further obstacles to overcome when synthesizing TiN using CVD. CVD systems can be expensive and time-consuming to set up and run, necessitating specialized equipment and trained personnel. Precursor gases, such as  $TiCl_4$ , are very corrosive and poisonous, necessitating cautious handling throughout use. It is imperative to take precautions for the safety of workers and machinery. The tuning of deposition parameters may also be required to achieve homogeneous layer thickness and composition over vast substrate surfaces. Additionally, achieving uniform film thickness and composition over large substrate areas can be challenging and may require optimization of deposition parameters. Despite these challenges, TiN synthesis using CVD remains a versatile and effective method for producing high-quality TiN films with controlled properties. Ongoing research and development efforts continue to refine CVD processes, enabling the synthesis of TiN coatings with enhanced



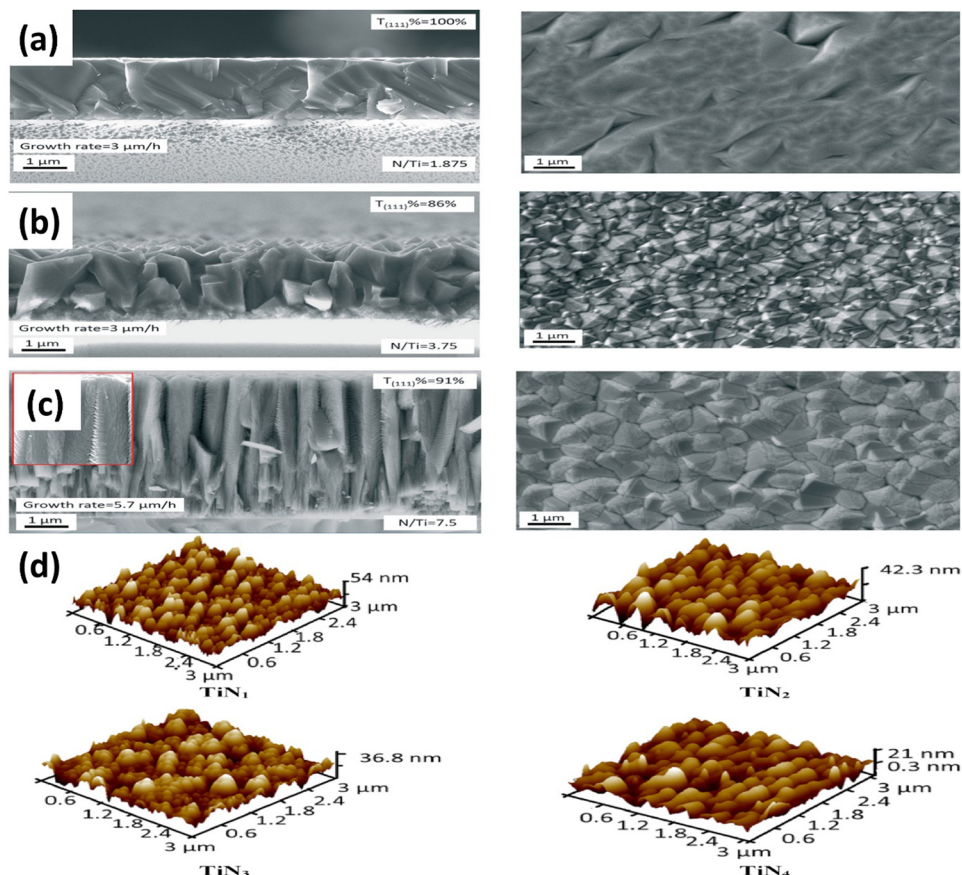


Fig. 3 Cross-sectional and surface morphology of TiN layers with a (a) golden; (b) brown; and (c) brown color on sapphire (reproduced from ref. 54 with permission); (d) AFM images of TiN coating grown at a different  $N_2$  flow rate (reproduced from ref. 35 with permission).

performance for various materials science and engineering applications.

## 2.2 Atomic layer deposition (ALD)

Thin films are also known as conformal coatings, which adhere closely to the form of the structures they cover, are an essential constituent in an extensive range of contemporary technologies, including optical and optoelectronic components,<sup>56</sup> magnetic storage devices,<sup>57</sup> membranes<sup>58</sup> and catalysts.<sup>59</sup> Particularly in microelectronics, the majority of manufacturing processes demand the growth of thinfilms to facilitate the *in situ* assembly of capacitors, metal interconnects, diodes, transistors, and other components within integrated circuits.<sup>60</sup> Nowadays electronic devices are frequently manufactured with individual structures measuring less than 100 nm, possessing extremely high aspect ratios and many narrow, deep cavities and trenches.<sup>61</sup> Physical deposition methods,<sup>62</sup> being primarily directional, may not be well-suited for certain applications, whereas chemical-based processes offer isotropy and excel in depositing films evenly, especially on irregular surfaces. Additionally, their strength lies in creating uniform and dense films consistently. Moreover, the wide range of available chemical constituents ranging from hydrides and halides to organometallics enables the deposition of a diverse array of substances.<sup>63</sup>

In addition to the aforementioned advantages, the CVD technique is not without its drawbacks, including the need

for elevated temperatures and challenges in regulating the thickness and morphology of the developing layers. To overcome such issues, a modified form of CVD known as atomic layer deposition (ALD) is utilized nowadays. In ALD, two complementary self-limiting reactions are employed in a sequential and alternating fashion to construct solid films one monolayer at a time.<sup>63</sup> Musschoot *et al.* investigated TiN films *via* atomic layer deposition (ALD), comparing thermal and plasma-assisted processes. The optimized thermal method achieved 0.06 nm per cycle growth rate and  $53 \times 10^3 \mu\Omega$  cm resistivity, while plasma-enhanced  $NH_3$  produced 0.08 nm per cycle growth and  $180 \mu\Omega$  cm resistivity. High resistivity in thermal ALD films is correlated with oxygen (37%) and carbon (9%) contamination, reduced to below 6% in optimized plasma films. Their research highlighted that TiN films from plasma-assisted processes exhibit excellent copper diffusion barrier properties similar to or better than those from physical vapor deposition (PVD).<sup>64</sup> In a pioneering work, H. J. Lee and team developed an innovative ALD surface reaction pathway using  $H_2S$  after the  $TiCl_4$  pulse, leading to a remarkable reduction in the resistivity of TiN films ( $< 130 \mu\Omega$  cm) at lower ALD process temperatures ( $< 400^\circ C$ ). This unconventional approach transformed titanium sulfide into titanium nitride by subsequent  $NH_3$  gas exposure, reducing Cl impurities ( $\sim 1\%$ ) and resulting in a ( $> 20\%$ ) decrease in resistivity compared to conventional



ALD methods ( $\text{TiCl}_4 + \text{NH}_3$ ). The resistivity decrease of the TiN film can enable a reduction of power consumption in the dynamic random-access memory (DRAM) operation, which offers an aggressive scaling of DRAM capacitors for high-density integration, showcasing the distinctive potential of this novel ALD synthesis pathway.<sup>65</sup> Further, J. Shin *et al.* studied plasma-enhanced atomic layer deposition (PEALD) parameters on TiN film properties. Their findings revealed that higher nitrogen plasma power and longer exposure times yielded highly dense, crystallized TiN films with minimal impurities, notably enhancing adhesion to Si substrates by 50%. The research underscores the potential for tailored plasma parameters in PEALD to produce TiN thin films with enhanced mechanical stability and electrical conductivity, promising for various applications in semiconductor technology.<sup>66</sup>

Recently, B. Lee explored the impact of deposition temperature on TiN thin films using thermal atomic layer deposition (ALD). They demonstrated a decrease in resistivity to  $177 \mu\Omega \text{ cm}$  at  $600^\circ\text{C}$  but noticed increased surface roughness and decreased step coverage. To enhance film quality at lower temperatures, they performed a post-treatment using a  $\text{N}_2/\text{He}$  plasma mix (3:2 ratio), resulting in a 25% decrease in resistivity for films deposited at  $400^\circ\text{C}$ . This innovative approach offers insights into improving TiN thin film quality for semiconductor applications *via* ALD processes.<sup>67</sup> The evolution from conventional techniques like CVD to advanced methodologies such as ALD and PEALD has revolutionized the fabrication of TiN thin films, addressing challenges related to temperature, thickness control, and material purity. However, further advancements are required to mitigate some challenges related to ALD, such as the slow deposition rate, undesirable contaminants due to the decomposition of precursors, and carrier gas impurities in some films. Further research will mitigate such challenges, and TiN films with improved performance will be obtained for various material and engineering related applications.

### 2.3 Solvothermal and hydrothermal methods *via* nitridation

Solvothermal and hydrothermal approaches are employed to fabricate nanomaterials, such as TiN, through distinct reaction environments.<sup>53</sup> These methods involve using a solvent or water under specific temperature and pressure conditions to facilitate the reaction between precursor materials and nitrogen sources, resulting in the formation of TiN. In solvothermal synthesis, an organic solvent is used as the reaction medium. The titanium precursors and a nitrogen source, such as ammonia or amines, are dissolved in the solvent. The reaction mixture is then sealed in a high-pressure autoclave and heated to an elevated temperature. The high temperature and pressure conditions facilitate the reaction between the precursors and nitrogen, forming TiN nanoparticles or thin films. The solvothermal synthesis method enables meticulous manipulation of the TiN material's particle size, shape, and composition.<sup>68</sup> On the other hand, hydrothermal synthesis utilizes water as the reaction medium. The titanium precursors and a nitrogen source are dissolved in water, typically with the addition of a mineralizer or a pH adjuster. The reaction mixture is then

placed in a high-pressure vessel called an autoclave and subjected to elevated temperature and pressure conditions. The hydrothermal environment enables the chemical interaction between the precursor chemicals and nitrogen, resulting in the formation of TiN.<sup>69</sup> Hydrothermal synthesis offers advantages such as using water as an environmentally friendly solvent, relatively low reaction temperatures, and carefully manipulating the TiN material's particle size, shape, and composition.<sup>53</sup> These methods help modify the nanoscale TiN NPs in terms of their form, size, and crystallinity. These characteristics can be fine-tuned by altering factors like solvent type, reaction time, and temperature during the TiN NPs' synthesis. This synthetic method can be used to create materials with desired phase characteristics, metastable states, vapor pressures, and melting points. The technology has some substantial downsides, the most significant being the need for prolonged exposure, which may result in the aggregation of nanoparticles. In addition, the autoclave can get dangerously overheated and explode if high pressure and temperatures ( $80^\circ\text{C}$  to  $400^\circ\text{C}$ ) are used.

The solvothermal method has successfully produced TiN nanostructures with diverse morphologies, including multifaceted shapes and spherical rings featuring a central void.<sup>53,70</sup> Balogun *et al.* conducted a study where they synthesized TiN nanowires (NWs) using hydrothermal methods and annealed them on a carbon fabric.<sup>71</sup> The SEM analysis showed that the morphological features of the  $\text{TiO}_2$  nanoparticles remained unchanged after curing at temperatures of  $1000^\circ\text{C}$ ,  $900^\circ\text{C}$ , and  $800^\circ\text{C}$ . The TEM image of the TiN-900 sample confirmed the synthesis of TiN nanoparticles with a size of approximately 160 nm and a nanowire structure (see Fig. 4(e-i)). This study demonstrates the successful synthesis of TiN nanowires through hydrothermal synthesis and highlights their stability during the annealing process. Qin *et al.* produced nanopillars of hierarchical TiN nanoparticles using a simple hydrothermal technique.<sup>72</sup> The electrode is fabricated through the nitration process of  $\text{TiO}_2$  nanotubes, resulting in the formation of H-TiN nanopillars (see Fig. 4(a-d)). These nanopillars possess a surface area of  $23.1 \text{ m}^2 \text{ g}^{-1}$ , with a diameter ranging from 100 to 150 nm and a length of 6 m. The H-TiN nanoparticles, when used as an electrode, demonstrated a capacitance of  $69 \text{ F cm}^{-3}$  at a current density of  $0.83 \text{ A cm}^{-3}$ . The authors additionally asserted that the remarkable electrochemical performance can be attributed to the significant specific surface area and enhanced electroactive sites. Coatings made of various materials can increase TiN nanostructures' stability. A hydrothermal procedure is ideally suited for this purpose. TiN electrodes degrade structurally during cycling because electrolyte ions are constantly intercalating and deintercalating, as noted by Lu *et al.* To protect the carbon fabric from the TiN nanowires, the team employed a hydrothermal approach to produce a thin coating of amorphous carbon on top of the nanowires.<sup>73</sup> The resultant TiN@C electrode has a specific capacitance of  $124.5 \text{ F g}^{-1}$  at a current density of  $5 \text{ A g}^{-1}$ , compared to  $107 \text{ F g}^{-1}$  for a pure TiN electrode. TiVN, a bimetallic nitride synthesized by a solvothermal technique, has recently been reported for SC applications by Wei *et al.* TiVN composite's mesoporous hollow spheres

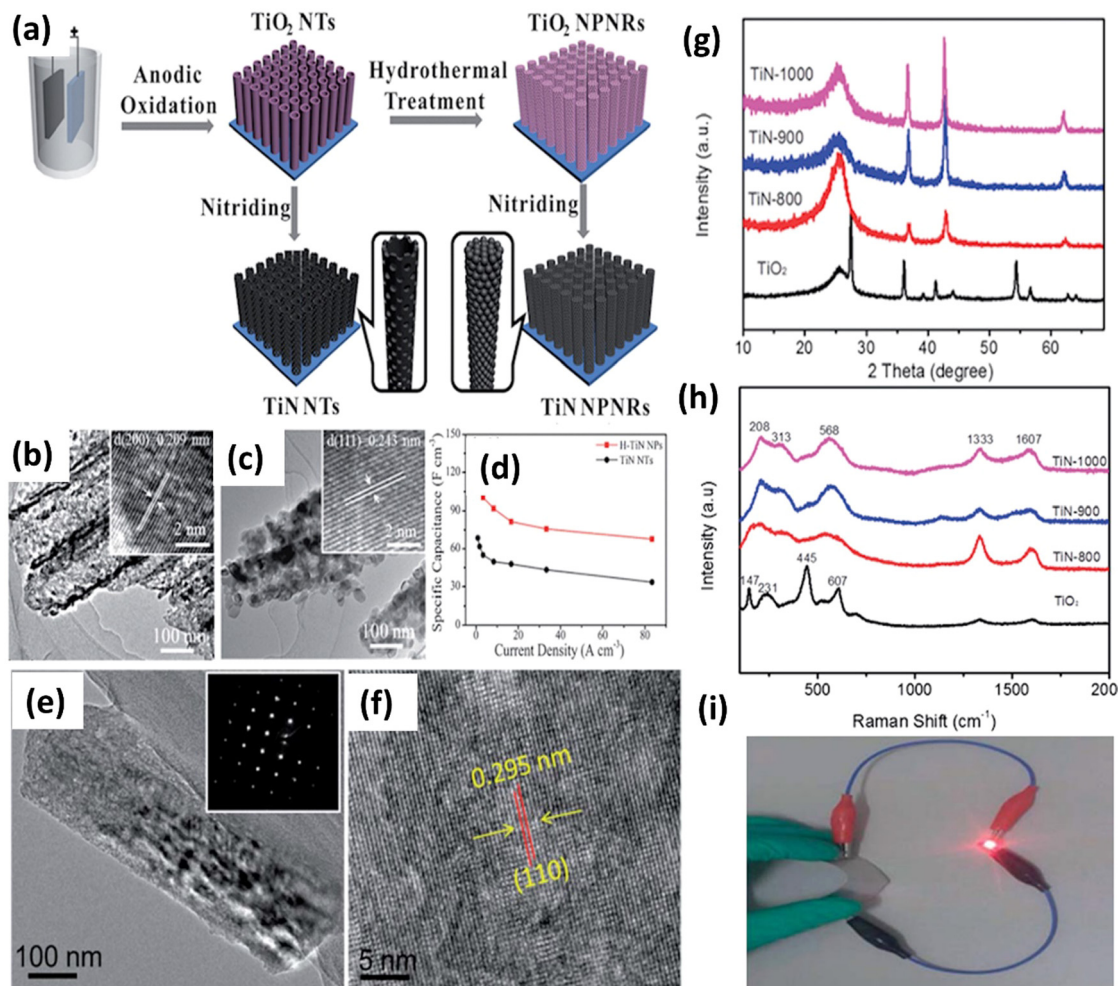


Fig. 4 (a) Schematic illustration of the formation process of TiN NTs and H-TiN NPs; (b) TEM images of TiN NTs; (c) H-TiN NPs; (d) rate performance of H-TiN NPs and TiN NTs (reproduced from ref. 72 with permission); (e) TEM image; (f) HRTEM image of the TiN-900 sample; (g) XRD patterns; (h) Raman spectra of the TiO<sub>2</sub> and different TiN samples; and (i) a red LED in the bent position is seen being powered by a fully charged LiCoO<sub>2</sub>/TiN-900 battery (reproduced from ref. 71 with permission).

contribute to its enhanced electrical conductivity and specific capacitance.<sup>74</sup> The exceptional result can be ascribed to the combined effects of both counterparts.

Recently, Bai and colleagues studied hydrothermally oxidized multi-arc ion-plated (MAIP) titanium nitride (TiN) coatings. Hydrothermal oxidation of TiN at temperatures above 200 °C produced a thick oxide layer with a 20–50 nm thickness. The oxide layer comprised 50–150 nm-long anatase particles covered in smaller anatase nano crystallines.<sup>75</sup> Passivation range, corrosion current, and impedance were all significantly boosted for TiN after oxidation treatment in simulated saliva. This study demonstrates the beneficial effects of hydrothermal oxidation on the structural, corrosion, and wear properties of TiN coatings. Yang *et al.* employed a solvothermal technique to achieve the formation of ruthenium nanorods supported on TiN nanosheets, thereby inducing a robust metal-support interaction (SMSI) effect.<sup>76</sup> The Ru NRs/TiN catalyst demonstrates remarkable hydrogen evolution reaction (HER) efficiency in a KOH solution with a concentration of 1.0 M. It exhibits a minimal overpotential of only

25 mV. The substance exhibits exceptionally high mass activity and demonstrates superior turnover frequency values. The SMSI effect results in the redistribution of charges at the interface between ruthenium and TiN, thereby increasing the catalytic action of the catalyst for the HER (see Fig. 5). The stability of the catalyst is deemed exceptional, as it has demonstrated a remarkable endurance of 10 000 cycles without any observable decay. This study broadens the scope of ruthenium-based catalysts for the HER and provides novel perspectives on surface modification by the SMSI engineering.

Both solvothermal and hydrothermal approaches offer convenient and controllable methods for synthesizing TiN materials. These methods provide flexibility in tuning the properties of the TiN products by adjusting reaction parameters such as temperature, pressure, precursor concentration, and reaction time. The ability to control particle size, morphology, and crystal structure makes these methods suitable for several applications, such as catalysis, energy storage, and optoelectronics. Overall, solvothermal and hydrothermal approaches



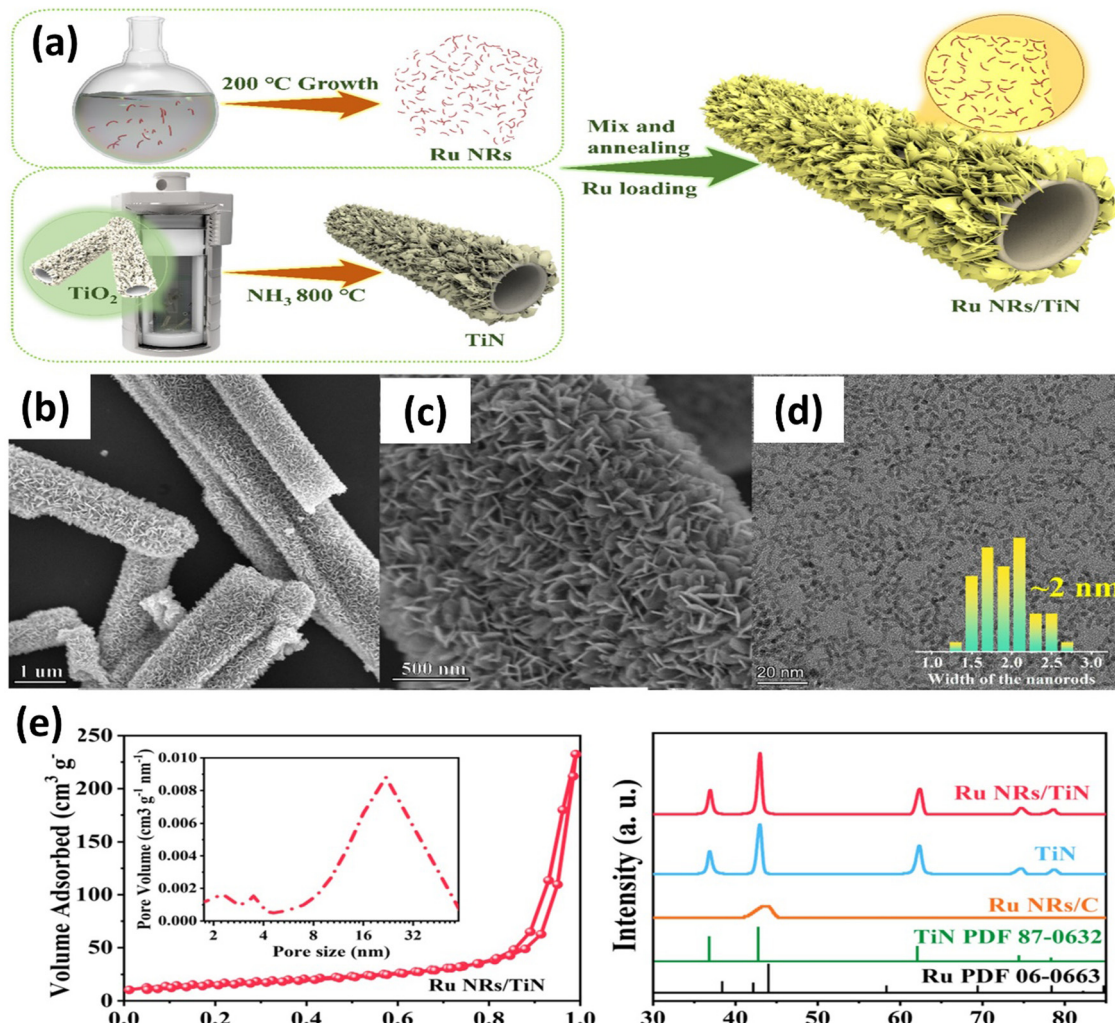


Fig. 5 (a) Schematic synthesis processes and structure of Ru NRs/TiN catalyst; (b) and (c) SEM of Ru NRs/TiN; (d) TEM of Ru NRs; (e) N<sub>2</sub> adsorption–desorption isotherms and XRD patterns of Ru NRs/TiN, TiN, and Ru NRs/C (reproduced from ref. 76 with permission).

contribute to the development of TiN materials with tailored properties for specific applications.

#### 2.4 Magnetron sputtering technique

Magnetron sputtering has evolved into an advanced technique for precisely applying extremely pure and evenly thin layers of metal oxides, nitrides, and sulfides.<sup>77</sup> This method finds applications in a wide range of fields, including memory storage, optics, semiconductors, decorative coatings, and electronic devices, among various other uses. The two types of sputtering in a magnetron are radio frequency (RF) and direct current (DC). A sputtering target is hit with fast, powerful ions to deposit the target's film onto the substrate. As a result, atoms are emitted from the target and deposited in thin layers on the surface of the substrate, which is elevated and positioned directly opposite the target. Defect-free thin films are formed when the operating conditions, including pressure, temperature, and voltage, are precisely controlled.<sup>78</sup> The production of TiN nanostructures through alternative methods like the hydrothermal process necessitates the involvement of different gases, including O<sub>2</sub>

and NH<sub>3</sub>, as well as the application of exceedingly high temperatures, typically around 800 °C. Since no binders or conducting agents are required, the electrochemical performance is improved when TiN nanostructures are deposited directly onto the substrates.<sup>79</sup> Magnetron sputtering allows the direct depositing of binder-free, highly conformal, and pure TiN thin films onto substrates. In this context, Arif *et al.* employed DC sputtering with a power supply of 80 W to fabricate nanostructured TiN thin films in a pyramid shape.<sup>80</sup> The resulting films exhibited an atomic percentage ratio of Ti:N as 54.24:15.26%. A symmetrical supercapacitor device utilizing thin films of TiN demonstrated a capacitance of 112 F g<sup>-1</sup> at 1 A g<sup>-1</sup>, exhibiting impressive capacitance retention of 92.6% over a prolonged cycle count of 30 000.

The need for micro-supercapacitors has grown significantly in recent years, primarily attributed to their excellent robustness and capability to energize other integrated apparatus effectively. Nevertheless, the primary criteria for achieving enhanced performance are reliable cyclic stability and increased energy density. Utilizing magnetron sputtering for the deposition of TiN

thin films contributes significantly to the enhancement of micro supercapacitor fabrication. Achour *et al.* employed a sputtering-based technique to produce TiN thin films on planar silicon substrates.<sup>81</sup> The prepared films exhibited regulated porous structure and demonstrated a volumetric capacitance of 146.4 F cm<sup>-3</sup> while exhibiting a minimal decline in capacitance over a span of 20 000 cycles. Nitrogen doping of the TiO<sub>2</sub> layers and the film's inherent porosity are both likely responsible for the observed performance. Later, the same team of researchers created a micro-SC using a TiVN thin film composite by employing DC magnetron sputtering based on binary metal nitrides.<sup>82</sup> It has been determined that the greatest areal capacitance is delivered at a 1:1 Ti-V ratio, translating to 15 mF cm<sup>-2</sup>. In addition, after being subjected to 10 000 cycles, the TiVN thin film-based electrode displayed almost no degradation in capacitance (see Fig. 6a). This excellent capacitance retention can be attributed to the combined efforts of both components.

Recently, there has been a notable surge in the exploration of flexible and wearable electronic devices.<sup>83</sup> In these devices, the movement of electrolyte ions through nanostructured and porous thin films is enhanced, as these films effectively shorten the paths for ionic diffusion. To illustrate, Sial *et al.* employed DC magnetron sputtering to fabricate a flexible solid-state supercapacitor (SC) device. They achieved this by depositing a TiN-Ni thin film under specific conditions: a power of 150 W and a pressure of 10 mTorr, carried out for 30 minutes.<sup>84</sup> The generated porous TiN thin films have a consistent thickness of 103 nm. A thin layer of Ni improved the TiN-Ni electrode's electrical performance, resulting in a specific capacitance of 10.21 mF g<sup>-1</sup> and decent energy and power densities in the constructed device (see Fig. 6(b and c)). In another study, Xie *et al.* produced tunable TiN films to study the effect of substrate bias current ( $I_s$ ) on film characteristics.<sup>85</sup> Upon increasing the value of  $I_s$  from 0.1 to 3.0 A, it was observed that the films exhibit a preferred orientation for growth along the TiN(111) crystal plane. Additionally, a significant transformation in the morphology of the films was observed, transitioning from a loosely packed columnar microstructure to a densely packed and smooth microstructure devoid of distinct features.

In a recent study, Anas *et al.* analyzed the impact of N<sub>2</sub> content on the structural, mechanical, and corrosion properties of TiN coatings.<sup>86</sup> X-Ray diffraction analysis showed that as N<sub>2</sub> flow was increased, so too did the average grain size. Nitrogen content seemed to have the most significant impact on hardness. One advantage of TiN synthesis using magnetron sputtering is the ability to achieve highly adherent and uniform films on various substrate materials, including metals, semiconductors, and ceramics. The technique also offers good control over the film's stoichiometry, enabling the production of stoichiometric TiN with a desirable nitrogen-to-titanium ratio.

Magnetron sputtering allows for the deposition of TiN films with excellent mechanical and physical properties. TiN exhibits high hardness, excellent wear resistance, and good thermal stability, making it suitable for protective coatings, cutting tools, and wear-resistant components.<sup>80,87,88</sup> However, there are some limitations to consider. Magnetron sputtering equipment can

be costly and requires a well-controlled vacuum environment. Additionally, the process may lead to high residual stresses in the deposited films, which can affect their mechanical performance. Careful optimization of the deposition parameters and post-deposition treatments may be necessary to mitigate these effects.

## 2.5 Electrochemical deposition technique

TiN synthesis using the electrochemical deposition technique involves the electrodeposition of TiN films onto a conductive substrate from an electrolytic bath containing suitable precursor materials.<sup>89</sup> This method offers advantages such as simplicity, cost-effectiveness, and the ability to deposit TiN coatings on complex geometries or large-area substrates.<sup>9</sup> The process typically begins by preparing an electrolyte solution containing titanium salts, such as titanium chloride or titanium sulphate, along with a nitrogen source, usually in the form of ammonium salts or urea. The conductive substrate, often made of stainless steel or copper, serves as the cathode, while an inert or sacrificial anode is employed. During electrochemical deposition, a current is applied between the anode and the cathode, inducing a reduction reaction at the cathode surface. This promotes the formation of TiN nuclei on the substrate, which then grows into a continuous TiN film. The thickness, composition, and quality of the deposited film depend on the precise regulation of the deposition parameters, which include current density, bath composition, pH, and temperature. As an application in energy storage, Gray and colleagues sought to clarify the role that surface oxide layers play in diminishing the electrochemical functioning of TiN thin films.<sup>90</sup> After the electrodeposition, Ti foils were anodized in ammonia to produce TiN thin films. Their cyclic voltammetry analysis suggested that more oxidative treatment would not improve the initial cycles' capacitance values. However, at a high scan rate of 100 mV s<sup>-1</sup>, the capacitance of the succeeding cycles was 39 F cm<sup>-2</sup>. Zhao and co-workers developed mesoporous TiN nanotube arrays (TiN NTAs) as a substrate for ultra-low platinum (Pt) loadings.<sup>91</sup> The resulting TiN NTAs exhibited uniform structures with 80 nm inner diameter and 7 μm in length, featuring mesoporous holes on the nanotube walls with excellent stability. Mao *et al.* developed Ni-Cu/TiN for direct methanol fuel cells.<sup>92</sup> Electrochemical techniques are used to coat Ni-Cu nanoparticles on the surface of a TiN film. For the electrochemical oxidation of methanol, the prepared Ni-Cu/TiN has greater electrocatalytic activity than its counterparts. Xie *et al.* successfully incorporated MoN<sub>x</sub> with TiN to create MoN<sub>x</sub>-TiN nanotube arrays (NTAs) using electrodeposition and nitration in ammonia.<sup>93</sup> The resulting nanotubes had an average diameter of 110–130 nm and a length of approximately 4 μm.

The combined influence of MoN<sub>x</sub> and TiN resulted in an enhanced capacitance, reaching a measure of 121.50 mF cm<sup>-2</sup>, coupled with an impressive peak rate capability of 93.8% sustained throughout 1000 consecutive charge-discharge cycles. In another study, Jiangjing *et al.* produced two distinct types of nanocomposites through the electrochemical deposition of poly(3,4-ethylene dioxythiophene) (PEDOT) into porous hard template films containing TiC or TiN nanoparticles.<sup>94</sup> This



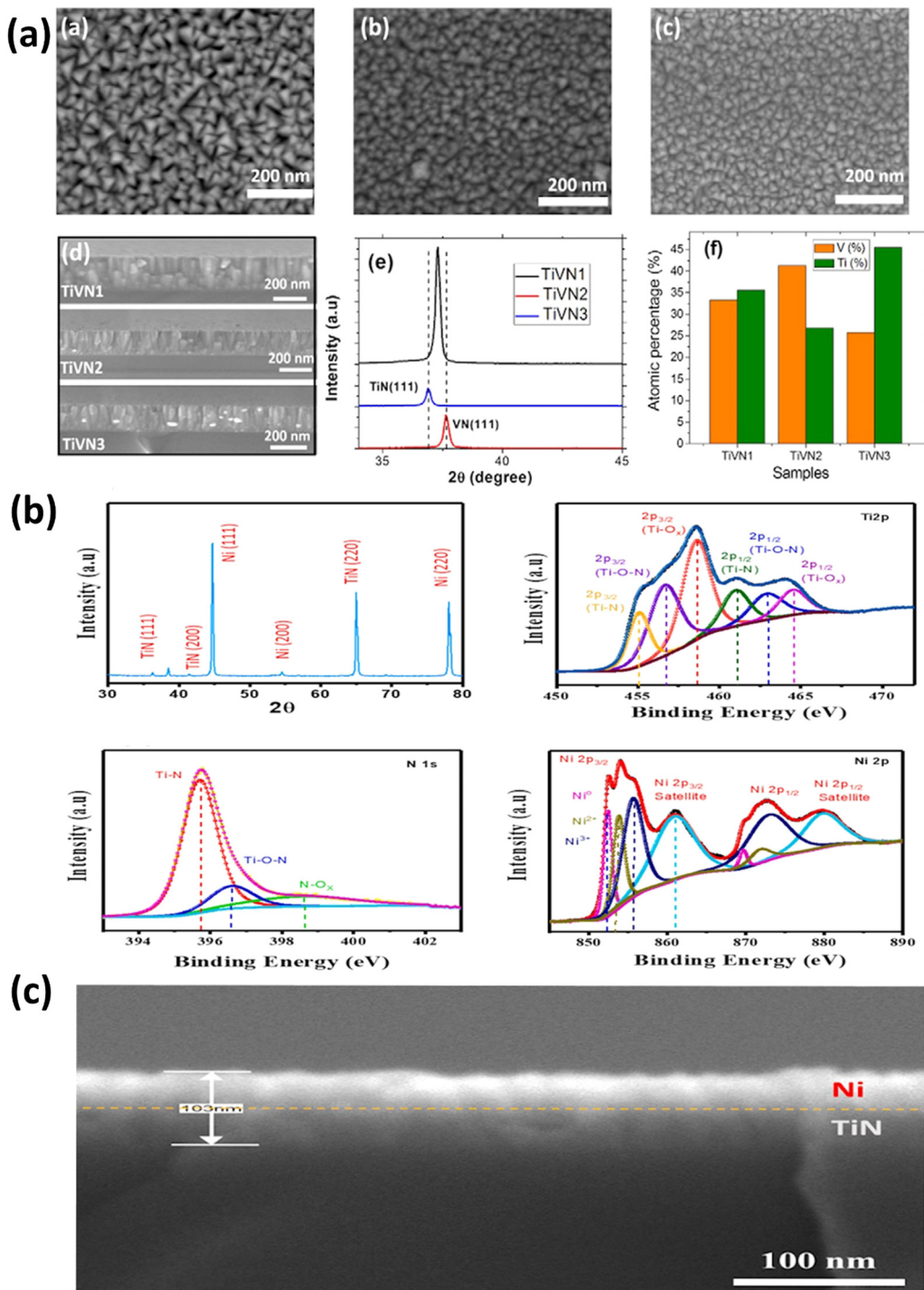


Fig. 6 (a) SEM images from a top view capturing TiVN electrodes, categorized as TiVN1, TiVN2, and TiVN3. The SEM cross-section of these three samples is also presented, along with the XRD pattern of TiVN electrodes, and the atomic percentages of Ti and V (reproduced from ref. 82 with permission); (b) the XRD pattern for a TiN/Ni nanocomposite, accompanied by deconvoluted spectra of Ti 2p, N 1s, and Ni 2p; (c) cross-sectional images of TiN/Ni nanocomposite (Reproduced from ref. 84 with permission).

investigation aimed to assess these nanocomposites' viability as potential catalysts in dye-sensitized solar cells (DSSC) that utilize a  $\text{Co}^{2+}/\text{Co}^{3+}$  polypyridyl redox mediator. Recently, Zhang *et al.* investigated the synthesis of an efficient catalyst for the HER using a combination of TiN and platinum (Pt) nanoparticles.<sup>95</sup>

The catalyst was prepared on carbon cloth (CC) through a two-step process involving nitridation of  $\text{TiO}_2$  in ammonia ( $\text{NH}_3$ ) followed by electrodeposition of Pt nanoparticles (see Fig. 7). The researchers found that introducing TiN as a plasmonic booster and Pt nanoparticles as a cocatalyst significantly improved HER

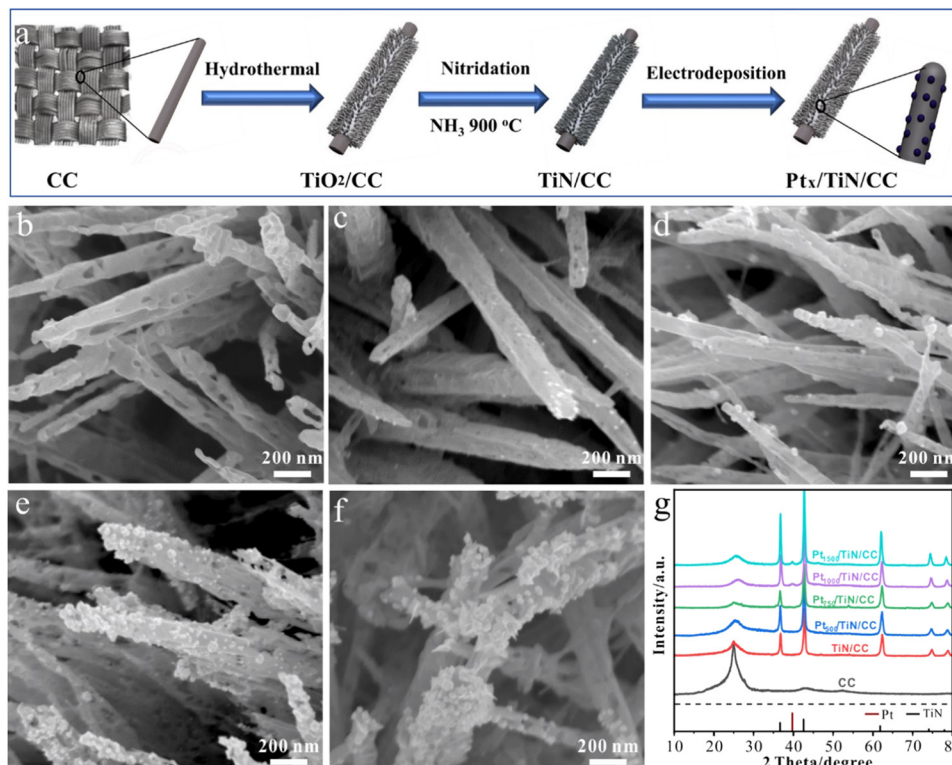


Fig. 7 (a) Schematic illustration of electrode preparation; SEM images of (b) TiN; (c) Pt500/TiN/CC; (d) Pt7500/TiN/CC; (e) Pt1000/TiN/CC; and (f) Pt1500/TiN/CC NWs; (g) XRD spectra of different samples (reproduced from ref. 95 with permission).

properties. The catalyst exhibited a small overpotential of 16 mV at a current density of 10 mA cm<sup>-2</sup>, indicating its high catalytic activity.

Electrochemical deposition of TiN offers several benefits. Adjusting the deposition parameters allows for precise control over the film's properties, including thickness, morphology, and crystal structure. The method also enables the formation of conformal coatings on complex-shaped substrates, making it suitable for applications where uniform coverage is essential, such as microelectronics and corrosion protection.<sup>9,96</sup> Furthermore, TiN films synthesized *via* electrochemical deposition exhibit desirable characteristics.<sup>97,98</sup> However, there are certain considerations to take into account. The electrochemical deposition process requires careful optimization of parameters to ensure uniform film growth and minimize defects or impurities. The choice of electrolyte composition and operating conditions can impact the film's properties and deposition efficiency. Additionally, post-treatment steps like annealing may be necessary to enhance the crystallinity and performance of the deposited TiN film.

## 2.6 Sol-Gel technique for TiN nanoparticles synthesis

The sol-gel method is a wet chemical technique that produces a wide range of nanomaterials, specifically metallic oxide nanostructures. In a conventional methodology, the dissolution of the precursor, commonly a metal alkoxide, in either alcohol or water is conducted, followed by its transformation into a gel through heat and agitation *via* alcoholysis or hydrolysis.<sup>99,100</sup>

TiN synthesis using the sol-gel approach involves forming a sol, a colloidal suspension of nanoparticles, followed by gelation and subsequent thermal treatment. A precursor solution containing titanium and nitrogen sources is prepared in this process. Common titanium precursors include titanium alkoxides or titanium salts, while nitrogen sources can be organic or inorganic compounds. The sol-gel process begins with the hydrolysis of the titanium precursor, which reacts with water to form metal hydroxides. Subsequently, a condensation reaction takes place, leading to the formation of a three-dimensional network or gel. The gel is then subjected to a thermal treatment process, typically at high temperatures, to promote the conversion of the gel into the desired TiN phase. During the thermal treatment, the gel undergoes various chemical reactions, such as nitridation, reduction, and decomposition, resulting in the formation of TiN nanoparticles. The exact conditions of the thermal treatment, including temperature, duration, and atmosphere, are critical factors influencing the properties of the TiN material.<sup>53</sup>

The low reaction temperature makes the sol-gel method a labour and material saving procedure that precisely manipulates product chemical composition, size distribution, and shape.<sup>99</sup> In addition to its many other applications, the sol-gel method can be used during the ceramics manufacturing process as a molding product and as a bridge between metal oxide thin films.<sup>101</sup> The methods used to create these materials have several potential uses in fields as diverse as electronics, optics, surface engineering, energy, pharmacology, and separation science.<sup>102,103</sup> The



sol-gel approach offers several advantages for TiN synthesis. It allows for controlling particle size, morphology, and composition by adjusting the precursor concentration, reaction conditions, and additives. It also enables the incorporation of dopants or the formation of composite materials. The resulting TiN coatings or films can exhibit enhanced hardness, stability, and thermal resistance properties.<sup>53,104</sup>

An instance of the fabrication of nanostructured TiN was carried out by Kim and Kumta using a hydrazide sol-gel (HSG) process.<sup>105</sup> The process involves the reaction of anhydrous hydrazine with titanium isopropoxide in the presence of anhydrous acetonitrile, resulting in the formation of a solid titanium alkoxy hydrazide precursor. Integrating sol-gel technology with complementary methodologies enables synthesising nanostructured materials with tailored properties. Using a combination of microwave carbothermal reduction and sol-gel methods, Zhang *et al.* created ultrafine TiN powders from sucrose and tetra butyl titanate.<sup>104</sup> The molar ratio of titanium to carbon, the impact of NH<sub>4</sub>F concentration, and the role of crystal seeds were also studied in this study. The results of the studies indicate that the created TiN NPs are favourably affected by the inclusion of crystal seeds, an excess amount of carbon, and NH<sub>4</sub>F at low temperatures. In a different study, Zhang *et al.* conducted a synthesis of sol-gel derived TiN nano powder, resulting in the production of crystallite sizes smaller than 10 nm.<sup>106</sup> Additionally, they successfully achieved a TiN coating with exceptional conductivity. The study utilized an optimized TiN coating containing 10 wt% TiN to coat LiFePO<sub>4</sub> particles, commonly used as a battery material. The resulting materials demonstrated notable enhancements in electrochemical performance compared to uncoated LiFePO<sub>4</sub>. These improvements were observed in terms of increased specific capacity, enhanced cycle stability, and improved rate capability. Hengyong *et al.* successfully prepared a TiN thin film by direct nitriding a TiO<sub>2</sub> thin film at various temperatures in the presence of NH<sub>3</sub>.<sup>107</sup> This study aimed to analyze the thin films' composition, microstructure, and optical properties to examine their impact on the surface-enhanced Raman scattering (SERS) capabilities exhibited by the thin films.

In another study, Yi-Min and colleagues employed a sol-gel technique with phase separation and nitridation to produce a macro and mesoporous TiN structure on carbon paper.<sup>108</sup> The surface area and pore size of TiN were adjusted by varying the concentrations of polyvinylpyrrolidone (PVP) in the solvent. The deposition of Pt nanoparticles onto TiN was achieved through atomic layer deposition, forming a Pt@TiN@carbon paper electrode. This electrode exhibits potential for utilization in proton exchange membrane fuel cells. In a recent report, the optical, electrical, and mechanical properties of TiN films were investigated by Valour *et al.* through the utilization of a direct rapid thermal nitridation process.<sup>109</sup> This process involved the transformation of a photo-patternable TiO<sub>2</sub> sol-gel layer (see Fig. 8). The findings suggest that TiN thin films synthesized using this approach hold great potential for developing optical metasurfaces devices and novel plasmonic materials. Qin *et al.* recently employed a sol-gel-assisted Fe-catalysed carbon thermal reduction nitridation reaction to synthesize ultrafine

TiN.<sup>110</sup> The reaction was conducted at temperatures ranging from 900 °C to 1100 °C. The purpose of this research was to examine iron's (Fe) catalytic influence on the dry gel carbon's heat reduction nitridation reaction. The results showed that Fe greatly improved the dry gels' carbothermal reduction nitridation reaction. The dry gel was supplemented with 4 wt% of Fe and subjected to calcination at a temperature of 900 °C. This process produced ultra-fine TiN nanoparticles with an average particle size of approximately 24 nm. Overall, the sol-gel method provides a versatile and tunable route for the synthesis of TiN, offering opportunities for various applications, including protective coatings, catalysis, electronics, and energy storage.

## 2.7 Laser ablation technique

Integrating nanotechnology with the concept of "light" has given rise to a new and dynamic field called "laser-assisted synthesis." This field has garnered significant attention worldwide due to its extensive applications in catalytic activity, energy resources research, biomedical science, and optics.<sup>111,112</sup> When comparing laser ablation synthesis in the air to other methods, it is important to consider the potential risks it poses to the health of researchers. One such risk is the contamination of their work environments with aerosols, which can adversely affect their well-being.<sup>113</sup> Laser ablation synthesis in liquid is a relatively safe and controlled method for laser processing and synthesis, offering the advantage of containing the resulting nanoparticles.<sup>114</sup> In contrast to pulsed laser deposition (PLD), a method that utilizes vacuum techniques to create and immobilize nanostructured materials or thin films on a material surface, liquid processing promotes the transportation of nanoparticles onto various substrates and necessitates straightforward processing equipment typically consisting of a water-filled vial and a solid plate.<sup>114,115</sup>

TiN synthesis using the laser ablation approach involves a high-power laser to ablate a TiN target in a controlled atmosphere. The process utilizes the interaction between the laser beam and the target material to generate a plasma plume containing TiN species. These species then condense and deposit onto a substrate to form TiN thin films or nanoparticles. In the laser ablation technique, a pulsed laser with high energy density is focused onto the surface of the TiN target. The intense laser pulse rapidly heats and vaporizes the target material, creating a plasma plume of energetic ions, atoms, and clusters. The plume expands and cools, allowing the TiN species to condense and deposit onto a substrate placed in the deposition chamber. The deposition parameters, such as laser fluence, repetition rate, target-to-substrate distance, and gas environment, can be optimized to control the properties of the synthesized TiN films. By adjusting these parameters, it is possible to influence the film's morphology, crystallinity, composition, and thickness.<sup>116,117</sup> The production of size-adjustable, highly pure TiN NPs was presented by Popov *et al.* through the utilization of femtosecond (fs) laser ablation in liquid and fragmentation techniques in acetone and water.<sup>118</sup> The synthesized nanoparticles exhibited high crystallinity, with only negligible TiO<sub>2</sub>. The authors have demonstrated the potential to manipulate the nanoparticles' size by adjusting the laser pulses' energy.



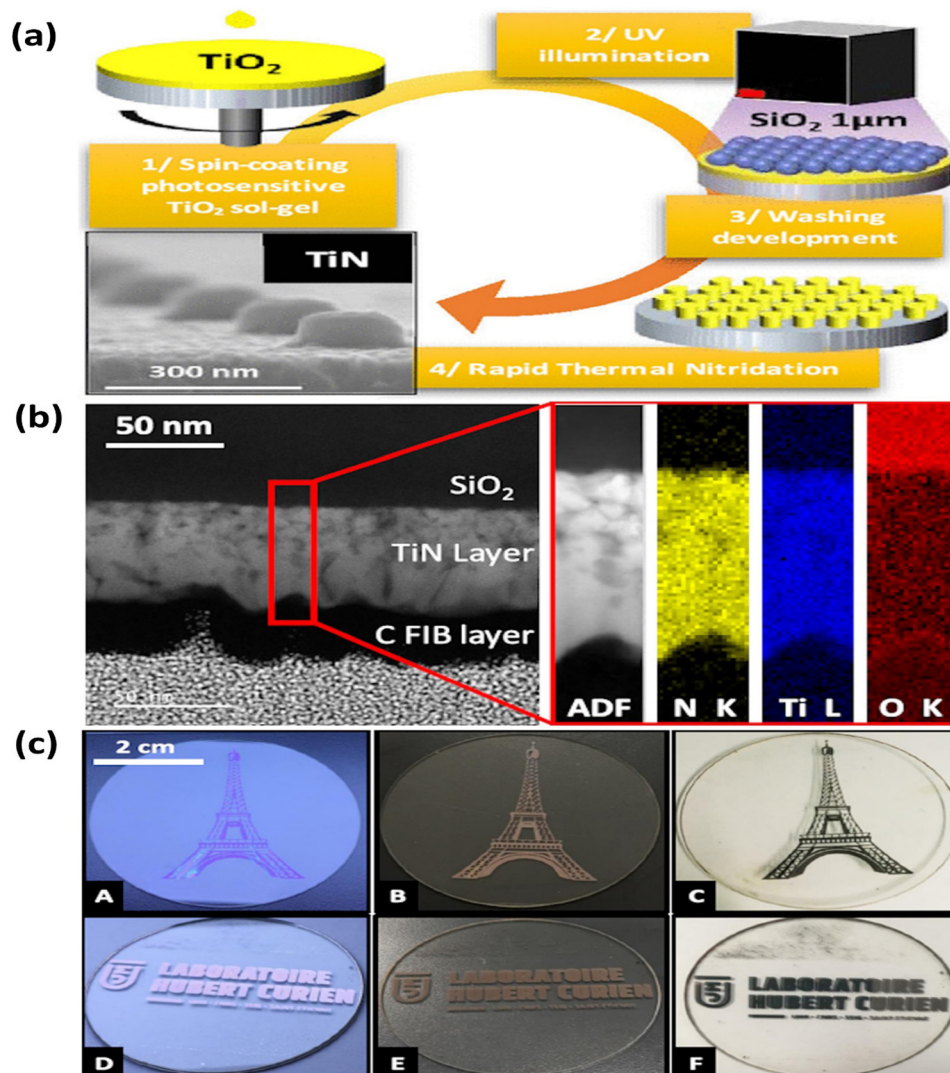


Fig. 8 (a) Scheme for the preparation; (b) cross-sectional HRTEM of the TiN thin film, annular dark field (ADF), and element mapping images for the N, Ti, and O; (c) photographs of structured  $\text{TiO}_2$  thin films after UV exposure (A) and (D), after nitridation (B) and (E) and in transmission (C) and (F) elements in the TiN layer (reproduced from ref. 109 with permission).

Bonse *et al.* studied TiN coated with various substrate materials, generating 2.5  $\mu\text{m}$  thick TiN layers.<sup>119</sup> They developed large surface areas of laser-induced periodic surface structures (LIPSS) using femtosecond laser pulses. The tribological performance of the nanostructured surfaces was determined using tribological tests against hardened 100 Cr6 steel. Tribological performance was sensitive to substrate material, laser fluence, and lubrication. However, LIPSS did not significantly reduce friction and wear compared to reference TiN surfaces. Researchers investigated the nanostructured surfaces' wear patterns using morphology, depth, and chemical composition. Fedorov *et al.* employed a femtosecond laser process with a power output of 100 W to carry out treatments on titanium and silicon substrates under different atmospheric conditions.<sup>120</sup> The experimental procedure resulted in uniform coatings consisting of titanium oxynitride (TiON) and silicon carbide (SiC) on a titanium substrate. This was achieved by subjecting the titanium substrate to nitrogen and ethene/argon

atmospheres, which facilitated rapid surface transformation and yielded coatings with excellent spatial resolution. The surfaces exhibited enhanced mechanical resistance and a discernible microstructure in contrast to those produced through vapor deposition methods. Marzieh *et al.* used nanosecond Ce:Nd:YAG pulsed laser ablation in different solvents to create TiN nanoparticles.<sup>121</sup> Spectroscopic, structural, and compositional methods were used to characterize the NPs. TiN NPs in *N,N*-dimethylformamide exhibited high near-infrared optical absorption, whereas those in toluene and acetonitrile were encased in a carbon matrix. TiN NPs devoid of carbon were obtained through thermal oxidation of the carbon matrix. When surface Raman spectroscopy was performed on methylene blue molecules, these carbon-free TiN NPs were shown to have almost the same enhancement factors as gold. Radhakrishnan *et al.* pioneered ultrafast laser processing to produce superhydrophobic nanostructured TiN surfaces.<sup>122</sup> The method



includes changing the shape of a surface to speed up the adsorption of volatile organic compounds (VOC). The nanostructures are porous and spongy on a nanoscale scale. The nanostructures act as air traps, which helps to promote a wetting condition known as Cassie–Baxter. A study comparing vacuum-processed and atmospherically-aged materials found that water molecules passivate reactive sites, reducing VOC adsorption.

In a recent report, Farooq and colleagues carried out the synthesis of TiN NPs through the utilization of pulsed laser ablation in acetone as a nanofluid.<sup>123</sup> TiN NPs exhibit low dispersion, possess a broad absorption peak, and demonstrate a solar-weighted absorption coefficient of 95.7%. TiN nanofluids exhibit a thermal efficiency that surpasses Au-based counterparts by 80%. This notable enhancement, coupled with their superior photothermal efficiency and colloidal stability, positions TiN nanofluids as a significant breakthrough in direct absorption solar collectors (DASC) technology. In another report, Chen *et al.* developed a picosecond laser ablation method for modifying CrTiN thin films for cell culture processes.<sup>124</sup> The method effectively controlled surface roughness and ripple characteristics of periodic corrugated nano pod structures, improving mechanical and electrochemical properties (see Fig. 9). The laser-material interaction also influenced wetting behaviours and enhanced A549 cell proliferation and viability. This method can potentially

develop new micro composites and *in vivo* detection in biomedical applications.

The laser ablation approach offers several advantages for TiN synthesis. It enables the growth of TiN films with high purity and stoichiometry. The non-equilibrium conditions during laser ablation can promote the formation of metastable phases and unique nanostructures. Furthermore, the process is relatively fast, allowing for rapid deposition of TiN films over large areas. Laser ablation synthesis of TiN results in outstanding mechanical, electrical, and optical characteristics, rendering it apt for diverse application possibilities. These include wear-resistant coatings, corrosion protection, semiconductor devices, optoelectronics, and biomedical implants.<sup>53,125</sup> In summary, the laser ablation technique provides a versatile and precise method for synthesizing TiN films and nanoparticles. It offers control over the film properties and enables the production of superior TiN materials for various technological applications.

### 3 Emerging applications of TiN nanostructures

The emergence of TiN nanostructures has opened up exciting avenues across various technological landscapes. These

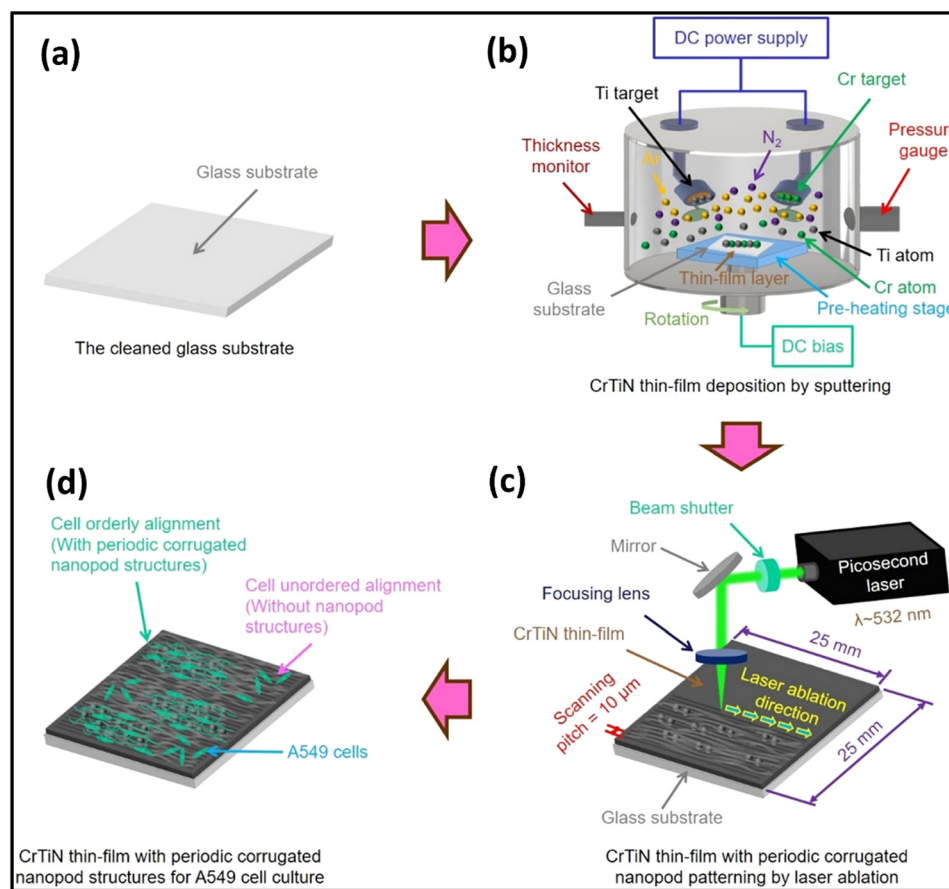


Fig. 9 Illustration of CrTiN thin films (a–d), having regularly patterned nanopod structures, generated via picosecond laser ablation, designed for applications in cell culture procedures (reproduced from ref. 124 with permission).



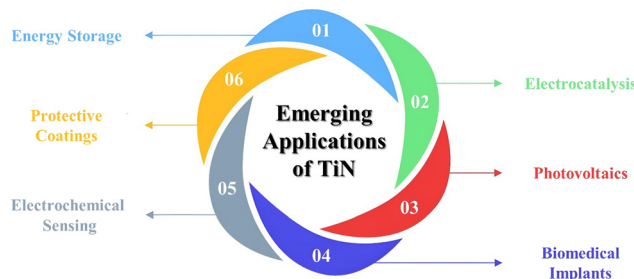


Fig. 10 Emerging applications of TiN in various allied areas.

nanostructures, characterized by their unique properties and tunability, are finding applications in cutting-edge fields.<sup>126–128</sup> In electronics, TiN nanostructures are being explored as components for nanoscale devices, owing to their exceptional electrical conductivity and compatibility with semiconductor processes. In the realm of energy, TiN nanostructures are being integrated into energy storage systems and catalytic converters due to their high surface area and reactivity.<sup>129,130</sup> The biomedical field is witnessing the incorporation of TiN nanostructures in implant coatings and drug delivery systems, taking advantage of their biocompatibility and tailored surface properties.<sup>131,132</sup> Moreover, TiN nanostructures are playing a pivotal role in advanced sensors and detectors, harnessing their sensitivity to changes in physical and chemical parameters.<sup>133,134</sup> As research continues to unravel their potential, TiN nanostructures are poised to revolutionize a spectrum of industries and technologies, showcasing their versatility and promising a future marked by innovation. The aforementioned characteristics render them highly suitable candidates for various applications, encompassing energy generation, storage and other allied applications (see Fig. 10). This section focuses on the practical implementation of TiNs in the context of energy storage, catalysis, photovoltaics, biomedical implants, electrochemical sensing, and protective coatings.

### 3.1 Supercapacitor electrode material

As the need for effective energy storage solutions continues to rise, there is a constant evolution in the development of state-of-the-art equipment. Supercapacitors (SC), also known as “ultracapacitors,” have gained significant attention due to their higher capacitance values compared to regular capacitors. Various materials have been explored to fabricate supercapacitor electrodes, including conducting polymers,<sup>135–138</sup> carbon-based materials,<sup>139–142</sup> transition metal oxides,<sup>143</sup> dichalcogenides,<sup>144–147</sup> nitrides,<sup>47,148</sup> and carbides.<sup>149</sup> Among these materials, TiN has emerged as one of the most suitable choice for supercapacitor electrodes. TiN, along with other ternary metal nitrides such as VN and MnN, has garnered considerable interest due to its potential for high-performance supercapacitors.<sup>17,150</sup> The unique properties of TiN make it well-suited for energy storage applications. TiN electrodes offer several advantages in supercapacitor systems. Firstly, their high electrical conductivity allows for efficient charge transfer, facilitating rapid charging and discharging processes. Additionally, TiN exhibits good chemical stability, ensuring the long-term durability and performance of the supercapacitor device. The high

surface area of TiN electrodes allows for enhanced electrochemical activity, leading to improved energy storage capabilities. In the subsequent section, we explore various amalgamations of TiN with different carbon allotropes, conducting polymers, and metal oxides in the context of their potential utilization in supercapacitor applications.

**3.1.1. Pure nanostructured TiN.** In general, several TiN morphologies, such as cauliflower,<sup>151</sup> Chrysanthemum-like,<sup>152</sup> corn-like,<sup>153</sup> or nanotube-TiN<sup>72</sup> have been synthesized using a variety of methods.<sup>154</sup> We will discuss some of them in this section. For instance, Yang *et al.* created corn-like TiN structures (see Fig. 11(d)) using both the hydrothermal method and atomic layer deposition (ALD) technique.<sup>153</sup> These corn-like TiN electrodes exhibited a remarkable volumetric capacitance of  $1.5 \text{ mW h cm}^{-3}$  and maintained their capacitance with minimal loss even after undergoing 20 000 cycles of operation. In their study, Hou *et al.* synthesized chrysanthemum-like titanium nitride (CL-TiN) using a hydrothermal technique which exhibits excellent capacitive performance and structural stability, achieving a specific capacitance of  $23.35 \text{ F g}^{-1}$  and maintaining 90.0% capacitance retention after 10 000 cycles.<sup>152</sup> Moreover, a symmetric flexible solid-state supercapacitor (FSS-SC) based on CL-TiN demonstrates high volumetric capacitance, energy density, and ultrafast-charging/discharging performance, with a remarkable capacitance increase of 36.7% after 20 000 cycles. The TiN-based flexible supercapacitors with rapid charging/discharging might be successfully used as a reliable and adaptable energy storage technology (see Fig. 11(a)).

Achour *et al.* reported that nitrogen ( $\beta$ -N) doping in the oxidized surface of TiN thin films (see Fig. 11(b) and (c)) significantly improves the specific capacitance and cycling stability, with a 3-fold increase in areal capacitance achieved through vacuum annealing without compromising electrode performance even after 10 000 charge/discharge cycles.<sup>155</sup> Using binder-free electrodes promotes rapid ion transport through conducting networks, removing the requirement for conducting agents and binders and thus increasing the electrochemical performance of TiN-based electrodes. For instance, Qin *et al.* produced nanopillars of hierarchical TiN nanoparticles using a simple hydrothermal technique.<sup>72</sup> The electrode is fabricated through the nitration process of  $\text{TiO}_2$  nanotubes, resulting in the formation of H-TiN nanopillars. The H-TiN nanopillars, when used as an electrode, exhibited a capacitance of  $69 \text{ F cm}^{-3}$  at a current density of  $0.83 \text{ A cm}^{-3}$  and high energy density ( $0.53 \text{ mW h cm}^{-3}$ ), presenting a novel approach for improving the supercapacitive performance of metal nitrides.

A large surface area is crucial for achieving high-performance supercapacitor electrodes because it allows for more charges to accumulate on the electrode's surface, thereby increasing capacitance. Moreover, the synthesis of TiN with an expanded specific surface area holds the potential to greatly enhance the performance of supercapacitors.<sup>154</sup> Adopting the same strategy, Choi *et al.* conducted a synthesis of TiN nanocrystals, resulting in a specific surface area of  $128 \text{ m}^2 \text{ g}^{-1}$ .<sup>156</sup> The researchers noted a decline in specific capacitance, from 238 to  $24 \text{ F g}^{-1}$ , in a 1 M KOH aqueous electrolyte as both the synthesis temperature and



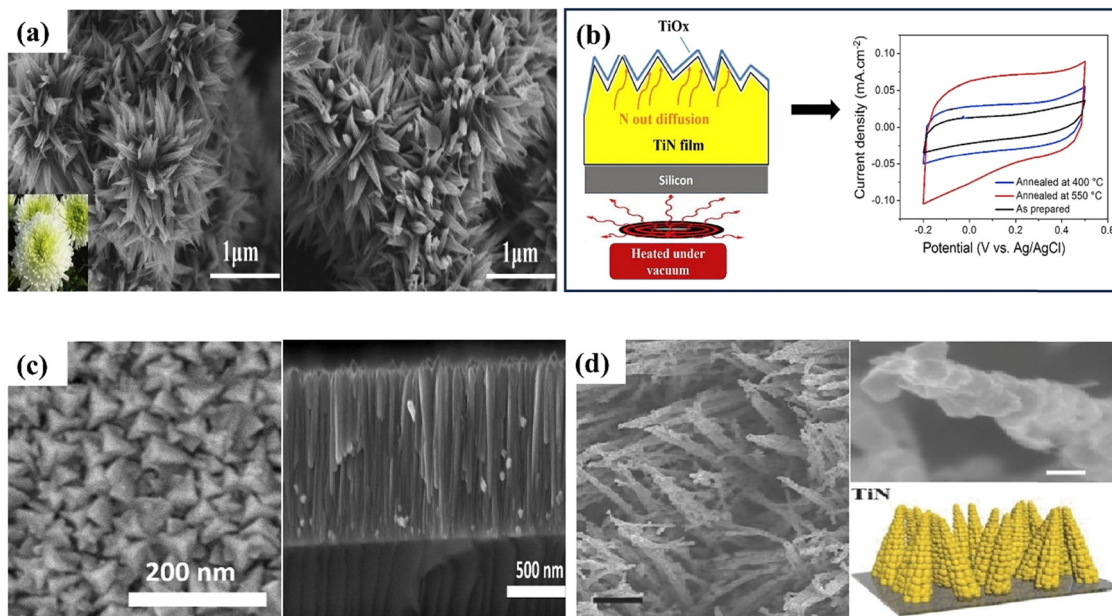


Fig. 11 SEM images of (a) CL-TiN (reproduced from ref. 152 with permission); (b) this diagram illustrates the annealing of TiN thin films in vacuum and cyclic voltamogram curves for both the pre-and post-annealing state of TiN electrodes, (c) pyramid-shaped TiN nanostructures (reproduced from ref. 155 with permission); (d) corn like TiN nanostructure (reproduced from ref. 153 with permission).

scan rates were elevated. The investigation of nanostructured TiN as a potential supercapacitor electrode is motivated by its robust mechanical and electrical conductivity. Nevertheless, the constrained specific surface area of the material and the lack of electroactive sites for charge storage offer significant challenges.

**3.1.2. TiN–carbon-based nanocomposites.** In order to achieve both high energy density and improved power density, researchers often create TiN/C nanocomposite electrodes that possess exceptional electrochemical properties. These electrodes are synthesized by combining nanostructured carbon materials with elevated surface area, alterable pore size, and TiN, which offers superior conductivity.<sup>154</sup> Haldorai *et al.* reported TiN/rGO nanocomposite fabrication by a two-step process.<sup>157</sup> The nanocomposite demonstrated a notable capacitance of 415 F g<sup>-1</sup> when subjected to a current density of 0.5 A g<sup>-1</sup>. This enhanced electrochemical functionality can be ascribed to the robust interaction and efficient dispersion of TiN nanoparticles within the reduced graphene oxide (rGO) sheets (see Fig. 12(a)). Using a two-step process, Lu *et al.* developed TiN NWs on carbon cloth (TiN/C).<sup>158</sup> The electrode obtained exhibited a significant volumetric specific capacitance of 0.33 F cm<sup>-3</sup> when subjected to a current density of 2.5 mA cm<sup>-3</sup>. This value is comparable to the recent findings reported for solid-state graphene-based supercapacitors, specifically 0.42 F cm<sup>-3</sup>. The TiN nanowire/carbon electrode demonstrated excellent stability, retaining 82% of its initial capacitance following 15 000 cycles in a 1 M potassium hydroxide electrolyte solution (see Fig. 12(b–e)).

CNTs have shown outstanding charge transfer properties surpassing other materials, establishing them as excellent conductive materials.<sup>148</sup> Consequently, in recent years, numerous TiN/CNT composite electrodes for supercapacitors have been extensively studied and reported due to their promising

performance. Tremendous research is going on to develop hybrid supercapacitors, following the same trend Achour *et al.* developed high-performance composite electrodes for micro-supercapacitors, combining vertically aligned carbon nanotubes (CNTs) with hierarchically structured porous TiN.<sup>151</sup> These electrodes, deposited on silicon substrates, demonstrate exceptional performance with an impressive areal capacitance of 18.3 mF cm<sup>-2</sup> at 1 V s<sup>-1</sup>, which can be further improved by increasing the thickness of the TiN layer. Moreover, this capacitance is maintained even after 20 000 cycles. This outstanding performance is attributed to the electrode's large surface area, nanoporous structure, and specific surface chemistry, which includes a significant presence of oxygen vacancies on the electrode's surface. Furthermore, the researchers demonstrated that the concentration of oxygen vacancies could be increased by introducing nitrogen (N) into the TiO<sub>2</sub> surface layer during the synthesis and aging processes. This nitrogen doping strategy effectively enhances the capacitance of supercapacitors (SCs).

In another study, Kao *et al.* used atomic layer deposition (ALD) to coat TiN onto carbon nanotube (CNT) electrodes for supercapacitors.<sup>159</sup> The ALD technique allowed precise and conformal coatings, resulting in a >500% increase in capacitance compared to bare CNTs. TiN-coated CNTs showed superior performance with areal capacitance values of 81 mF cm<sup>-2</sup>, outperforming bare CNTs and planar TiN at a scan rate of 10 mV s<sup>-1</sup>. Recently, Liu *et al.* developed a method using carbon nitride to synthesize TiN/carbon nanosheets and TiC/carbon nanosheets with a hierarchical structure.<sup>160</sup> These materials performed exceptionally well as the cathode and anode in a capacitor in an aqueous electrolyte. The asymmetric supercapacitor constructed with TiN/C cathode and TiC/C anode demonstrated a wide operating voltage range (0.3–1.8 V), high specific capacitance (103 F g<sup>-1</sup>), and

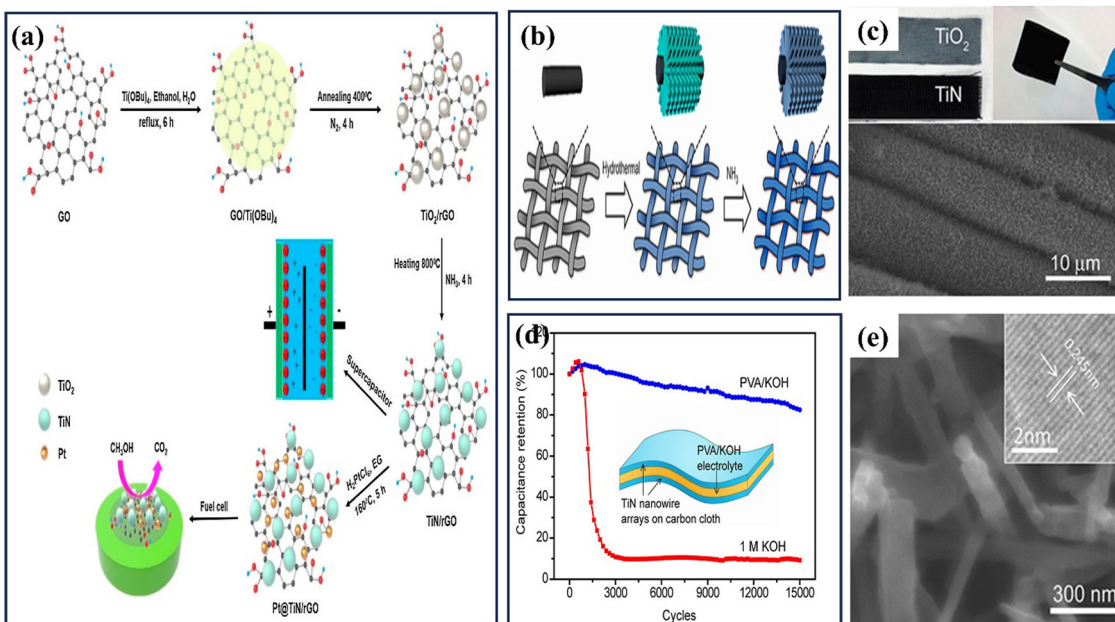


Fig. 12 (a) The production processes of the Pt@TiN/rGO ternary hybrid and the TiN/rGO composite (reproduced from ref. 157 with permission); (b) schematic of a two-step growth method for generating TiN nanowires (NWs) on carbon cloth; (c) images of carbon cloth coated with TiO<sub>2</sub> and TiN nanoparticles, as well as a SEM image showcasing TiN NWs growth on carbon fabric; (d) comparison of H-TiN NPs and TiN NTs electrode electrochemical performances; (e) an enlarged SEM perspective of a single carbon fiber embellished with TiN nanowires (reproduced from ref. 158 with permission).

remarkable energy density ( $45.2 \text{ W h kg}^{-1}$ ), outperforming previous TiN- and TiC-based SCs. The excellent performance was attributed to reversible redox reactions, electro-adsorption of anions, fast adsorption/desorption of cations, unique surface morphology, and heterostructure. The authors presented a novel methodology for synthesising transition metal nitride (or carbide)/carbon composites, which holds promise for their utilization in cutting-edge energy-related applications.

**3.1.3. TiN/conducting polymer-based composites.** Currently, researchers are actively exploring the use of organic-inorganic composite materials as electrodes for supercapacitors. These composites typically consist of an inorganic component, such as metal oxides, metal sulfides, or metal nitrides, combined with an organic component composed of conductive polymers (CPs).<sup>161–163</sup> The integration of these materials enables charge storage through pseudocapacitance, offering high energy storage capacity. Conductive polymers possess several favorable characteristics that make them highly suitable for supercapacitor electrodes. They exhibit a wide operating potential window, allowing for efficient charge storage over a broad range of voltages. Additionally, these polymers are environmentally friendly, cost-effective, and relatively simple to produce, making them attractive for large-scale production.

Various polymers, including polypyrrole (PPy), polypropylene (PP), polyaniline (PANI), polyvinyl alcohol (PVA), and polyacrylamide (PAM), are being investigated for their potential applications in supercapacitors.<sup>164</sup> These polymers offer unique properties and can be tailored to meet specific requirements, providing versatility in designing and optimizing the performance of supercapacitor electrodes. Researchers aim to enhance supercapacitors' energy storage capacity and overall performance by exploring the

synergistic combination of inorganic materials and conductive polymers. This research field holds significant promise for developing efficient and sustainable energy storage systems to meet the growing demands of various applications, ranging from portable electronics to electric vehicles and renewable energy grids.<sup>165</sup> For example, Du *et al.* reported a comparison between polypyrrole-TiN and polypyrrole-TiO<sub>2</sub> hybrids.<sup>98</sup> Both of them were prepared *via* an electrodeposition process called normal pulsed voltammetry. The resulting structures show that the polypyrrole fully coats the TiN and TiO<sub>2</sub> nanotubes, forming coaxial heterogeneous nanohybrids. The exceptional conductivity of the TiN substrate significantly enhances the electrochemical capacitance of polypyrrole, leading to enhanced supercapacitance capabilities in the Ppy-TiN nanohybrid compared to the Ppy-TiO<sub>2</sub> nanohybrid at a current density of  $0.6 \text{ A g}^{-1}$ . Both nanohybrids show similar cyclability, with stable capacitances of  $459 \text{ F g}^{-1}$  for PPy-TiN and  $72 \text{ F g}^{-1}$  for PPy-TiO<sub>2</sub> (see Fig. 13(a and b)). Lu *et al.* have successfully reported a unique composite electrode consisting of phosphomolybdic acid, polyaniline, and a TiN core-shell structure.<sup>166</sup> The effective dispersion of polymers and the highly conductive TiN backbone in binder-free electrodes, fabricated *via* electrodeposition (Fig. 13(c–e)), enabled the device to achieve a specific capacitance of  $469 \text{ F g}^{-1}$  at  $1 \text{ A g}^{-1}$  and an impressive energy density of  $216 \text{ W h kg}^{-1}$  within a  $1.5 \text{ V}$  operating voltage range. Xia *et al.* integrated TiN nano wire array with polyaniline (PANI) and manganese oxide ( $\text{MnO}_2$ ) to obtain PANI/MnO<sub>2</sub>/TiN ternary nanocomposite for SC application.<sup>167</sup> They started with synthesising TiN NWA and then coating the NWA with electroactive MnO<sub>2</sub> and PANI layer by layer to form a heterogeneous



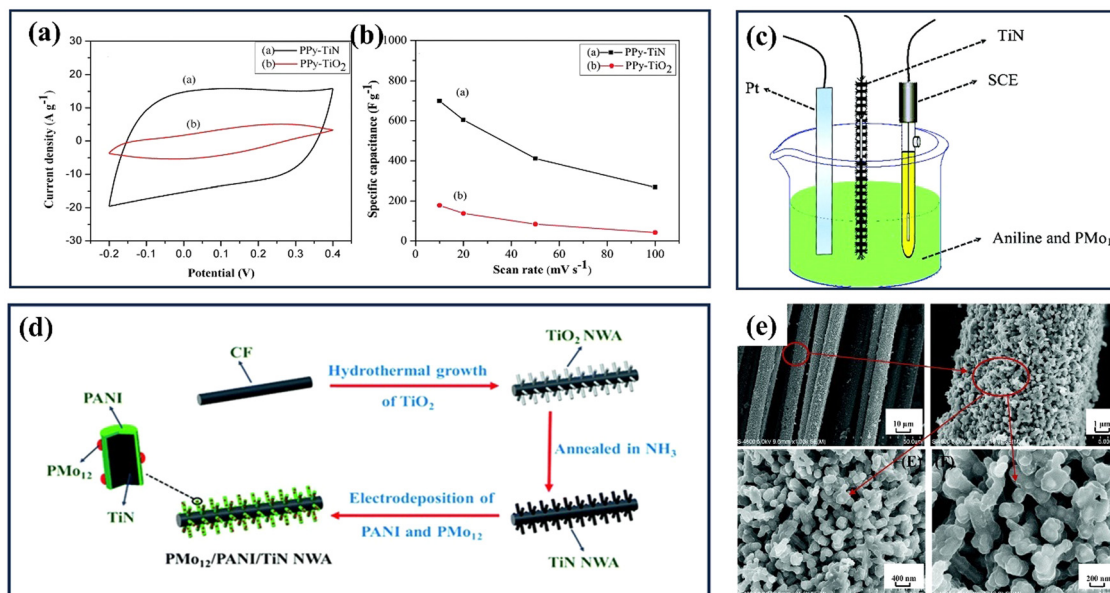


Fig. 13 (a) The PPy–TiO<sub>2</sub> and PPy–TiN nanotube hybrid cyclic voltammetry curves in the 1 M H<sub>2</sub>SO<sub>4</sub> electrolyte at 20 mV s<sup>-1</sup>; (b) the corresponding specific capacitance in terms of the CV scan rate (reproduced from ref. 98 with permission). (c) This diagram shows how PMo<sub>12</sub> and PANI can be electrochemically polymerized in one step on the surface of TiN NWA supported on CF; (d) a schematic showing how PMo<sub>12</sub>/PANI/TiN NWA supported on CF grows; (e) SEM images of PMo<sub>12</sub>/PANI/TiN NWA (reproduced from ref. 166 with permission).

coaxial structure through a stepwise electrodeposition process. The PANI/MnO<sub>2</sub>/TiN NWA achieved a significantly higher specific capacitance of 674 F g<sup>-1</sup> at 1 A g<sup>-1</sup> compared to previously reported PANI/MnO<sub>2</sub>/carbon-cloth composites.

Incorporating both a *n*-type and *p*-type conducting polymer with highly conductive TMN is another way to increase the capacitance of electrodes, providing efficient and narrow routes for fast electrolyte diffusion.<sup>168</sup> In this regard, Xie *et al.* produced a PPy/TiN/PANI coaxial nanotube composite *via* normal pulse voltammetry and cyclic voltammetry electrodeposition, which was further utilized as SC electrode along with H<sub>2</sub>SO<sub>4</sub>-included polyvinyl alcohol gel electrolyte. The PPy/TiN/PANI nanotube hybrid obtained with P/N type doping properties demonstrated a high specific capacitance of 1471.9 F g<sup>-1</sup> at 0.5 A g<sup>-1</sup> along with good capacitance retention of 78.0% after 200 cycles. The findings of this study provide strong evidence that the hybrid nanotube under investigation exhibits considerable potential as a viable option for supercapacitor electrodes.<sup>169</sup> To enhance the performance of supercapacitors, it is important to find alternative methods for synthesizing hybrid nanostructures of TiN and conducting polymers, as current techniques are limited. Using polymers as templates can result in TiN with larger surface areas, varied pore sizes, and efficient conducting channels, leading to higher capacitance.<sup>168</sup> In this regard, Kin *et al.* fabricated mesoporous TiN thin films by incorporating an amphiphilic graft copolymer as a template.<sup>170</sup> The SC device fabricated using these thin films demonstrated excellent capacitance retention even when bent, delivering a capacitance of 266.8 F g<sup>-1</sup> and exhibiting high cycling stability.

**3.1.4. TiN/metal oxides/nitrides-based composites.** Metal oxides are commonly used as electrode materials for pseudocapacitors due to their high energy density and capacitance. However, they face

challenges of low conductivity and limited surface area. To address this, incorporating metal oxides with conducting titanium nitrides (TiNs) as a conducting substrate or composite material is a strategy employed to enhance electric conductivity.<sup>171</sup> For instance, Yadav and colleagues conducted research that showcased how the development of hierarchical porous flower-shaped NiCo<sub>2</sub>O<sub>4</sub>@TiN core/shell nanosheet arrays on Ni foam led to heightened electrochemical effectiveness. Notably, these nanosheet arrays exhibited remarkable outcomes, with a specific capacity of 402.57 C g<sup>-1</sup> under a current density of 1 A g<sup>-1</sup>, while maintaining an impressive cycling stability of 90% across 2000 charge–discharge cycles.<sup>172</sup> The superior electrochemical performance of the electrode can be ascribed to the optimized thickness and enhanced conductivity of the TiN thin film, as well as the synergistic interaction between NiCo<sub>2</sub>O<sub>4</sub> and TiN. This unique core/shell structure holds promise for high-performance supercapacitors and opens avenues for new electrode fabrication.

In a similar report, Peng *et al.* fabricated porous double-layered MoO<sub>x</sub>/TiN/MoO<sub>x</sub> nanotube arrays.<sup>173</sup> The inclusion of TiN, which exhibits high conductivity, facilitates efficient electron transfer. Simultaneously, the porous structure of MoO<sub>x</sub> allows for easy infiltration of the electrolyte, thereby maximizing the number of active sites available on the MoO<sub>x</sub> material. This, in turn, enhances the system's specific capacitance and rate capability. The electrode demonstrated an impressive capacitance of 97 mF cm<sup>-2</sup> when subjected to a current density of 1 mA cm<sup>-2</sup>. Moreover, it retains 60% of its capacitance even when the current density is increased by a factor of 20. A symmetrical device developed using this electrode maintains a capacitance of 24 F cm<sup>-3</sup> and exhibits excellent cycling stability over 10 000 charge/discharge cycles. The enhanced performance of the device was attributed to the incorporation

of a thin TiN layer and dual-layered  $\text{MoO}_x$  nanotube arrays, which provide both high mass loading and surface area.

The combination of two distinct metal nitrides exhibits the potential to enhance the swift mobility of electrons and ions, thereby augmenting the capacity for storing electric charge.<sup>168</sup> Following a similar approach, the fabrication of core–shell TiN–VN fibers with high porosity and a large surface area was reported by Zhou *et al.* using the co-axial electrospinning technique.<sup>174</sup> Utilizing a composite material comprising TiN and VN led to the achievement of a specific capacitance value of  $247.5 \text{ F g}^{-1}$ , along with a remarkable capacitance retention rate of 88% over a span of 500 cycles. The presence of a fibrous structure facilitated increased accessibility to electrolyte ions, while the incorporation of TiN and VN in the composite material resulted in enhanced performance of the supercapacitor electrode.

The main challenge in the widespread use of supercapacitors is their low energy density. Optimizing voltage window and capacitance through suitable electrode materials and device configuration is crucial to address this. Creating an asymmetric supercapacitor device is a key strategy to achieve higher energy density.<sup>168</sup> Furthermore, one can increase the capacitive performance of TiN electrodes *via* transition metal incorporation (heteroatom incorporation). Recently, Wei *et al.* utilized both of these strategies in their supercapacitor as described here; by incorporating niobium (Nb) into TiN, the performance of TiNbN is significantly enhanced due to the combined effect of Ti and Nb.<sup>175</sup> This results in a superior capacitance of  $59.3 \text{ mF cm}^{-2}$  at  $1.0 \text{ mA cm}^{-2}$ , surpassing the capacitance of TiN, NbN, and other reported transition metal nitrides. They combined this TiNbN electrode with VN to obtain an asymmetric TiNbN/VN supercapacitor demonstrating a high energy density of  $74.9 \text{ mW h cm}^{-3}$  at a power density of  $8.8 \text{ W cm}^{-3}$  and exceptional stability. This study introduces a high-performance asymmetric supercapacitor and provides a comprehensive approach to improve the electrochemical characteristics of metal nitride thin films.

While TiN-based supercapacitors show great potential, ongoing research focuses on improving their performance characteristics, such as energy density and rate capability. Scientists and engineers are exploring strategies such as nanostructuring, hybridization with other materials, and developing novel electrode architectures to enhance the overall performance of TiN-based supercapacitors. TiN-based supercapacitors represent a promising avenue for advanced energy storage devices. Their high specific capacitance, excellent cycling stability, and ease of fabrication make them attractive for various applications, including portable electronics, electric vehicles, renewable energy systems, and more.<sup>47,154</sup> With continued research and development, TiN-based supercapacitors have the potential to contribute significantly to the advancement of energy storage technologies.

### 3.2 Batteries electrode material

In response to the growing requirements for energy storage solutions, scientists have thoroughly explored a range of battery types. These encompass lithium-ion batteries (LIBs), sodium-ion batteries (SIBs), potassium-ion batteries (KIBs), zinc-air batteries (ZABs), and lithium–oxygen batteries (LOBs).<sup>176–178</sup>

An essential aspect of enhancing the performance of these batteries is the choice of anode material. In recent years, researchers have explored a wide range of anode materials, with metal nitrides gaining significant attention due to their reversible redox reactions and potential advantages for battery performance.<sup>17</sup> TiN, in particular, has emerged as a promising candidate due to its excellent electronic conductivity and chemical stability, making it desirable for applications in Li–S batteries.<sup>179</sup> In this regard, Balogun and colleagues effectively created TiN nanowires by employing a hydrothermal technique followed by annealing on a carbon fabric substrate.<sup>71</sup> These TiN nanowires demonstrated impressive electrochemical performance as anode materials in flexible LIBs. They exhibited a high reversible capacity of  $567 \text{ mA h g}^{-1}$  and remarkable capacity retention of 80% after 100 cycles at a current density of  $335 \text{ mA g}^{-1}$ . This highlights the potential of TiN nanowires for flexible LIBs, offering excellent electrochemical performance and flexibility.

Cui *et al.* have successfully developed a novel cathode material known as mesoporous TiN–sulfur for application in lithium–sulfur batteries (LSBs). This material exhibits noteworthy characteristics, including a high specific capacity, exceptional rate capability, and superior cycling stability. Notably, the capacity decay observed over 500 charge/discharge cycles is a mere 0.07% per cycle. These findings underscore the considerable potential of mesoporous TiN as a viable solution for mitigating the capacity fade problem encountered in LSBs.<sup>180</sup> In another study, to address the issue of low sulfur utilization and poor redox kinetics in lithium–sulfur (Li–S) cells, Wang and collaborators designed carbon hollow nanosphere-based TiN (C@TiN) nanospheres, serving as versatile polysulfide mediators. This innovation facilitated accelerated reaction kinetics, elevated polysulfide entrainment efficiency, and enhanced longevity in Li–S batteries. The achieved outcomes include a commendable reversible capacity of  $453 \text{ mA h g}^{-1}$ , remarkable Coulombic efficiency (~99.0%), and minimal capacity degradation (0.0033% per cycle) throughout 300 cycles. These findings underscore the substantial potential of this strategy for advancing high-performance Li–S batteries.<sup>181</sup>

Several studies have been reported on integrating TiN with carbon allotropes for the potential application in batteries. For example, Zeng *et al.* devised a straightforward approach for fabricating composite electrodes consisting of TiN and graphene.<sup>184</sup> This method involved the integration of ultrasonication with the melt-diffusion process of elemental sulfur. As a consequence, a composite structure exhibiting porosity was obtained, thereby leading to enhanced electrical conductivity. The Li–S batteries utilizing different composites of TiN (with different morphology such as nanotubes and nanoparticles) and graphene demonstrated specific capacitance of 1229 and 1085  $\text{mA h g}^{-1}$ , respectively, outperforming pure TiN nanostructures. By optimizing the TiN nanotube to graphene ratio, the best 1:1 TiN/graphene ratio exhibited a high-capacity retention of 87.5% after 180 cycles. This 3D hybrid structure balances specific capacity and electrochemical stability, enabling superior energy storage over an extended period. Li–S batteries exhibit considerable potential as a viable solution for future energy storage owing to their advantageous characteristics, including their



cost-effectiveness and high energy density. However, they suffer from issues such as slow reaction kinetics and capacity loss caused by the shuttle effect, which leads to poor performance over time. In a study conducted by Wang *et al.*, they developed a CNT@TiON/S electrode by incorporating oxidized TiN (TiON) onto carbon nanotubes (CNTs).<sup>182</sup> At a current rate of 0.2C, the electrode exhibited an initial discharge capacity of  $1044.9 \text{ mA h g}^{-1}$ , accompanied by an encouraging capacity retention rate of approximately 80.6% following 100 cycles (see Fig. 14(a and b)).

In pursuit of enhanced cycle stability and reversibility within Li-S batteries, Chen *et al.* achieved successful synthesis of a composite material by combining TiN nanoparticles with N-doped graphene through a hydrothermal reaction.<sup>185</sup> As a cathode in Li-S batteries, this composite material exhibited marked advancements in both cycling stability and reversibility. The incorporation of TiN nanoparticles and N dopants into graphene amplified the electrochemical conversion of lithium polysulfides ( $\text{LiPS}_x$ ), yielding improved reaction kinetics and curbing the shuttle effect. Consequently, the system's reversible capacity witnessed a substantial elevation, reaching an impressive  $1390 \text{ mA h g}^{-1}$ . Furthermore, the rate capability demonstrated enhancement to  $860 \text{ mA h g}^{-1}$ , while the enduring cycling performance showcased capacity retention of  $730 \text{ mA h g}^{-1}$  after 300 cycles. These enhancements are notably superior when compared to the  $\text{TiO}_2@\text{rGO/S}$  system. Cao *et al.* successfully synthesized 2D mesoporous B, N co-doped carbon/TiN (BNC-TN) composites through a hydrogel method, demonstrating adjustable doping levels and TiN content, as well as alleviating the shuttle effect in Li-S batteries.<sup>186</sup> The cathode composed of S@BNC-TN showcased an impressive initial discharge capacity of

$1130.9 \text{ mA h g}^{-1}$  under a current rate of 0.2C, with a commendable capacity retention rate of 84.1% following 50 cycles, showcasing its potential in addressing challenges in Li-S battery technology. In their recent study, Wang and colleagues pursued the creation of carbon-free sulfur hosts geared towards flexible Li-S batteries.<sup>170</sup> Their efforts yielded the successful fabrication of thin films composed of carbon-free titanium nitride nanobelts (TiN-NB) featuring flexible, conductive, and hierarchically porous architectures. These designs facilitated the establishment of sulfur electrodes boasting high-sulfur-loading and elevated-energy-density attributes. The initial electrode capacity was gauged at  $1436.7 \text{ mA h g}^{-1}$  for a sulfur loading of  $1.0 \text{ mg cm}^{-2}$ . Impressively, the electrodes maintained a reversible capacity of  $1032.6 \text{ mA h g}^{-1}$  after 150 cycles at 0.5C. Furthermore, they exhibited a discharge capacity of  $403.1 \text{ mA h g}^{-1}$  after 50 cycles at a high sulfur loading of  $7.1 \text{ mg cm}^{-2}$  at 0.1C. These findings address the significant challenge of enhancing sulfur content and loading in Li-S batteries while maintaining energy density (see Fig. 14(c–e)).

In a similar work, Liu *et al.* prepared a novel TiN composite anode coated with 2D carbon nanosheets (TiN@C) for sodium-ion batteries to enhance their cycling stability and specific capacity, demonstrating a high reversible capacity of  $170 \text{ mA h g}^{-1}$  and excellent cycling stability with  $149 \text{ mA h g}^{-1}$  retained after 5000 cycles at a current density of  $0.5 \text{ A g}^{-1}$  and  $1 \text{ A g}^{-1}$ , respectively, opening new possibilities for metal nitride anodes in energy conversion and storage applications.<sup>187</sup>

**Bottom of form.** In a different study, Zhang *et al.* attempted to enhance the performance of Si anodes in LIBs.<sup>188</sup> They proposed a novel approach where Si nanoparticles are coated

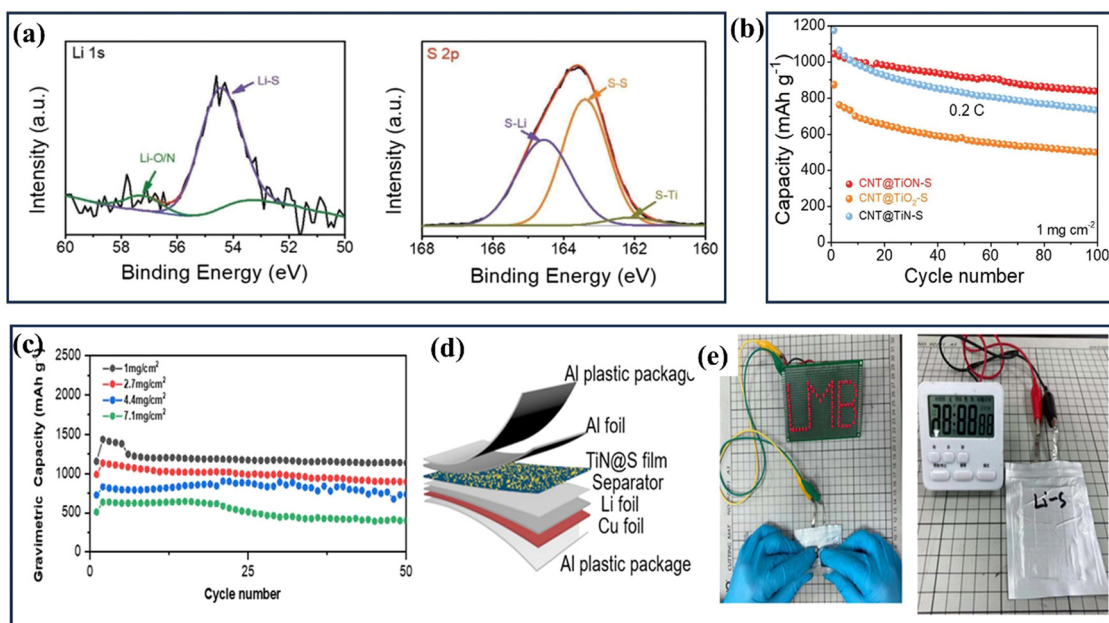


Fig. 14 (a) The detailed Li 1s and S 2p XPS spectra of CNT@TiON/Li<sub>2</sub>S<sub>6</sub> are illustrated; (b) cycling performance of CNT@TiON-S, CNT@TiO<sub>2</sub>-S, and CNT@TiN-S at 0.2C is illustrated (reproduced from ref. 182 with permission). (c) Cycling performance data for TiN-900@S cathodes with various sulphur loadings. (d) This diagram illustrates the TiN-900@S//Li pouch cell. (e) Photographs showcasing the operation of a timer activated by a Li-S battery pouch (on the right) and a collection of LED lamps illuminated by a Li-S battery pouch (on the left) (reproduced from ref. 183 with permission).



with TiN in a yolk–shell structure, addressing volume expansion issues and enhancing the performance of Si anodes in LIBs. The TiN coating accommodates volume expansion, promotes stable solid electrolyte interphase (SEI) formation, and ensures efficient charge transfer. The yolk–shell Si@TiN nanoparticles displayed an excellent conductivity of  $4 \times 10^4$  S cm $^{-1}$ , an impressive capacity of 2047 mA h g $^{-1}$  at 1000 mA g $^{-1}$  after 180 cycles. Further, Si@TiN nanoparticles displayed improved rate performance and suppressed volume expansion compared to pure Si nanoparticles. The present study exhibits considerable potential in augmenting Si anodes within forthcoming iterations of LIBs.

In recent years, iron-chromium redox flow batteries have gained significant interest due to their low cost. To enhance the electrochemical activity of the Cr $^{3+}$ /Cr $^{2+}$  redox couples in these batteries, researchers have explored the integration of TiN nanorods and nitrogen-doped porous graphitic carbon hybridized with oxygen-doped titanium nitride (O-TiN@N-PGC) as electrode materials. Recently, Liu *et al.* (2023) developed a binder-free composite electrode by growing TiN nanorods arrays on 3D graphite felt.<sup>189</sup> This composite electrode exhibited improved electrochemical activity, leading to a significant increase in maximum power density (427 mW cm $^{-2}$ , 74.0% higher compared to TiN nanoparticles). The electrode also demonstrated excellent coulombic efficiency (93.0%), voltage efficiency (90.4%), and energy efficiency (84.1%) at a current density of 80 mA cm $^{-2}$ . Notably, the electrode maintained stability during cycle tests, highlighting its potential for iron-chromium redox flow batteries. In another recent report, Sun *et al.* used a one-pot synthesis method to successfully synthesize nitrogen-doped porous graphitic carbon (O-TiN@N-PGC), a hybrid material composed of nitrogen-doped PGC and O<sub>2</sub>-doped TiN.<sup>190</sup> Outstanding performance in Li–S batteries was attributed to this composite material's remarkable chemisorption and electrocatalytic performance within sulfur cathodes. Noteworthy attributes of high specific capacity (1408 mA h g $^{-1}$  at 0.1C), impressive rate capacity (604 mA h g $^{-1}$  at 4C), and enduring cycling stability (513 mA h g $^{-1}$  after 1000 cycles at 0.5C) were demonstrated by Li–S cells utilizing O-TiN@N-PGC as their sulfur host. In addition, despite a high sulfur loading of 5.7 mg cm $^{-2}$ , a remarkable areal capacity of 7.6 mA h cm $^{-2}$  was observed. This study presents a prospective approach to incorporate metal nitrides into porous carbons, thereby creating potential avenues for advancements in modern energy technologies.

These studies highlight the significant contributions of TiN-based materials in advancing the performance of iron-chromium redox flow batteries and lithium–sulfur batteries. Integrating TiN nanostructures with other potential materials for making composites offers improved electrochemical activity, stability, and efficiency, paving the way for developing more efficient and reliable energy storage technologies.

### 3.3. Electrocatalysis

**3.3.1. Hydrogen evolution reaction (HER).** Hydrogen is acknowledged as an eco-friendly substitute for conventional fossil fuels owing to its elevated energy density and minimal ecological footprint.<sup>191</sup> Researchers are focusing on the hydrogen

evolution reaction (HER) as a cost-effective method for large-scale hydrogen production.<sup>192</sup> The utilization of electrode materials is of paramount importance in augmenting the efficiency of HER systems. TiN has been recognized as a highly efficient catalyst owing to its exceptional electrical conductivity and corrosion-resistant properties. Their comparable performance to noble metal-based catalysts makes them an attractive option for advancing HER technology and promoting sustainable energy solutions. Initiative for utilizing TiN as an electrocatalyst for HER was taken by Yujie Han and his colleagues.<sup>193</sup> They used the chemical vapor deposition (CVD) technique to synthesize single-crystalline TiN nanowires (TiN NWs) directly. In a first-of-its-kind experiment, these nanowires were tested as catalysts for the HER. The electrochemical tests demonstrated that the TiN NWs exhibited excellent HER performance, with a low overpotential of 92 mV at a current density of 1 mA cm $^{-2}$  and a Tafel slope of 54 mV dec $^{-1}$ . Additionally, the current density hardly changed after 20 000 cycles and a 100 h durability test in acidic environments, demonstrating the exceptional chemical stability of the produced TiN NWs for HER applications. This work presents a comparative analysis of various electrodes' HER activities, including bare glassy carbon electrodes, commercially available bulk TiN, and conventional Pt/C electrocatalysts (see Fig. 15). The improved performance of TiN nanowires can be attributed to their smaller charge transfer resistance ( $R_{ct}$ ) and increased number of active surface sites, resulting in enhanced HER performance compared to bulk TiN.

A composite material named MoS<sub>2</sub>/TiN was fabricated by Yu *et al.* and utilized as a highly efficient electrocatalyst for the HER activity.<sup>194</sup> They first grew a layer of TiN on carbon cloth through hydrothermal deposition of TiO<sub>2</sub> followed by nitridation using NH<sub>3</sub> gas. Then, they hydrothermally coated MoS<sub>2</sub> on the TiN layer. In an acidic solution, the MoS<sub>2</sub>/TiN catalyst exhibited a low overpotential of 146 mV at a current density of 10 mA cm $^{-2}$ . This composite structure allowed for rapid electron transfer, elevated surface-active sites, and enhanced ion diffusion, contributing to its improved performance in the HER. Wang *et al.* developed an advanced electrocatalyst for the HER by fabricating Pt-anchored TiN nanorods (Pt/TiN NRs).<sup>195</sup> The Pt/TiN nanorods displayed remarkable HER performance, with overpotentials of 139 mV and 39.7 mV at a current density of 10 mA cm $^{-2}$  in alkaline and acidic environments. Under acidic conditions, the performance of Pt/TiN NRs was found to be comparable to that of the standard Pt/C electrocatalyst. Still, they showcased superior stability, retaining 91.6% of the current after 60 h in 0.5 M H<sub>2</sub>SO<sub>4</sub>, compared to Pt/C's 46.9% retention after 30 h of cycling. The remarkable performance of the Pt/TiN NRs can be ascribed to their large surface area and the synergistic effect between the Pt and TiN nanorods. Furthermore, Peng *et al.* developed an advanced HER electrocatalyst called Ni–FeP/TiN/CC.<sup>196</sup> This catalyst, consisting of hierarchically structured Ni-doped FeP on TiN nanowires and graphitic carbon fibers (CC), exhibited exceptional performance. It demonstrated a low overpotential of 75 mV at 10 mA cm $^{-2}$  and excellent stability for more than 10 h of continuous cycling. The exceptional HER performance of the catalyst was attributed to the significant surface area made possible by the presence of



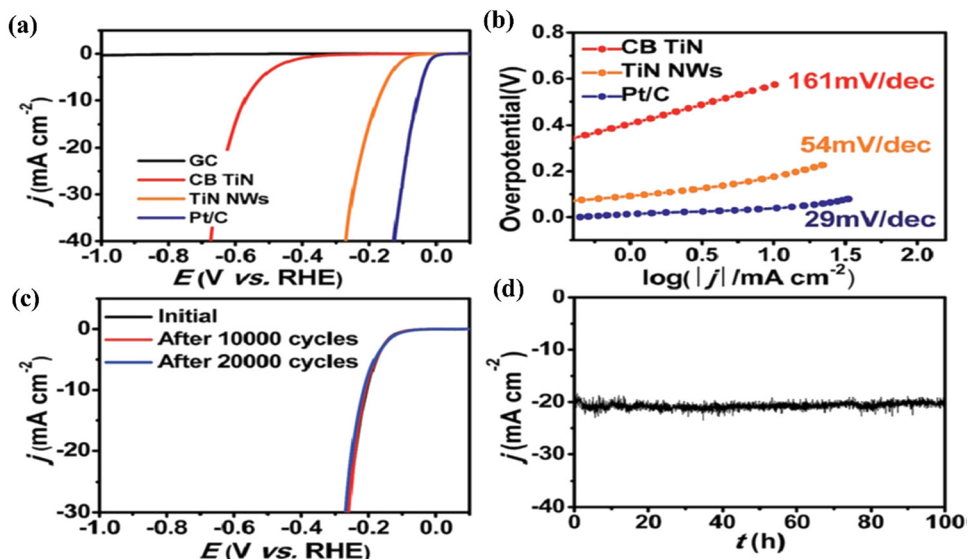


Fig. 15 (a) Represents polarization curves for the hydrogen evolution reaction (HER); (b) showcases Tafel plots. These comparisons encompass bare GC electrodes, TiN nanowires, commercially available bulk TiN, and Pt/C electrodes, all examined in a 1 M  $\text{HClO}_4$  environment; (c) highlights  $J$ – $E$  curves for TiN nanowires pre and post 10 000 and 20 000 potential cycles in a stability assessment; (d) provides insight into the current density pattern during a 100-hour electrolysis, maintained at a constant overpotential of 240 mV (reproduced from ref. 193 with permission).

nickel (Ni) and iron (Fe) atoms in Ni–FeP. Furthermore, the presence of these atoms also played a role in forming active sites located at the edges, thereby augmenting the HER activity. In a different study, Shanker *et al.* successfully developed a catalyst with exceptional performance for the HER activity using nitrogen-doped graphene and TiN nanocrystals (TiN–NFG).<sup>197</sup> The fabrication process and surface characteristics of TiN–NFG (see Fig. 16(a–c)). Incorporating TiN in the TiN–NFG nanocomposites

resulted in an abundance of electrons, enhancing electrical conductivity. The N-doped graphene (NFG) also improved charge transfer and increased the available surface area. As a result, the TiN–NFG nanocomposites displayed remarkable HER performance, achieving an overpotential of 161 mA at 10  $\text{mA cm}^{-2}$ .

In 2020, Zhang *et al.* successfully produced systematically arranged arrays of Nb–TiN nanotubes (NNAs) on Nb–Ti alloy panels by implementing an anodization and nitridation technique.<sup>198</sup> The

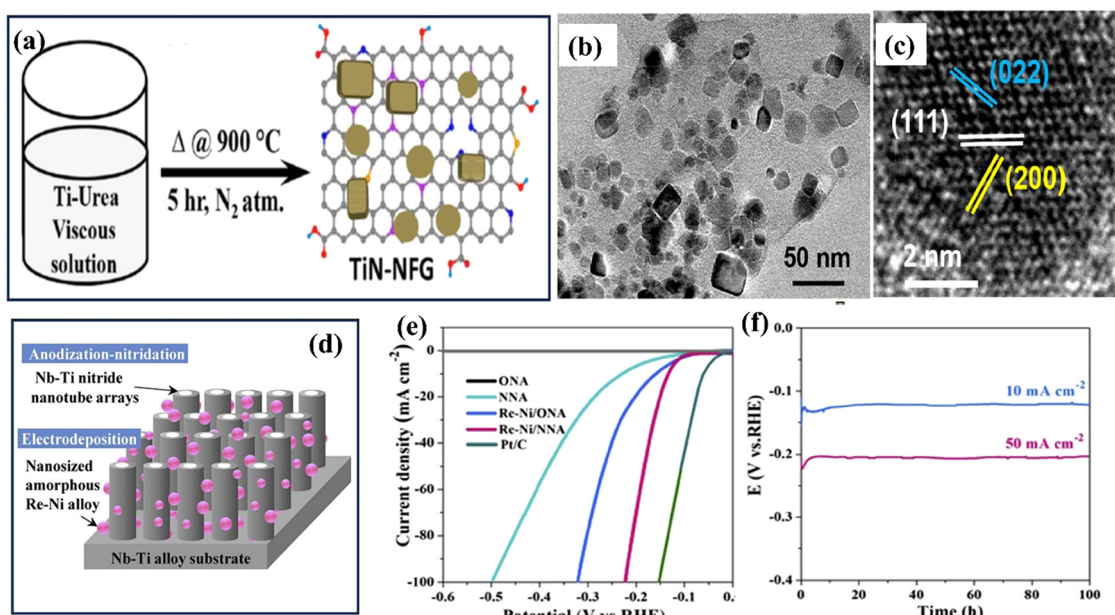


Fig. 16 (a) Synthesis of TiN–NFG represented schematically; (b) TEM; (c) HRTEM images of TiN–NFG (reproduced from ref. 197 with permission). (d) Nanoscale amorphous Re–Ni alloy electrodeposited on Nb–Ti NNA support; (e) LSV curves for the Nb–Ti ONA, NNA, Re–Ni/ONA, and Re–Ni/NNA in 1 M KOH; (f) chronopotentiometric responses of Re–Ni/NNA at current density of 10 and 50  $\text{mA cm}^{-2}$  in 1 M KOH for 100 h (reproduced from ref. 198 with permission).



NNA architecture comprised  $\text{Nb}_4\text{N}_5$  and TiN, providing notable benefits such as enhanced hydrophilicity, corrosion resistance, and improved conductivity. The researchers then created a Re–Ni/NNA composite electrode by electrodepositing a nanostructured Re–Ni alloy over the NNA support. The electrochemical experiments demonstrated that the Re–Ni/NNA composite electrode exhibited a current density of  $50 \text{ mA cm}^{-2}$  when tested in a  $1.0 \text{ M KOH}$  solution at a potential of  $-0.18 \text{ V}$  *vs.* RHE. Furthermore, the electrode displayed excellent stability for more than 100 h. The enhanced performance of the HER can be attributed to the synergistic effect of Re–Ni particles and the Nb–Ti NNA support, which results in increased catalytic activity and decreased charge transfer resistance (see Fig. 16(d–f)).

Furthermore, in the same year, to reduce platinum (Pt) usage in electrocatalysts for HER activities, Zhao *et al.* developed mesoporous TiN nanotube arrays (TiN NTAs) as a substrate for Pt loadings in small quantities.<sup>91</sup> TiN NTAs were synthesized through the thermal treatment of  $\text{TiO}_2$  NTAs in the  $\text{NH}_3$  atmosphere. The platinum (Pt) species that were dissolved from the platinum counter electrode underwent redeposition on mesoporous TiN NTAs, leading to the formation of Pt–TiN NTAs with an extremely low platinum loading of  $8.3 \text{ }\mu\text{g cm}^{-2}$ . The Pt–TiN NTAs demonstrated a mass activity that was 15 times greater than 20 wt% Pt/C. This enhanced performance was observed at an overpotential of  $71 \text{ mV}$  *vs.* RHE while maintaining a current density of  $10 \text{ mA cm}^{-2}$ . The Tafel slope, a measure of the electrochemical reaction kinetics, was determined to be  $46.4 \text{ mV dec}^{-1}$ . Furthermore, the Pt–TiN NTAs exhibited exceptional stability under experimental conditions. The mesoporous structure facilitated electron and mass transfer, outperforming non-mesoporous nanotube arrays with deposited Pt species.

Recently, Yang *et al.* presented a successful approach for creating an HER catalyst by loading ruthenium nanorods (Ru NRs) onto a TiN support, utilizing the strong metal–support interaction (SMSI) effect.<sup>76</sup> The Ru NRs/TiN catalyst demonstrated outstanding performance, including high activity, long-term stability, and accelerated hydrogen evolution kinetics in alkaline environments. The porous and hollow structure of the tube assembled with TiN nanosheets played a pivotal role in attaining noteworthy mass activity for the HER and enhanced turnover frequency values, despite utilizing a low amount of Ru. More recently, Chandrasekaran *et al.* developed a catalytic site-rich hybrid nanostructure composed of TiN decorated on graphitic carbon nitride ( $\text{g-C}_3\text{N}_4$ ) using a straightforward ultrasonication technique.<sup>199</sup> The TiN/ $\text{g-C}_3\text{N}_4$  hybrid showed excellent bifunctional activity, with an overpotential of  $-0.35 \text{ V}$  for the HER and  $0.32 \text{ V}$  for the OER at  $10 \text{ mA cm}^{-2}$  current density. The hybrid material demonstrated a notable increase in electrical conductivity due to the synergistic interaction between TiN and graphitic carbon nitride ( $\text{g-C}_3\text{N}_4$ ). The inclusion of  $\text{g-C}_3\text{N}_4$  offered structural reinforcement to TiN, while the existence of nitrogen atoms in both substances contributed to the creation of supplementary catalytic sites that facilitated efficient electron transport during water splitting.

The studies mentioned above have shown that TiN-based catalysts can achieve competitive HER performance compared to traditional catalysts, such as Pt and other transition

metal-based materials. The unique combination of TiN's conductivity, surface chemistry, and stability allows it to efficiently catalyze the HER, enabling the production of hydrogen gas with high efficiency and low overpotential. However, it is important to note that further research is still ongoing to fully understand the underlying mechanisms and optimize the performance of TiN-based catalysts for HER. Scientists are exploring various synthesis methods, catalyst morphologies, and surface modifications to enhance the catalytic activity, selectivity, and durability of TiN in HER systems. With continued research and development, TiN-based catalysts have the potential to contribute significantly to the advancement of hydrogen-related technologies and the realization of a sustainable energy future.

**3.3.2. Oxygen evolution reaction (OER).** Developing efficient and affordable electrocatalysts for the oxygen evolution reaction (OER) is of utmost importance in numerous renewable energy applications, such as water splitting, metal–air batteries, and electrolyzers.<sup>200,201</sup> TiN has emerged as a highly effective electrocatalyst for the OER, a crucial process in electrochemical water splitting for sustainable energy generation. TiN is an appealing option due to its unique features, which include excellent electrochemical stability, high electrical conductivity, and cost-effectiveness compared to noble metal catalysts. The OER, which involves converting water into molecular oxygen, requires effective electrocatalysts to minimize energy barriers and increase reaction rates. TiN's exceptional conductivity allows for quick electron transport, reducing energy losses during the process.<sup>199,202</sup>

TiN's tunable surface properties, high surface area, and excellent durability also contribute to its catalytic efficiency and long-term stability. Its resistance to corrosion and disintegration, even under extreme conditions, adds to its practicality.<sup>202</sup> Furthermore, TiN may be synthesized using scalable processes, allowing for large-scale manufacturing. Ongoing research aims to improve TiN's catalytic performance by alloying, doping, and enhanced characterization methods. TiN has enormous promise in realizing a greener and more efficient future due to its ability to drive sustainable energy solutions. In this context, Zhang *et al.* presented a novel water-splitting device utilizing hierarchical TiN@ $\text{Ni}_3\text{N}$  nanowire arrays inspired by *Myriophyllum*, demonstrating exceptional performance as both HER and OER catalysts.<sup>203</sup> The TiN@ $\text{Ni}_3\text{N}$  nanowire arrays exhibited a low onset overpotential of  $15 \text{ mV}$  *vs.* RHE for HER and high stability, showing less than 13% degradation after 10 h of operation (see Fig. 17(a–e)). For OER, the nanowire arrays displayed an onset potential of  $1.52 \text{ V}$  *vs.* RHE. They retained 72.1% of the current after 16 h of operation, enabling the assembly of a symmetric water splitting device with a water splitting onset of approximately  $1.57 \text{ V}$  and current retention of 63.8% after 16 h. Guo *et al.* successfully constructed an efficient and durable OER electrocatalyst, TiN@ $\text{Co}_{5.47}\text{N}$ , through plasma nitriding and ALD  $\text{Co}_x\text{N}$  process, demonstrating impressive electrocatalytic performance and long-term stability.<sup>204</sup> At a current density of  $50 \text{ mA cm}^{-2}$ , the overpotentials for the oxygen evolution reaction (OER) stand at  $398 \text{ mV}$ ,  $248 \text{ mV}$ , and  $411 \text{ mV}$  in acidic, basic, and neutral electrolytes. Impressively, the material showcases consistent catalytic activity over 1500 hours, with just a marginal 1.3% rise in



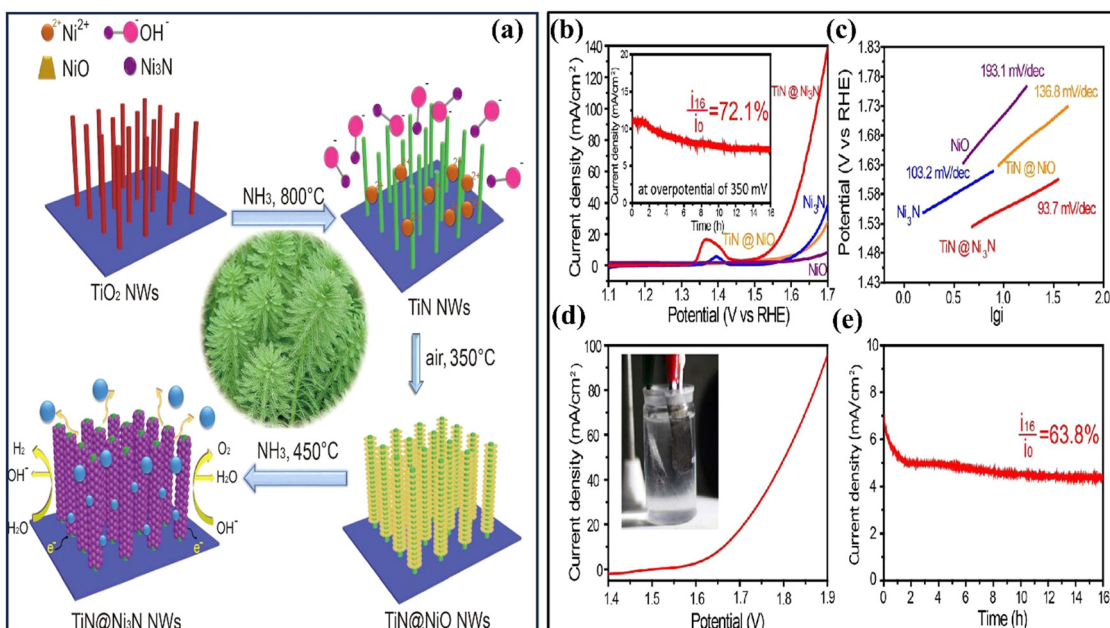


Fig. 17 (a) Schematic depiction of the synthesis and manufacturing process of TiN@Ni<sub>3</sub>N nanowire arrays on Ti foil; (b) linear sweep voltammetry (LSV) polarization curves, and (c) corresponding Tafel plots for TiN@Ni<sub>3</sub>N, Ni<sub>3</sub>N, TiN@NiO, and NiO catalysts within a 1 M KOH electrolyte, employing a scan rate of 5 mV s<sup>-1</sup>. The inset in panel (b) illustrates the potentiostatic measurement of TiN@Ni<sub>3</sub>N nanowire arrays at an overpotential of 350 mV; (d) polarization curves for the symmetric water splitting device in a 1 M KOH solution; (e) potentiostatic measurement of a water splitting device utilizing a TiN@Ni<sub>3</sub>N nanowire two-electrode water splitting system at a potential of 1.62 V within a 1 M KOH medium (reproduced from ref. 203 with permission).

overpotential. This heightened OER performance is attributed to the harmonious electronic interplay between TiN and atomic layer deposition (ALD) Co<sub>5.47</sub>N. Additionally, the formation of a CoTi layered double hydroxides layer at the interface/surface of TiN@Co<sub>5.47</sub>N during the electrocatalytic process contributes to this enhanced efficiency. This study provides additional evidence regarding the potential of TiN in the realm of OER electrocatalysts.

In a pioneering work by Zhang *et al.* a support-type composite catalyst, TiN/IrO<sub>2</sub>, was synthesized using a colloidal method.<sup>205</sup> The catalyst exhibited ultra-fine nanoclusters of IrO<sub>2</sub> dispersed on the TiN support, resembling the arrangement of strawberry seeds. The distinctive configuration of this structure resulted in an increased active surface area and greater exposure of unsaturated Ir atoms on the surface. Consequently, the catalytic performance of the OER in acid electrolytes was significantly enhanced. The TiN/IrO<sub>2</sub> catalyst, with an IrO<sub>2</sub> loading of 31 wt%, demonstrated an impressive mass-normalized OER activity of 874.0 A g<sup>-1</sup> (IrO<sub>2</sub>) at a potential of 1.6 V, approximately five times higher than unsupported IrO<sub>2</sub>. The exceptional performance of this composite catalyst, combining the advantages of TiN support and ultra-fine IrO<sub>2</sub> nanoclusters, showcases the groundbreaking work of researchers in developing efficient electrocatalysts for OER applications. In another work, Bele *et al.* developed an inexpensive, oxygen-evolution catalyst by synthesising a thin-film composite electrode with a unique morphology, ultralow iridium loading, and high stability.<sup>206</sup> The composite electrode, consisting of a TiO<sub>2</sub> nanotubular film subjected to nitridation and efficient immobilization of iridium nanoparticles, exhibits high OER activity and remarkable stability. The electrode's exceptional durability can be attributed to the self-passivation phenomenon occurring on the

titanium oxynitride (TiON) surface, which forms a protective layer of TiO<sub>2</sub>. This TiO<sub>2</sub> layer effectively incorporates the iridium nanoparticles and ensures electrical connectivity. The TiON layer's nitrogen atoms suppress iridium nanoparticle growth, contributing to enhanced durability. Advanced electrochemical characterizations provide valuable insights into the thin film's morphological, structural, and compositional aspects, making this research significant in electrocatalysis and other fields.

In a similar work, Pan *et al.* fabricated a highly efficient bifunctional electrocatalyst for the CO<sub>2</sub> reduction reaction (CO<sub>2</sub>RR) and the OER, utilizing Cu–Ni alloy electrodeposited onto TiN NPs on carbon mesh, resulting in enhanced catalytic activity.<sup>207</sup> The bifunctional system exhibits a high level of durability, maintaining a stable performance for a period of 24 h at an overpotential of 670 mV with a current density of 2 mA cm<sup>-2</sup>, producing 19.1% CO and 6.7% formate as CO<sub>2</sub>RR products and showing significantly improved catalysis due to preferential deposition of Cu–Ni on TiN as observed through cyclic voltammetry and X-ray diffraction studies, respectively. Recently, Chandrasekaran and colleagues fabricated a hetero nanostructure composed of TiN and graphitic carbon nitride (g-C<sub>3</sub>N<sub>4</sub>) through ultrasonication.<sup>199</sup> The hybrid material demonstrated dual functionality in the HER and OER, with an overpotential of  $-0.35$  V and 0.32 V, respectively. The enhanced electrical conductivity of the composite could be due to the combined effect of metal nitride and carbonaceous material. Both materials contain nitrogen atoms that serve as additional catalytic sites for electron transport during water-splitting.

The aforementioned studies have demonstrated that TiN-based catalysts exhibit comparable performance in the OER

when compared to conventional catalysts, such as iridium oxide ( $\text{IrO}_x$ ) and ruthenium oxide ( $\text{RuO}_x$ ). The distinctive amalgamation of TiN's electrical conductivity, chemical stability, and surface characteristics endow it with the capability to serve as an efficient catalyst for the OER, facilitating the generation of oxygen gas with notable efficiency and minimal overpotential. Nevertheless, it is imperative to acknowledge that additional investigations are being conducted to comprehensively comprehend the fundamental mechanisms and enhance the efficiency of TiN-based catalysts for the OER. Researchers are investigating different approaches to improve the catalytic activity, selectivity, and durability of TiN in OER systems. These approaches include exploring various synthesis methods, catalyst morphologies, and surface modifications.

**3.3.3. Oxygen reduction reaction (ORR).** The oxygen reduction reaction (ORR) plays a vital role in diverse energy conversion applications, such as fuel cells and metal-air batteries.<sup>208</sup> The enhancement of performance and affordability of energy systems necessitates the development of electrocatalysts for ORR that are both efficient and cost-effective. TiN exhibits several advantageous characteristics that make it a desirable electrocatalyst for ORR. It possesses high electrical conductivity, enabling efficient charge transfer during the ORR process. Moreover, TiN demonstrates remarkable stability and resistance to harsh conditions, making it a durable catalyst for long-term operation.<sup>209,210</sup> The strong metal–support interaction between TiN and active species further enhances its catalytic performance by promoting favorable surface reactions and preventing catalyst degradation.<sup>211</sup> In a groundbreaking study, Avasarala *et al.* introduced TiN, synthesized through a polyol process, as a supportive material for Pt-based catalysts in the ORR. TiN was chosen for its excellent electrical conductivity and remarkable oxidation and acid corrosion resistance.<sup>212</sup> Later, Pan *et al.* presented findings on a durable non-carbon catalyst that utilized TiN nanotubes (TiN NTs) as a supporting material for platinum (Pt).<sup>213</sup> The catalyst exhibited remarkable performance and stability in the ORR, as demonstrated by the accelerated durability test (ADT). Notably, the catalyst retained 77% of its initial electrochemically active surface area even after undergoing 12 000 ADT cycles, surpassing the performance of the commercially available Pt/C (E-TEK) catalyst. The observed empirical data strongly supports a notable interaction between platinum nanoparticles and the TiN nanotubes (NTs) support. The TiN NTs' surface exhibited dendrite nanocrystals, which acted as effective agents for capturing and revitalizing dissolved platinum species. This mechanism effectively curtailed the loss and migration of platinum nanoparticles. This innovative approach paves the way for designing TiN NT-supported catalysts with enhanced performance and potential applications in various energy conversion processes.

In the succeeding year, Yousefi *et al.* successfully synthesized TiN–carbon nanocomposites through a supercritical benzene medium, investigated their electrocatalytic properties for the ORR under different heating conditions and identified the sample heat-treated under  $\text{NH}_3$  atmosphere at 1000 °C for 10 h as the most promising catalyst with significantly enhanced ORR activity, reduced  $\text{H}_2\text{O}_2$  production, and improved stability

attributed to its unique carbon structure, nitrogen and oxygen doping, and higher electrochemical surface area.<sup>214</sup> Creating an effective and durable catalyst for commercializing fuel cells is challenging. To address this, a simple method is suggested by Zheng *et al.* to produce 3D TiN with interconnected nanowire assemblies, forming a porous structure.<sup>215</sup> This structure promotes efficient electron transfer, offers many accessible active sites, and enhances the interaction between the catalyst and electrolyte. The research presents a prospective method to enhance ORR performance and longevity by utilizing a distinctive corrosion-resistant configuration coupled with a robust metal–support interaction. The resulting Pt/TiN catalyst exhibits unusual activity and stability, with experimental evidence highlighting the crucial role of innovative TiN support. Tian *et al.* have effectively devised a straightforward hydrothermal technique for the synthesis of hierarchical tubular structures composed of metal nitride nanosheets.<sup>216</sup> Among various assemblies, one particular assembly,  $\text{Ti}_{0.8}\text{Co}_{0.2}\text{N}$ , demonstrated noteworthy oxygen reduction activities in both acidic and alkaline fuel cells. Thus, this study introduces a potentially effective and adaptable method for developing and synthesizing stable and efficient binary nitride nanostructures, which hold promise for affordable applications in catalysis and energy conversion.

In 2019, Chen *et al.* conducted a study on utilising TiN hollow spheres (TiN HSs) as an electrocatalyst for the ORR.<sup>217</sup> They employed a carbon-template-assisted strategy to synthesize TiN HSs composed of TiN nanosheets. The researchers observed that the TiN HSs possessed a porous and uniform shell structure with a thickness of approximately 30 nm. Moreover, their investigation revealed that subjecting TiN HSs to heat treatment at 325 °C resulted in exceptional catalytic prowess for the ORR. Notably, TiN HSs-325 showcased an even more favorable onset potential of 0.85 V *vs.* RHE and an elevated limiting current density reaching 4.5 mA cm<sup>-2</sup>. These results underscore the significant promise held by hollow transition metal nitrides, exemplified by TiN HSs, as immensely effective catalysts not only for the ORR but also for diverse electrochemical devices. Later, Liu *et al.* successfully synthesized a facile *in situ* self-template strategy to construct a composite material, TiN/Fe–N–CNS, which exhibits outstanding ORR activity with a positive half-wave potential of 0.87 V, large limiting current density of 4.43 mA cm<sup>-2</sup>, high selectivity in alkaline media, enhanced stability, and improved methanol tolerance compared to commercial Pt/C catalyst.<sup>210</sup> The exceptional performance characteristics of the ORR can be attributed to the collaborative effect resulting from the uniform dispersion of TiN on Fe–N–CNS catalysts and the increased specific surface area.

In a different report, Al-Dhaifallah *et al.* reported a cost-effective and stable non-precious catalyst for fuel cells by preparing Co NPs composite with TiN on rGO, which exhibited a superior onset potential of 0.926 V *vs.* Ag/AgCl, surpassing the standard Pt/C catalyst, with an optimum Co and TiN ratio maximizing the ORR activity.<sup>32</sup> The catalyst exhibited no discernible reactivity towards methanol oxidation, thereby presenting itself as a potentially advantageous cathode catalyst for direct alcoholic fuel cells. Furthermore, it displayed remarkable



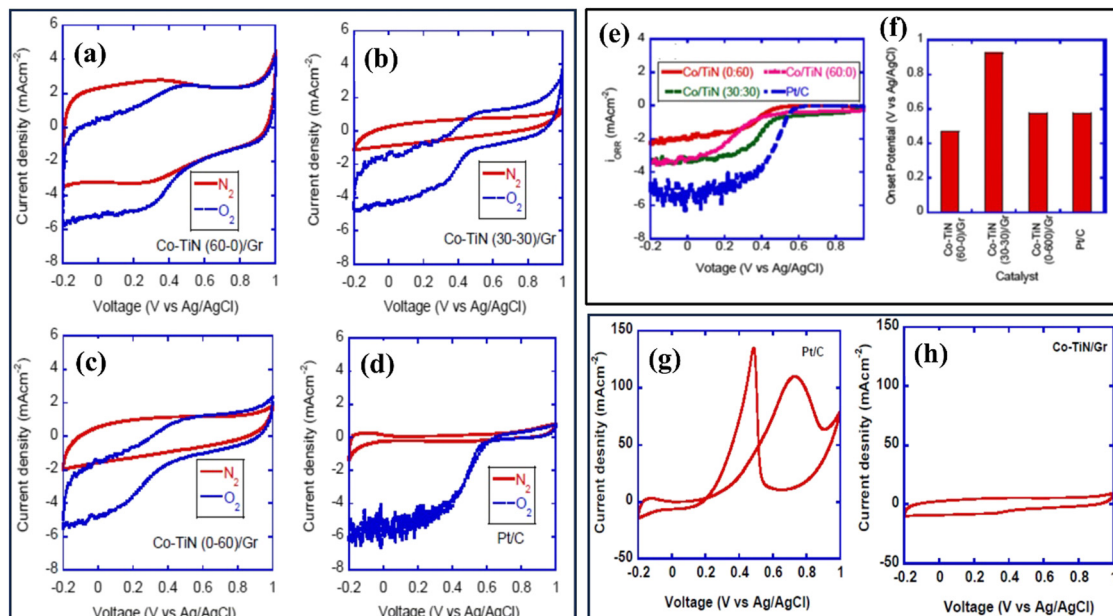


Fig. 18 Figures (a)–(d) display cyclic voltammograms of Co-TiN (60–0)/Gr, Co-TiN (30)/Gr, Co-TiN (0–60)/Gr, and Pt/C in  $N_2$  and  $O_2$  environments at  $200\text{ mL min}^{-1}$  flow rate, utilizing  $0.5\text{ M H}_2\text{SO}_4$  at  $5\text{ mV s}^{-1}$ . In (e), the calculated oxygen reduction current ( $i_{\text{ORR}}$ ) is represented, derived from the difference between the current under  $O_2$  and  $N_2$  flow. Panel (f) showcases the onset potential for oxygen reduction (ORR) across different samples – Co-TiN (60–0)/Gr, Co-TiN (30)/Gr, Co-TiN (0–60)/Gr, and Pt/C – at  $5\text{ mV s}^{-1}$ , employing  $0.5\text{ M H}_2\text{SO}_4$ . Cyclic voltammograms in (g) exhibit Pt/C and (h) Co-TiN/Gr in  $0.5\text{ M H}_2\text{SO}_4$  supplemented with  $0.5\text{ M}$  methanol at  $20\text{ mV s}^{-1}$  (reproduced from ref. 32 with permission).

durability, as evidenced by the absence of any decline in activity even after undergoing 1000 cycles, contrasting the 20% reduction in activity observed for Pt/C under identical operating conditions (see Fig. 18(a–h)). The improved catalytic effectiveness of the catalyst can be attributed to the cooperative interplay between TiN and Co. Yuan *et al.* successfully fabricated TiN nanospheres featuring dendritic surface structures, which were employed as carriers for platinum nanoparticles.<sup>218</sup> The catalyst exhibited remarkable performance in the ORR, demonstrating a mass activity of  $0.44\text{ mA g}^{-1}$  Pt and a specific activity of  $0.33\text{ mA cm}^{-2}$ . It exhibited improved stability by retaining 61% of its initial activity after undergoing 3000 cycles. The present study presents a potentially effective framework for developing catalysts with reduced platinum loading, which can exhibit prolonged durability. Numerous researchers are currently endeavouring to offer a feasible substitute for commercially available Pt/C catalysts in energy conversion devices. In this regard, Zheng *et al.* recently developed N-doped carbon-supported Fe-doped TiN NPs ( $\text{Ti}_{x}\text{Fe}_{1-x}\text{N/NC/C}$  catalyst) as an exceptional cathode catalyst for Zn-air batteries, outperforming the standard Pt/C catalysts.<sup>219</sup> The  $\text{Ti}_{0.95}\text{Fe}_{0.05}\text{N/NC/C}$  catalyst, which has been optimized, exhibits exceptional catalytic performance and stability in the ORR. This leads to enhanced power density and specific capacity identical to Pt/C catalysts. These improvements can be attributed to the incorporation of Fe dopant into the TiN lattice, which promotes the graphitization of carbon matrices. Additionally, optimising TiN nanoparticle size, modulation of the electronic structure and active sites, and reducing the barrier for the rate-determining step in the ORR contribute to the enhanced activity of the catalyst.

Consequently, the performance of Zn-air batteries is significantly improved. These findings highlight the potential of the  $\text{Ti}_{0.95}\text{Fe}_{0.05}\text{N/NC/C}$  catalyst as a promising alternative to commercially available Pt/C catalysts in energy conversion devices.

While TiN possesses some desirable properties like high conductivity and corrosion resistance, it lacks the necessary catalytic activity for efficient ORR performance. Catalysts commonly employed for the ORR include platinum (Pt) and other transition metal-based materials due to their high activity and selectivity towards the reaction. Efforts in the research community have primarily focused on developing alternative materials with improved ORR activity and durability. These materials often involve precious metals or transition metal-based catalysts with tailored surface structures, compositions, and nanostructures. It is worth mentioning that there have been studies exploring the potential use of TiN in other electrochemical reactions and energy storage applications, as discussed previously in the context of TiN-based supercapacitors and the hydrogen evolution reaction (HER).

### 3.4 Photovoltaic applications

TiN can be utilized in different components in solar cell applications to enhance device performance. TiN films can serve as efficient current collectors as a transparent conductive electrode, replacing traditional indium tin oxide (ITO) electrodes.<sup>220</sup> TiN offers superior conductivity, chemical stability, and lower sheet resistance, reducing energy losses and enhancing charge extraction efficiency.<sup>221</sup> Moreover, TiN-based electrode materials exhibit favorable light absorption properties, enabling efficient utilization of a broad range of solar wavelengths.<sup>222</sup> Furthermore, TiN can be



employed as a plasmonic material in solar cells, exploiting its localized surface plasmon resonance (LSPR) effect.<sup>223</sup> By incorporating TiN NPs or nanostructures, the light absorption and scattering within the active layer of the solar cell can be significantly enhanced, leading to improved photon absorption and light trapping.<sup>224</sup> Keeping this in mind, using a soft-template approach, Ramasamy *et al.* fabricated a structured TiN–carbon nanocomposite (TiN–C).<sup>225</sup> The resulting material exhibited a significant surface area of  $389\text{ m}^2\text{ g}^{-1}$  and possessed uniform hexagonal mesopores. The TiN–C nanocomposite outperformed platinum as a counter electrode (CE) material in dye-sensitized solar cells (DSSCs). Specifically, in an organic electrolyte system, DSSCs incorporating the TiN–C nanocomposite achieved a power conversion efficiency (PCE) of 6.71%, surpassing the efficiency of platinum at 3.32%. Likewise, within an iodide electrolyte environment, the integration of the OM TiN–C nanocomposite yielded a noteworthy 8% efficiency in DSSCs. The stellar performance of the TiN–C nanocomposite can be attributed to its orchestrated symphony of lowered charge transfer resistance, elevated electrical conductivity, a multitude of engaged active sites, and an augmented resilience within the organic electrolyte. Wang *et al.* successfully synthesized a porous TiN microspheres film on a titanium substrate through a hydrothermal technique and nitridation in the presence of  $\text{NH}_3$ , which not only displayed superior electrocatalytic activity for  $\text{I}_3^-$  reduction but also exhibited good electrical conductivity.<sup>226</sup> Utilizing this unique morphology as a CE in DSSCs led to an impressive PCE of 6.8% under  $100\text{ mW cm}^{-2}$  irradiation, surpassing the performance of cells using conventional Pt counter electrodes. Using TiN nanopatterned back electrodes, Magdi *et al.* showcased a notable advancement in organic solar cells by introducing a TiN nanopatterned back electrode, emerging as a cost-effective and abundant substitute for Ag. This innovative approach not only enhances the power conversion efficiency (PCE) but also holds the potential to expedite the commercialization of plasmonic organic solar cells.<sup>227</sup> The peak spectral response of TiN aligns with that of an Ag layer, occurring in the visible region at 550 nm. This similarity underscores TiN's efficacy in replicating the advantageous optical properties observed with traditional materials like silver.

In a research conducted by Li *et al.*, notable progress was achieved in elevating the efficiency of Cu (In, Ga)  $\text{Se}_2$  (CIGS) thin-film solar cells. This was accomplished by enhancing the adhesion, microstructure, and surface characteristics of the Mo films employed as back electrodes.<sup>228</sup> The researchers accomplished this feat by introducing a TiN diffusion barrier layer, expertly deposited through the process of reactive magnetron sputtering. The implementation of the TiN diffusion barrier layer proved to be highly beneficial, leading to improved cell efficiencies. This breakthrough finding suggests that the TiN/Mo bilayer design holds immense promise to enhance the overall efficiency of CIGS solar cells. The primary objective of the study was to investigate the influence of the TiN diffusion barrier layer on the physical characteristics of Mo back electrodes, specifically in the context of CIGS solar cell applications. By introducing the TiN layer, the researchers aimed to enhance the adhesion properties between the Mo film and the underlying

layers, as well as to improve the microstructure and morphology of the Mo film.

In contrast to noble metals, TiN is more affordable, abundant, and compatible with CMOS. Hence, Khezripour *et al.* suggested using a bilayer of Al–TiN nano square array to improve organic solar cells.<sup>231</sup> This technique leads to improved organic solar cells that exhibit heightened absorption rates ranging from 70% to 88% across the 300–625 nm spectrum. The enhancement is most pronounced at 665 nm, where the enhancement factor reaches a maximum of 2.16. Additionally, the photocurrent density experiences an augmentation, reaching  $13.7082\text{ mA cm}^{-2}$ . Under normal incidence, the suggested design is polarization insensitive and can potentially enhance other thin film solar cells. The exceptional photothermal conversion capabilities of TiN as a plasmonic nanofluid for solar energy harvesting applications are demonstrated by Wang *et al.* in their research. TiN significantly outperforms five conventional materials (carbon nanotubes, graphene, gold, silver, and copper sulphides) in terms of optical absorption characteristics, and the efficiency of converting light into heat is amplified due to the LSPR effect between Au and TiN NPs.<sup>232</sup> Further, the Au/TiN nanocomposite exhibited even higher optical absorption than TiN alone. Moreover, Au/TiN nanofluids with diverse amounts of Au showed superior temperature rise compared to TiN alone, demonstrating the beneficial effect of the dual LSPR on photo-thermal conversion performance.

In another study, to replace the Pt-based CEs in DSSCs, Gnanasekar *et al.* successfully synthesised TiN nanoflower buds (TiN NFBs), resulting in a PCE of 7.0%. This PCE value is marginally equivalent to the PCE achieved by Pt-based CE (7.4%) in DSSCs.<sup>229</sup> The TiN NFBs showed excellent catalytic activity towards the  $\text{I}^-/\text{I}_3^-$  electrolyte, favourable charge transport properties, and performance equivalent to the platinum electrode (see Fig. 19(a–c)). A 30-day stability investigation also demonstrated the TiN NFB CE-based DSSC's very stable performance and strong corrosion resistance against the  $\text{I}^-/\text{I}_3^-$  electrolyte, indicating the possibility of TiN NFBs as a practical substitute for Pt in large-scale DSSCs. In another study, Yi Di *et al.* created bifunctional TiN@Ni-MXene nanocrystals as an innovative catalyst for DSSCs.<sup>233</sup> By combining TiN's plasmonic properties to increase catalytic activity and utilising NIR light absorption to improve charge transfer, the researchers were able to achieve an impressive PCE of 8.45% under NIR irradiation and 8.08% under conventional irradiation conditions, outperforming the reference Pt-based DSSC with 7.59% efficiency, thus providing a promising approach for efficient utilization of wide-spectrum solar energy.

Recently, Mohamed *et al.* prepared  $\text{TiO}_2/\text{TiN}/\text{TiO}_2$  multilayer nanostructured films with mixed anatase and rutile phases of  $\text{TiO}_2$ .<sup>234</sup> The films showed tiny grains evenly spaced out and ranged in size from 5 to 9 nm. Thicker TiN layers have shown a lower refractive index and smaller real components of the dielectric constant but higher electrical conductivity. Increasing the thickness of the TiN layer resulted in a smaller optical band gap (3.32 eV to 3.01 eV) and more absorption between 650 and 1350 nm. The intensity of the photoluminescence was significantly reduced. These findings suggest that  $\text{TiO}_2/\text{TiN}/\text{TiO}_2$  multilayer films could be useful for solar energy harvesting due to their increased plasmonic



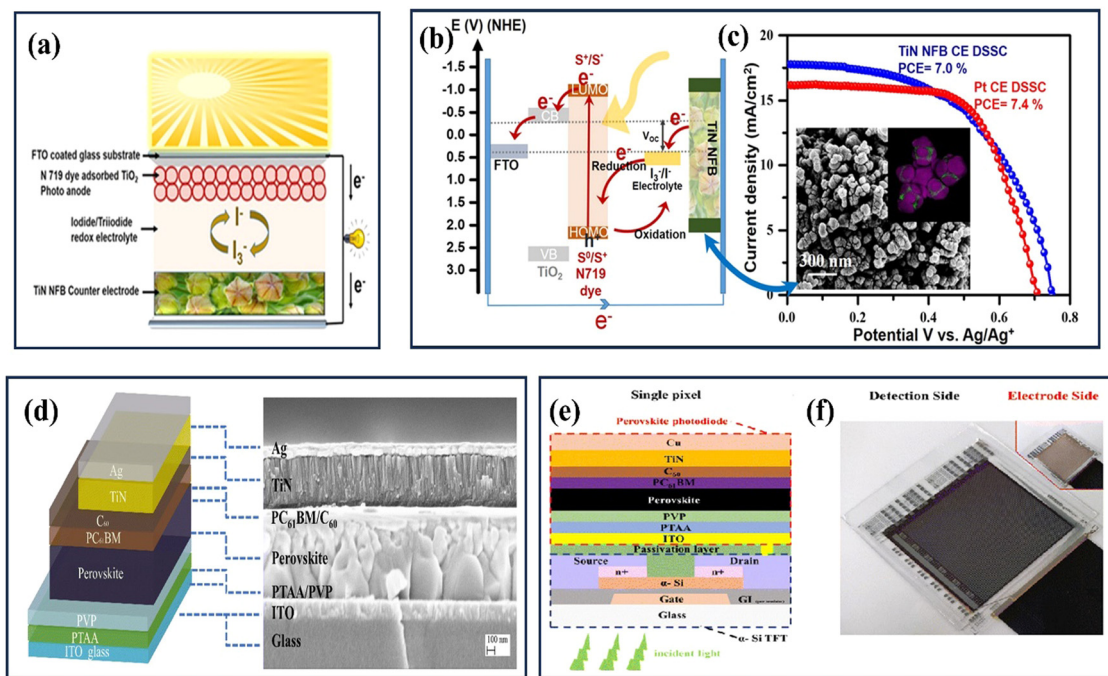


Fig. 19 (a) The illustration of the compiled DSSC featuring the TiN NFB CE; (b) a graphical representation of the energy band alignment within the DSSC constituents; (c) The  $J$ – $V$  traits of the DSSC unit embracing the TiN NFB CE and Pt CE (reproduced from ref. 229 with permission). (d) A cross-sectional SEM view capturing the essence of the TiN-based perovskite photodiodes; (e) schematic illustration of a single pixel of a perovskite photodiode; (f) image of the prepared TFT/perovskite photodetector array (reproduced from ref. 230 with permission).

characteristics, better absorbance, and reduced photoluminescence. More recently, Sun *et al.* examined the potential of utilizing a TiN layer as a stable electrode in a perovskite photodiode.<sup>230</sup> The researchers found that TiN-based photodiodes exhibited enhanced performance characterized by reduced dark current density and increased stability. These improvements can be attributed to the higher work function, hole-blocking capability, and permeation barrier properties of the TiN layer (see Fig. 19(d–f)). As a result, a photodetector was developed that exhibited a detectivity of  $1.21 \times 10^{14} \text{ cm W}^{-1} \text{ Hz}^{1/2}$ , a low dark current ratio (LDR) of 164 dB, and remarkable durability, as evidenced by a mere 5.73% attenuation after 576 000 light pulse cycles and 72% initial responsivity retention after 572 h of aging at a temperature of 85 °C. Overall, the application of TiN in solar cells holds great promise for achieving higher efficiency, improved stability, and cost-effective solutions for solar energy conversion. Ongoing research and development efforts are focused on optimizing TiN-based materials and device architectures to unlock the full potential of TiN in solar cell technologies. The diverse functions of TiN in photovoltaics underscore its adaptability and importance in elevating the effectiveness and productivity of solar cells. Ongoing exploration and innovation are directed towards refining TiN-related materials and methodologies, thereby playing a pivotal role in progressing towards more streamlined and economically viable solar energy conversion technologies.<sup>235</sup>

### 3.5 Biomedical implants

TiN is making remarkable strides in the field of biomedical implants, offering exceptional biocompatibility, durability, and performance. Its applications in biomedical implants are

revolutionizing the medical device industry and reshaping the future of patient care.<sup>236</sup> One of the key advantages of TiN is its seamless integration with the human body. It exhibits excellent biocompatibility, meaning it interacts harmoniously with living tissues and does not trigger adverse immune responses or rejection. This biocompatibility is crucial for successful implantation and long-term functionality.<sup>237</sup> In addition to its biocompatibility, TiN boasts remarkable mechanical strength. It is highly resistant to wear and corrosion, making it an ideal choice for orthopaedic implants that undergo repeated stress and friction within the body. The exceptional durability of TiN coatings ensures that implants can withstand the demanding mechanical conditions and maintain their functionality over extended periods.<sup>25</sup>

Furthermore, TiN demonstrates inherent antibacterial properties. Its surface has been shown to hinder the growth of bacteria, reducing the risk of infection around the implant site. This antibacterial characteristic is especially valuable for implants such as cardiovascular devices, where infections pose serious risks to patient health.<sup>238,239</sup> Integrating TiN into biomedical implants represents a significant advancement in the field. By leveraging TiN's unique properties, medical devices can provide safer, more reliable, and longer-lasting patient solutions. This translates into improved patient outcomes, reduced complications, and enhanced quality of life. For example, Subramanian *et al.* investigated the suitability of TiN, TiON, and TiAlN thin films prepared *via* reactive DC magnetron sputtering for biomedical applications.<sup>240</sup> They analyzed the coatings' chemical binding states, crystal structures, surface properties, corrosion



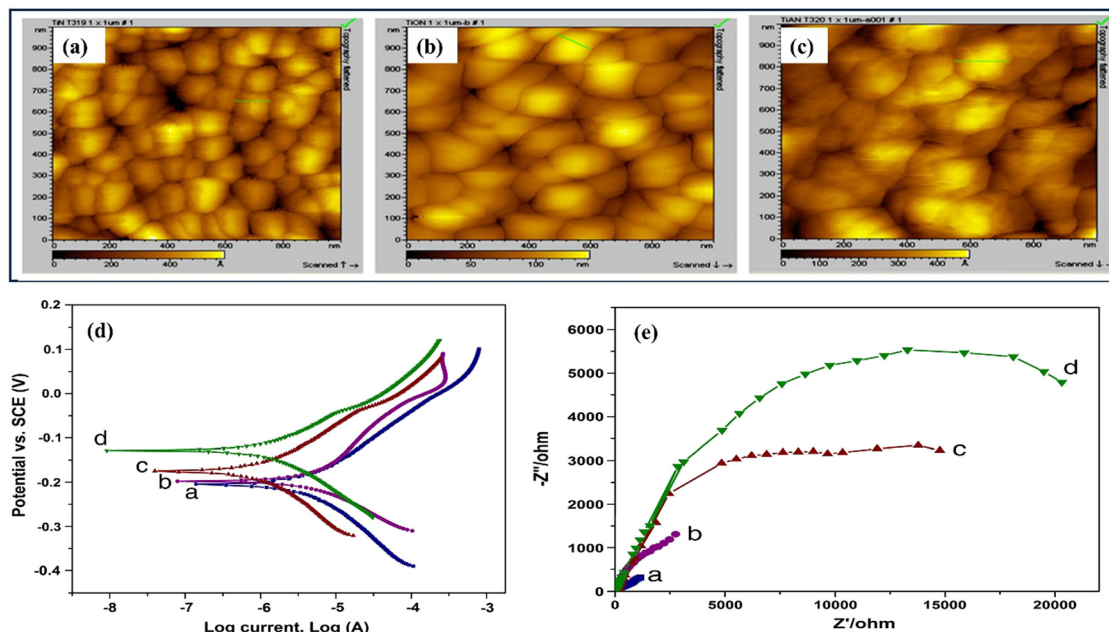


Fig. 20 AFM image of (a) TiN, (b) TiON and (c) TiAlN thin films on CP-Ti; (d) The potentiodynamic polarisation curve for the CP-Ti substrate, TiN, TiON, and TiAlN on CP-Ti in a simulated body fluid solution; (e) Nyquist plots for the CP-Ti substrate, TiN, TiON, and TiAlN on CP-Ti (reproduced from ref. 240 with permission).

resistance, and cytotoxicity (see Fig. 20). They found that TiAlN coatings exhibited superior corrosion resistance, making them promising candidates for biomedical applications, while all coatings showed non-cytotoxic behavior. Brunello *et al.* examined titanium coatings' biocompatibility and antibacterial properties.<sup>241</sup> Several coatings, including uncoated Ti<sub>64</sub>, anodized Ti<sub>64</sub>, TiN, and zirconium nitride, were prepared using physical vapor deposition (PVD) on titanium surfaces. Surface analysis showed zirconium nitride had the lowest roughness, while TiN and anodized samples were rougher than uncoated Ti<sub>64</sub>. Biocompatibility tests using MTT showed similar results for all samples, and the Ames test indicated no mutagenic activity. Notably, zirconium nitride and TiN demonstrated the highest antibacterial activity.

The effect of TiN coatings on implant surfaces was discussed by Hove *et al.*, according to their study, TiN coatings enhanced the compatibility of the implants with the human body.<sup>242</sup> However, there were also instances of the TiN coating delaminating and producing third-body wear, indicating the need for process standardisation and improvement. In another study, Lawand *et al.* validated the successful integration of TiN as a bio-compatible conductor in BiCMOS devices, allowing for the electrical integration of high-density biomedical electrode arrays on a single chip, which is especially important for devices like cochlear implants where space is limited.<sup>243</sup> Recently, Roberlo and coworkers deposited TiN thin films on AISI 316L stainless steel substrates using DC unbalanced magnetron sputtering, and they found that the TiN coatings exhibited promising characteristics, such as wear and corrosion resistance, making them suitable for biomedical applications.<sup>244</sup> The coatings exhibited improved performance in scratch tests using

a biomaterial pin, simulating body fluids, indicating potential durability and suitability for implants. With ongoing research and development, the potential of TiN in healthcare continues to expand. Its remarkable properties have opened up new avenues for implant design and functionality innovation. The future holds great promise for using TiN in biomedical implants, driving advancements in healthcare and positively impacting the lives of countless patients worldwide.

### 3.6 Electrochemical sensing

TiN has made a significant impact in the field of electrochemical sensing, reshaping the way we approach sensing applications. Its exceptional properties and versatile applications have positioned it as a game-changer in this realm.<sup>245,246</sup> One of the key advantages of TiN is its high electrical conductivity, which enables efficient electron transfer at the electrode interface. This characteristic enhances the sensitivity and accuracy of electrochemical sensing, allowing for precise detection and quantification of analytes. TiN electrodes exhibit excellent signal-to-noise ratios, improving detection limits and enhancing measurement performance.<sup>247</sup> Furthermore, TiN's biocompatibility is a crucial factor in biomedical sensing applications. It interacts favorably with biological systems, making it suitable for various biosensing platforms. When used as electrode material in bioelectrochemical sensors, TiN ensures minimal interference with biological samples, enabling safe and reliable biomedical monitoring. Its compatibility with living tissues facilitates the development of implantable sensors and wearable devices for continuous health monitoring.<sup>237,248</sup>

In addition to its electrical properties and biocompatibility, TiN demonstrates remarkable corrosion resistance. This

resistance to oxidation and degradation allows for long-term stability and durability of sensing electrodes, even in harsh or corrosive environments. It ensures the reliability and longevity of electrochemical sensing devices, making them suitable for various applications, including environmental monitoring and industrial sensing.<sup>25,249</sup> Integrating TiN into electrochemical sensing platforms has made significant advancements in healthcare, environmental monitoring, and beyond.<sup>129,250</sup> The unique properties of TiN enable the development of highly sensitive and accurate sensing devices, driving progress in disease diagnostics, environmental analysis, and quality control processes. As an example, Ali *et al.* developed a liquid-phase photopolymerization method to integrate a nanocomposite-based scaffold of graphene foam and TiN nanofibers into microfluidic channels, creating efficient microfluidic electrochemical sensors to detect nitrate ions in agricultural soils with ultralow detection limits and high sensitivity, providing a promising platform for sustainable agriculture.<sup>251</sup> Haldorai *et al.* demonstrated the synthesis of TiN NPs-decorated multi-walled carbon nanotube (MWCNTs) nanocomposite and used as a biosensor for nitrite detection.<sup>252</sup> The nanocomposite-modified electrode exhibited outstanding sensitivity ( $121.5 \mu\text{A} \mu\text{M}^{-1} \text{cm}^{-2}$ ) and a meager detection limit ( $0.0014 \mu\text{M}$ ) within a wide concentration range ( $1 \mu\text{M}$  to  $2000 \mu\text{M}$ ). The biosensor demonstrated good reproducibility, prolonged stability, and fruitful application in detecting nitrite in tap and seawater samples (see Fig. 21(a)). Kong *et al.* developed an electrochemical sensor using a nanohybrid of rGO and TiN, which demonstrated remarkable electrocatalytic performance in

detecting acetaminophen (ACOP) and 4-aminophenol (4-AP) simultaneously.<sup>253</sup> Furthermore, it displayed expansive linear detection spans and minimal detection thresholds, highlighting its potential as a favourable electrode substance for identifying diverse analytes in electrochemical sensing applications (see Fig. 21(b-d)). Feng *et al.* successfully synthesized a chrysanthemum-like TiN-rGO composite through a hydrothermal and nitridation process.<sup>254</sup> The researchers then utilized this composite to modify a glassy carbon electrode to develop an electrochemical sensor. The sensor showcased remarkable electrocatalytic effectiveness, capable of concurrently identifying dopamine and uric acid across linear detection spans of  $5\text{--}175 \mu\text{M}$  and  $30\text{--}215 \mu\text{M}$ , respectively. With commendable resilience against interference, coupled with stability and consistent performance, this sensor holds potential for real-world sample analysis.

Recently, using a solvothermal method and L-tyrosine as a template agent, Chu *et al.* prepared nano-Ag-TiO<sub>2</sub> hollow microsphere precursors, which were further transformed into nano-Ag-TiN hollow microsphere composites through nitride reduction.<sup>255</sup> The prepared composite demonstrated excellent electrochemical performance with low hydrogen peroxide (H<sub>2</sub>O<sub>2</sub>) detection limits and superior interference resistance, stability, and repeatability. Shylenra *et al.* improved a TiN solid-state pH sensor by creating a Nafion-modified TiN electrode, which significantly reduces the potential shift in the presence of oxidising or reducing agents, making it a promising tool for accurate pH measurement in high redox mediums and potentially has applications in real-time health monitoring and

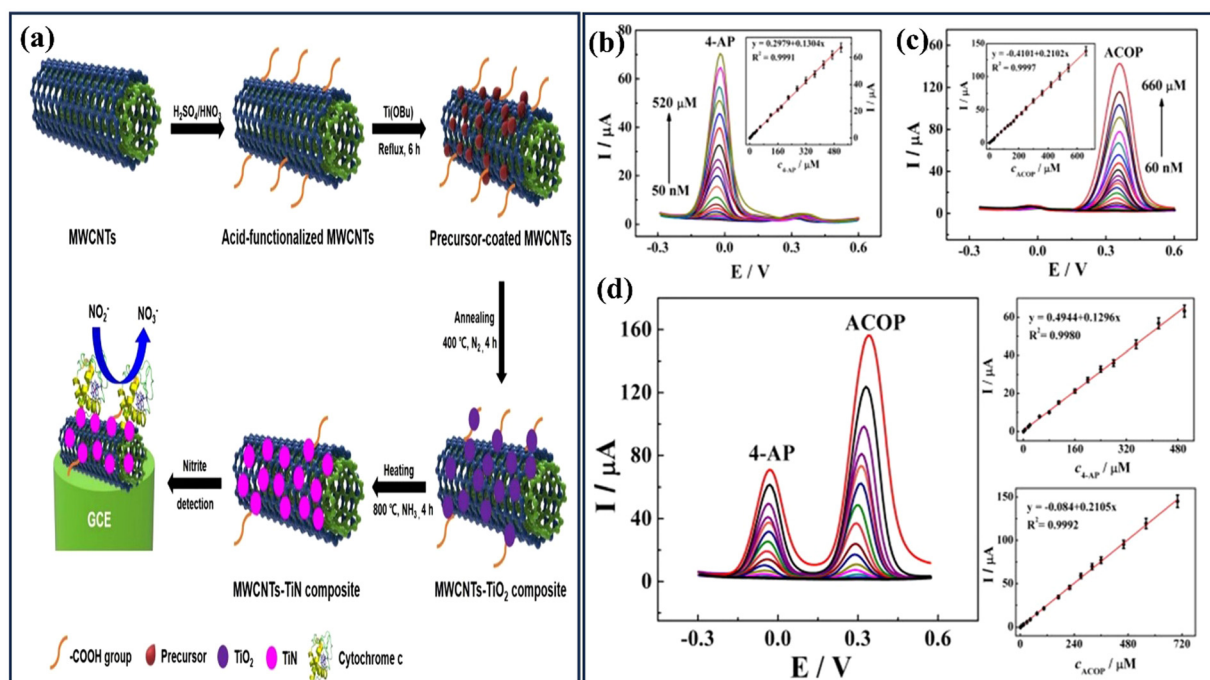


Fig. 21 (a) Illustration of the procedure to fabricate the MWCNTs-TiN composite for nitrite sensing (reproduced from ref. 252 with permission); (b) a mix containing  $10 \mu\text{M}$  ACOP and varying concentrations of 4-AP from  $50 \text{ nM}$  to  $520 \mu\text{M}$ , (c) a mix containing  $10 \mu\text{M}$  4-AP and varied ACOP concentrations from  $60 \text{ nM}$  to  $660 \mu\text{M}$ , (d) a combination of diverse 4-AP concentrations ( $0.05\text{--}500 \mu\text{M}$ ) and ACOP concentrations ( $0.5\text{--}700 \mu\text{M}$ ), alongside their corresponding calibration curves (reproduced from ref. 253 with permission).



medical diagnosis.<sup>256</sup> In another study, Wang *et al.* demonstrated a simple molten-salt synthesis method to create carbon–TiN nanocomposites, which displayed outstanding electrocatalytic activity for the sensitive detection of dopamine (DA).<sup>257</sup> The developed C–TiN-altered glassy carbon electrode (C–TiN/GCE) showed enhanced sensitivity ( $9620 \mu\text{A} \mu\text{M} \text{ cm}^{-2}$ ) and a low detection limit  $0.03 \mu\text{M}$  ( $\text{S}/\text{N} = 3$ ), making it a suitable choice for detecting DA in human serum with satisfactory recovery results. In their study, Annalakshmi *et al.* developed a nitrite sensor with high sensitivity by modifying a glassy carbon electrode using a nanocomposite of carboxylated multiwalled carbon nanotubes (c-MWCNT) and TiN NPs.<sup>258</sup> The modified electrode exhibited favorable characteristics, including low electrochemical resistance, a large electroactive surface area, and a high heterogeneous electron transfer rate. These qualities collectively contributed to the remarkable performance of the sensor in detecting nitrite. Notably, the sensor demonstrated a low limit of detection (LOD) of  $4 \text{ nM}$ , an extended useful analytical range from  $6 \text{ nM}$  to  $950 \mu\text{M}$ , and a rapid response time of  $4 \text{ s}$ . These results highlight the potential of the sensor for various applications in nitrite detection. The effectiveness of the sensor was further confirmed through the successful identification of nitrite in water and meat samples with satisfactory recoveries.

Integrating TiN with layered materials, such as reduced graphene oxide, holds significant potential in the sensing field. For example, An RGO–TiN nanocomposite was created by Wei *et al.* for the electrochemical detection of nerve growth factor (NGF).<sup>259</sup> This nanocomposite demonstrated excellent electrocatalytic activity with a linear response to NGF concentration ranging from  $10 \text{ nM}$  to  $5 \text{ M}$  and a low detection limit of  $2.6 \text{ nM}$ , highlighting its potential as a sensitive and reliable sensor for NGF determination in biological samples, particularly for assessing neurological impairment in patients after cerebrovascular accidents. Recently, Xu *et al.* devised an electrochemical sensor with enhanced sensitivity for the specific detection of bisphenol A (BPA) residues at a low detection limit of  $0.19 \text{ nmol L}^{-1}$  by integrating molecular imprinting with graphene-doped TiN.<sup>260</sup> The sensor exhibits remarkable repeatability and stability, thereby showcasing its viability for environmental monitoring and sensing applications.

As research and development in this field continue, the potential of TiN in electrochemical sensing will only grow. Its exceptional properties and diverse applications offer immense opportunities for innovation and advancement. TiN is truly revolutionizing the field, opening up new possibilities for precise and reliable sensing technologies with wide-ranging impacts on our lives.

### 3.7 Protective coatings

TiN has found extensive applications in protective coatings due to its exceptional properties, which make it highly desirable for enhancing the durability, wear resistance, and aesthetic appeal of various materials and surfaces.<sup>25</sup> Here, we will delve into some key applications of TiN coatings in the realm of protective coatings. One of the prominent uses of TiN coatings is in the field of cutting tools and wear-resistant applications. TiN-coated

cutting tools offer significantly improved hardness and wear resistance, allowing for extended tool life and enhanced cutting performance. The high hardness of TiN (approximately 2000 to 2500 HV) provides excellent resistance against abrasive wear, ensuring that the tools retain their sharpness and cutting efficiency for prolonged periods.<sup>20,261</sup> Moreover, TiN coatings reduce friction and provide a low coefficient of friction, reducing heat generation during cutting operations.<sup>25</sup> TiN coatings also find applications in decorative coatings, particularly in the watch and jewelry industry. The striking golden color of TiN-coated surfaces adds aesthetic appeal and offers an alternative to expensive gold plating. Additionally, TiN coatings provide excellent corrosion resistance, preventing tarnishing and ensuring the long-lasting beauty of the coated objects.<sup>262,263</sup>

In the automotive and aerospace industries, TiN coatings play an essential role in enhancing the durability and performance of various components. TiN-coated engine components, such as piston rings and valve stems, experience reduced friction and wear, improving engine efficiency and longevity. TiN coatings on aerospace parts, such as turbine blades, protect against high-temperature oxidation and erosion, extending the lifespan of critical components.<sup>264–266</sup> Furthermore, TiN coatings find applications in electronics, serving as protective layers on circuit boards and semiconductor devices. These coatings provide a barrier against moisture, chemicals, and electrical breakdown, ensuring the reliability and longevity of electronic components.<sup>267–269</sup> For example, In their study, Kao *et al.* subjected Ti<sub>6</sub>Al<sub>4</sub>V alloy substrates to a nitriding process at a temperature of  $900 \text{ }^\circ\text{C}$ , followed by the deposition of TiN coatings.<sup>270</sup> The scientists evaluated the microstructural attributes, hardness, and adhesion properties of TiN–N–Ti<sub>6</sub>Al<sub>4</sub>V substrates compared to untreated, nitrided, and TiN-coated specimens. The research investigated the tribological traits by implementing reciprocal sliding wear trials involving interactions with balls made of 316L, Si<sub>3</sub>N<sub>4</sub>, and Ti<sub>6</sub>Al<sub>4</sub>V materials (see Fig. 22). The biocompatibility was evaluated by affixing and cultivating purified mouse leukemic monocyte/macrophage cells onto the specimens. Applying a duplex nitriding/TiN coating treatment resulted in notable enhancements in the tribological, anti-corrosion, and bio-compatibility characteristics of the original Ti<sub>6</sub>Al<sub>4</sub>V alloy. Xia and colleagues effectively produced Ni–TiN composites with remarkable resistance to corrosion and wear using the ultrasonic pulse electrodeposition technique (UPED).<sup>271</sup> The findings of the study revealed a surface structure that was both fine and compact. The average diameter of the nickel (Ni) grains was  $68.4 \text{ nm}$ , while the average diameter of the TiN nanoparticles was  $26.8 \text{ nm}$ . The composite deposited by the UPED method exhibited superior microhardness, enhanced corrosion resistance, and displayed smooth worn surface morphologies characterized by minimal scratches (see Fig. 23).

In a separate study, Hong and co-authors investigated how process parameters influence the microstructure and wear resistance properties of TiN coatings created *via* electro-spark deposition.<sup>259</sup> The assessment involved the characterization of coating thickness, TiN concentration, and porosity. A statistical model was developed to identify the key factors influencing



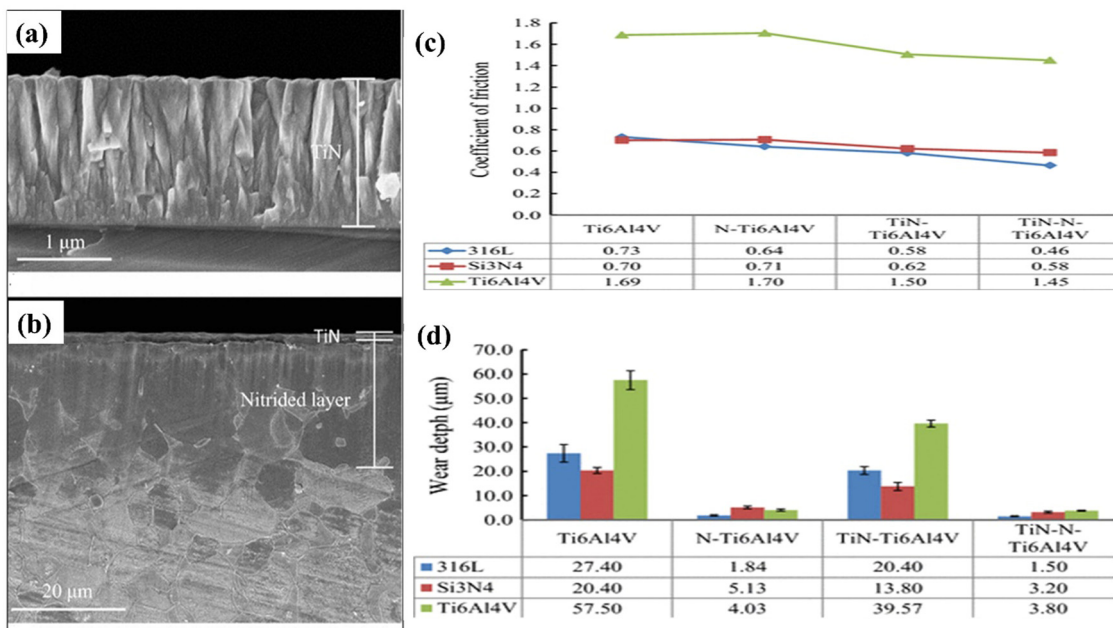


Fig. 22 (a) Cross-sectional SEM depictions of the TiN coating on a silicon wafer; (b) the TiN coating on a nitrided Ti<sub>6</sub>Al<sub>4</sub>V substrate; (c) the mean friction coefficients of diverse samples when in motion against 316L, Si<sub>3</sub>N<sub>4</sub>, and Ti<sub>6</sub>Al<sub>4</sub>V counterparts; (d) the levels of wear experienced by various samples as they glide against counterbodies constructed from 316L, Si<sub>3</sub>N<sub>4</sub>, and Ti<sub>6</sub>Al<sub>4</sub>V materials (reproduced from ref. 270 with permission).

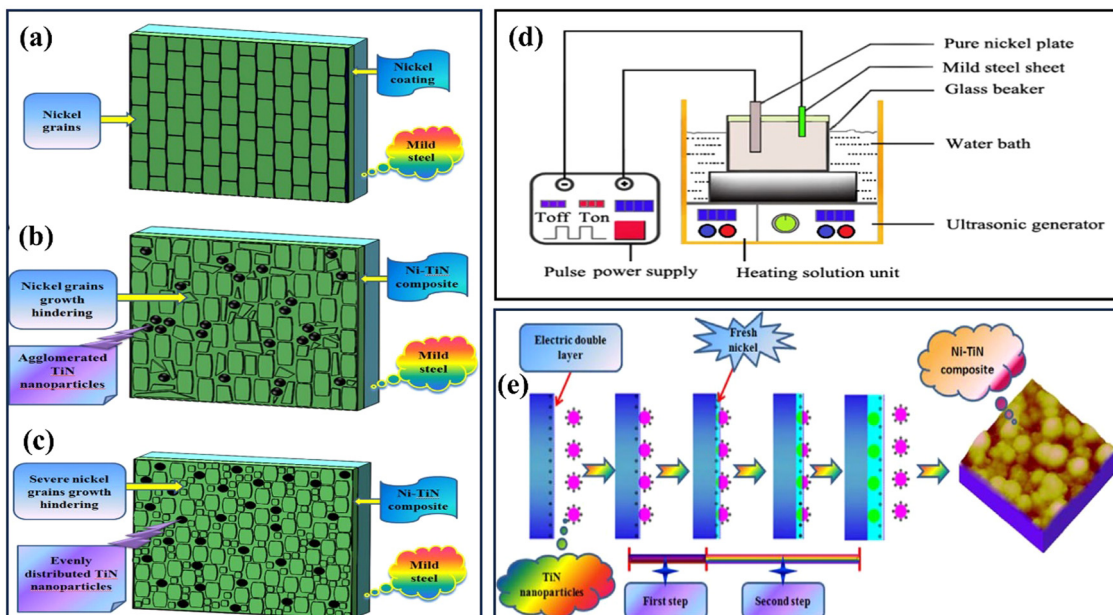


Fig. 23 (a) Ni-TiN composite's form and refinement mechanism with various preparation techniques: (a) PED-1, (b) PED-2, and (c) UPED-1; (d) experimental diagram for making composites of Ni-TiN composites; (e) diagrammatic illustration of the codeposition process between nickel ions and TiN nanoparticles (reproduced from ref. 271 with permission).

these characteristics. The output voltage, nitrogen flux, and specific strengthening duration were pinpointed the most favourable process parameters. The predominant wear mechanism identified in this study was micro-cutting wear, which was associated with micro-fracture wear.

In a different study, Martinu *et al.* fabricated nanolaminated ZrN/TiN systems by pulsed DC magnetron sputtering.<sup>272</sup> The

modulation periods of these systems ranged from 1 to 100 nm. The researchers discovered that coatings with a thickness less than 10 nm exhibited a homogeneous structure consisting of a single-phase solid solution characterized by a composition of Ti<sub>0.35</sub>Zr<sub>0.65</sub>N with a higher concentration of Zr. The size of the crystallites exhibited variation with the modulation periodicity. Specifically, the Ti<sub>0.35</sub>Zr<sub>0.65</sub>N solid solution displayed crystallite

sizes ranging from 11 to 12.5 nm, while the laminate structure exhibited sizes between 14.5 and 25 nm. The hardness of the hardened nanolaminate structure was found to be 32–35 GPa, notably greater than that of the individual TiN and ZrN single-layer coatings. The solution system, characterized by its hardness and solidity, demonstrated the highest wear resistance and toughness levels. Recently, Richter *et al.* investigated the effect of bipolar pulsed direct current (DC) magnetron sputtering on the evolution of TiN coating microstructure.<sup>273</sup> The researchers discovered that applying pulsed direct current (DC) voltage profiles transformed the material's texture, shifting it from a state of randomly oriented polycrystals to textured TiN coatings. Furthermore, it was observed that higher frequencies of the applied pulses contributed to reduced grain size and enhanced both hardness and resistance to wear. More recently, Liu *et al.* investigated the tribological properties of TiN ceramic coatings with a specific focus on the effects of sliding balls on wear.<sup>274</sup> The researchers fabricated TiN bioinert ceramic coatings doped with graphene oxide nanosheets (GO). These coatings were intended to serve as self-lubricating phases on a titanium alloy known as Ti<sub>6</sub>Al<sub>4</sub>V. Doping in the coating resulted in enhanced wear resistance and decreased friction coefficients. The observed phenomena exhibited by the coatings included oxidation, abrasive wear, and fatigue wear during the sliding motion with Si<sub>3</sub>N<sub>4</sub> balls, Ti<sub>6</sub>Al<sub>4</sub>V balls, and UHMWPE balls. The primary mechanism responsible for reducing friction was forming a lubricating film on the sliding surface by the substance known as GO. The application of GO-doped TiN bioinert ceramic coatings to artificial joints becomes feasible due to this development.

In summary, TiN coatings offer a range of protective benefits in various applications. They provide excellent wear resistance, corrosion resistance, and low friction properties, making them ideal for cutting tools, decorative coatings, automotive and aerospace components, and electronics. The versatility and effectiveness of TiN coatings have made them indispensable in industries where protection, durability, and enhanced performance are crucial considerations.

### 3.8 Plasmonic and metamaterial applications

Traditional photonics has undergone a transition due to the tremendous advancements made in the last ten years in the domains of plasmonics,<sup>275–277</sup> metamaterials,<sup>278–280</sup> and transformation optics.<sup>281</sup> With this evolution, new ideas such as light concentrators, invisibility cloaks, nanoscale imaging instruments, and materials with negative refractive index have emerged.<sup>282,283</sup> Together, these developments open the door to the development of gadgets with unmatched functionality. Although these devices show exciting potential in experiments, their practical use is still limited. A major obstacle to the application of transformation optics (TO) and metamaterials (MM) in physical devices is the significant loss resulting from the plasmonic components of these technologies.

For real-world device applications, traditional plasmonic materials such as gold and silver are less suitable since they experience significant losses when working at optical frequencies. Apart from loss issues, there is another major problem with

using normal metals in device applications: the real parts of metal permittivities are too big in scale, which makes them unusable for many MM and TO devices. Ideally, plasmonic substances in devices should have adjustable permittivity. Transparent conducting oxides (TCOs) were initially considered as potential substitutes for gold and silver in the near-infrared range.<sup>284</sup> However, TCOs lack metallic properties in visible wavelengths due to limited carrier concentration ( $\sim 10^{21} \text{ cm}^{-3}$ ). Transition-metal nitrides like titanium nitride and zirconium nitride offer higher carrier concentrations, surpassing those achievable in TCOs.<sup>285</sup> While the optical losses in metal nitrides aren't lower than those in noble metals, their real permittivity at visible wavelengths is significantly lower due to reduced carrier concentration. Moreover, unlike noble metals, the optical characteristics of these nitrides can be adjusted by altering processing conditions. Easy fabrication and integration with silicon manufacturing techniques is another significant benefit of ZrN and TiN. These attributes collectively position ZrN and TiN as highly promising substitutes for plasmonic materials in both the visible and near-IR spectra.<sup>286,287</sup> This section delves into the exploration of TiN as a foundational element for various applications, including SPP waveguides, localized surface plasmon resonance (LSPR) devices, hyperbolic metamaterials (MMs), and broader transformation optics devices.

In addition to its widespread application in the microelectronics sector,<sup>288</sup> TiN is a promising material for plasmonics as well because of its high melting point, corrosion resistance, biocompatibility, and other qualities.<sup>289</sup> N. Kinsey *et al.* explored an insulator–metal–insulator plasmonic interconnect using TiN, a CMOS-compatible material, at the telecommunication wavelength of 1.55  $\mu\text{m}$ . Their experimental results showcased that TiN waveguides have propagation losses less than 0.8 dB mm<sup>-1</sup> with a mode size of 9.8  $\mu\text{m}$  on sapphire, aligning with theoretical predictions. Additionally, their theoretical analysis of a solid-state structure with ultra-thin metal strips and Si<sub>3</sub>N<sub>4</sub> superstrates shows that even lower propagation losses below 0.3 dB mm<sup>-1</sup> with a mode size of 9  $\mu\text{m}$  are achievable. They proposed TiN as a useful plasmonic material for hybrid, integrated nano-optic, and solid-state photonic devices.<sup>290</sup>

Patsalas and team's review highlighted the TiN's optical intricacies, attributing its conductivity to the Ti semi-filled d-band. They propose a hybrid model amalgamating Drude and Lorentz oscillators to explain TiN's dielectric function. The parameter  $E_{\text{ps}}$ , tied to TiN's unscreened plasma energy, notably shapes TiN's plasmonic characteristics. They emphasize exceptional SPP performance in TiN/AlN and TiN/GaN interfaces and note that modifying TiN's composition and structure allows spectral control over LSPR in nanoparticles, although this can impact LSPR strength. Particularly, TiN nanoparticles showcase a dominant LSPR above 500 nm akin to gold's signature resonance.<sup>291,292</sup> Ultimately, this review is the crucial roadmap for researchers delving into the realm of TiN's optical properties, pivotal for advancing diverse technological applications.

According to a study by S. Ishii *et al.*, the lossy plasmonic resonances of nanoparticles are broad enough to cover the



majority of the solar spectrum and highly efficient for absorbing sunlight. TiN nanoparticles have higher sunlight absorption efficiency than gold and black carbon nanoparticles. Their experiments show that TiN nanoparticles dispersed in water heat water and generate vapor more efficiently than carbon nanoparticles. The results open possibilities for efficient solar heat applications with titanium nitride nanoparticles.<sup>292</sup>

Furthermore, H. Reddy *et al.* rigorously examined the temperature-induced alterations in optical traits within epitaxial TiN thin films (ranging from 30–200 nm) on sapphire. Their research showcased TiN's robust plasmonic behavior, demonstrating significantly lesser quality factor deterioration compared to noble metals like Au and Ag, particularly at elevated temperatures (>400 °C). The study emphasized TiN's structural resilience, hinting at its promising applications in high-temperature nanophotonics.<sup>293</sup>

A. Catellani and A. Calzolari investigated the optical attributes of TiN/(Al, Sc)N superstructures positioned on MgO substrates, employing first principles methodologies. Their study focused on deciphering the plasmonic behavior of extremely thin TiN layers at a microscopic scale, particularly emphasizing the electronic structure of the TiN/dielectric interfaces. Additionally, the study examined the hyperbolic properties of multilayer metamaterials, contrasting them with experimental results and emphasizing the significant impact of quantum confinement on these ultrathin dielectric layers. Their samples consisted of stacked sequences of TiN and (Al, Sc) N layers grown on MgO (001), all sharing the cubic crystal structure. In the same year, A. Catellani *et al.* scrutinized TiN's plasmon dispersion characteristics under pressure variations, outlining its optoelectronic behaviors in the visible spectrum. They uncovered a universal scaling law correlating mechanical and plasmonic properties under pressure. Additionally, their investigation shed light on the stability of surface-plasmon polaritons at various TiN-dielectric interfaces, indicating TiN's potential for robust plasmonic devices in extreme conditions, distinct from conventional noble metals.<sup>294</sup>

In a different study, Guo *et al.* utilized nitrogen-plasma-assisted molecular-beam epitaxy (MBE) for cultivating single-crystalline, stoichiometric TiN films on sapphire substrates. The study confirmed that MBE-produced TiN films exhibit superior plasmonic features, potentially replacing gold in the visible and near-infrared ranges. Spectroscopic ellipsometry reveals TiN's advantage over gold, notably below 500 nm, due to reduced interband transition losses. Contrary to predictions, surface plasmon interferometry proves the presence of surface plasmon polariton (SPP) modes at the TiN/air interface. Utilizing MBE-generated stoichiometric TiN, they crafted tailored TiN metasurfaces for visible spectrum applications.<sup>295</sup>

M. Wells & his colleagues explored several thin film materials including W, Mo, Ti, TiN, TiON, Ag, Au, SrRuO<sub>3</sub>, and SrNbO<sub>3</sub> for refractory plasmonic applications. Their results indicated that SrRuO<sub>3</sub> (SRO) maintains its metallic properties even after annealing at 800 °C, but SrNbO<sub>3</sub> loses its metallic properties at 400 °C. After annealing at 500 °C, the optical characteristics of TiN and TiON deteriorate due to oxidation and exhibit a loss of

metallic behavior, but Au's attributes do not change after 600 °C. Under vacuum, TiN and TiON can be more appropriate than Au or SRO for high-temperature applications.<sup>296</sup> Further, M. Gadalla *et al.* fabricated highly metallic TiN thin films on Si and MgO substrates, expanding the potential applications of TiN in plasmonics. Their research demonstrated TiN nanoantenna arrays' tunable plasmonic peaks in the near to mid-IR range and confirmed their capabilities akin to Au counterparts, validated through FTIR and S-SNOM experiments.<sup>297</sup>

In a similar study by T. Krekeler & A. Petrov, they investigated the oxidization behavior of TiN films, grown at 835 °C on Al<sub>2</sub>O<sub>3</sub> substrates. The study revealed that the TiN film structure exhibits exceptional structural stability at 1000 °C for 2 hours under medium vacuum conditions and thermal stability at 1400 °C for 8 hours under high vacuum conditions, without a protective coating layer. This is the first time the TiN film structure with columnar grains shows remarkable thermal stability at 1400 °C due to low-index interfaces and twin boundaries. Thus, providing critical knowledge for fabricating thermally stable photonic/plasmonic devices for harsh environment.<sup>298</sup> In their study, T. Reese and their team investigated the distinct photoexcited properties of TiN compared to noble metals like Au and Ag at ultrafast time scales. They explored the optical differences between TiN nanoparticle arrays supporting surface lattice resonances (SLRs) and those only exhibiting localized surface plasmons (LSPs). Their findings revealed asymmetric broadening in SLRs compared to symmetric broadening in LSPs during ps-time scale transient absorption measurements. Moreover, the robustness of TiN nanoparticle arrays was demonstrated by their ability to withstand high pump fluences for extended periods with minimal change in bleach wavelength.<sup>299</sup> To further explore TiN for its Photonic applications, J. Judek and his team investigated the plasmonic capabilities of polycrystalline TiN<sub>x</sub> that sputtered on silicon at room temperature. Their study revealed a continuous range of plasmonic properties spanning from 400 nm to 30 μm, with film composition (nitrogen to titanium ratio x) between 0.84 and 1.21 crucial for optimizing these properties. In the visible range, interband optical transitions governed the dielectric function, while longer wavelengths (>800 nm) aligned with a Drude model modified by an additional Lorentz term, essential for specific samples. It was the first study of its kind to explore the dielectric function of TiN at such long wavelengths.<sup>300</sup>

Recently, Mishra *et al.* explored TiN thin films' potential in fluorescence coupling within metal-dielectric structures. Through experimental and reflectivity calculations, they characterized the optical modes in these structures, adjustable by varying dielectric layer thickness. Their findings showcase that fluorophores on TiN substrates can couple with surface-plasmon modes or waveguide modes, yielding directional emission within narrow angular ranges. Notably, TiN demonstrates comparable performance to conventional Au substrates in surface plasmon-coupled emission (SPCE) and waveguide-coupled emission (WGCE), while offering the added advantage of reusability, a key feature for fluorescence sensing applications.<sup>301</sup>



As per our earlier discussion TiN has emerged as a promising material for plasmonics, but its typical high-temperature deposition methods have limited its applications and hindered integration into CMOS device architectures. Chang *et al.* showcased highly plasmonic TiN films and nanostructures using room-temperature, low-power reactive sputtering. Their TiN exhibits notably negative real dielectric values among reported plasmonic films. Their two-dimensional TiN nano disks validated robust plasmonic resonances. This deposition method enables the fabrication of intricate plasmonic TiN nanostructures, enhancing the functionality and performance of existing CMOS-based photonic devices.<sup>302</sup> Further, Dhruv and his team have made significant strides in the development of plasmonic materials compatible with CMOS technology. By carefully studying the plasma-enhanced atomic layer deposition process, they successfully deposited high-quality TiN layers on *c*-plane sapphire. They achieved low-loss, highly conductive TiN films with a plasma frequency below 500 nm at temperatures below 500 °C by fine-tuning parameters including chemisorption time, substrate temperature, and plasma exposure time. The fabricated 85 nm thick TiN films exhibited a remarkable plasmonic figure of merit of 2.8, showcasing potential applications in scalable and CMOS-compatible plasmonic devices.<sup>303</sup>

In the next year L. Mascaretti *et al.* reported RF substrate biasing during magnetron sputtering as a promising technique for preparing TiN thin films at room temperature. In their study, they examined how radiofrequency (RF) substrate biasing affected the structure, optical, and electrical properties of TiN films. Notably, moderate RF power exhibited a reduction in grain size while optimizing plasmonic quality factors and achieving low resistivity (<100  $\mu\Omega$  cm). The introduction of slight understoichiometry (TiN0.85) through this technique was key to achieving these desired properties.<sup>304</sup> Recently, S. Reiter *et al.* explored TiN nanohole arrays (NHAs) with varying thicknesses. Their findings uncovered Fano-shaped resonances between 950 and 1200 nm, attributed to extraordinary optical transmission (EOT) through NHAs. They demonstrated that increasing TiN layer thickness enhances sensitivity, leading to potential advancements in on-chip plasmonic refractive index sensors.<sup>305</sup> TiN's low-index surfaces enable the growth of ultra-smooth, thin crystalline films essential for high-performance plasmonic and metamaterial devices, including hyperbolic metamaterials (HMMs). G. Naik *et al.* constructed an epitaxial superlattice as a Hyperbolic metamaterial (HMM) using TiN, this study overcame fabrication limitations, achieving ultrasmooth layers of 5 nm thickness with sharp interfaces critical for superior HMM performance. The TiN-based superlattice HMM exhibited a higher enhancement of photonic densities of states (PDOS) compared to gold- or silver-based HMMs, showcasing its potential in quantum plasmonic applications.<sup>306</sup> To shed light on the future, we address the benefits of TiN plasmonic components through examples of applications centered around electromagnetic energy absorption.

**3.8.1. Therapeutic applications.** Resonant plasmonic nanoparticles serve as efficient collectors of electromagnetic energy, capable of heating a confined volume surrounding the

particles.<sup>307</sup> When nanoparticles are directed to a tumor area, they can be heated using near-infrared laser light, as this wavelength experiences minimal light attenuation through biological tissue. Conventionally, Au nanostructures are employed for this application, but the spectral mismatch between spherical Au nanoparticles and the biological transparency window necessitated the search for alternative materials.<sup>308</sup> In their study, Guler *et al.* explored lithographically crafted TiN nanoparticles with dipolar resonances. They revealed that TiN nanoparticles outperform identical-shaped Au counterparts when excited by an 800 nm laser light.<sup>309</sup> Notably, TiN nanoparticles displayed broader resonance peaks compared to Au nanoparticles, indicating their potential for photothermal therapy without size restrictions or complex shapes. Further, Guler *et al.* investigated the optical properties of colloidal TiN nanoparticles. They discovered 50 nm cubic nanoparticles exhibiting plasmon resonance within the biological transparency window, showcasing high absorption efficiency and a self-passivating oxide surface for versatile functionalization, paving the way for innovative applications in photothermal and photocatalytic domains.<sup>310</sup> In a pioneering work by L. Gui and H. Giessen, they engineered TiN nanoantenna arrays, offering tunable plasmonic resonances within the 950–1050 nm spectrum. Their analysis of second-harmonic (SH) spectroscopy, using a nonlinear oscillator model, provided the material's wavelength-dependent second-order response. These arrays surpassed gold counterparts in laser power sustainability by an order of magnitude, hence showcasing the potential of TiN nanoantennas for high-power/high-temperature applications as nanoscale heat sources and coherent nonlinear converters.<sup>311</sup> Due to TiN's existing use in biomedical implants and other biological applications, it emerges as a compelling alternative to Au nanostructures in therapeutic applications.

**3.8.2. Solar/thermophotovoltaics.** As the demand for alternative energy grows, light harvesting applications gain significance. Photovoltaics, crucial for future energy supply, faces hurdles in its maturity and reliability, notably in light conversion efficiency and long-term stability of semiconductor devices.<sup>312</sup> Excessive heating of semiconductors contributes to long-term stability issues, while environmental factors like humidity and UV radiation also degrade device performance. Solar/thermophotovoltaics can be a one-stop solution to various problems arising due to direct exposure of semiconductor components. In solar/thermophotovoltaics systems, a high-performance absorber captures solar energy, heating an intermediate layer. For a thermophotovoltaic device, the emitter gets heated from sources like chemical, nuclear, or waste heat sources.<sup>313</sup> Combining the solar absorber creates a hybrid, termed a solar/thermophotovoltaic device. The heated body re-emits infrared light based on Planck's law,<sup>314</sup> which can be tailored using optimized surface designs to emit light just above the semiconductor's bandgap.<sup>315</sup> This spectral match yields high efficiencies and prolonged lifetimes.

For years, theoretical discussions dominated the field, lacking practical demonstrations. Lenert *et al.* recently achieved a groundbreaking 3.2% efficiency in a solar-thermophotovoltaic device, a notable milestone.<sup>316</sup> However, limitations persisted in the spectral selectivity of the absorber and lower operational



temperatures due to material constraints. Plasmonic materials with refractory properties offer potential solutions to overcome these limitations and notably expand experimental boundaries. TiN's adaptable optical properties enable tailored impedance matching, facilitating efficient energy collection from sunlight with various perfect absorber designs. For this aim, Molesky *et al.* have proposed designs of selective emitters that use elements with high melting points, such as TiN.<sup>317</sup> Further, W. Li *et al.* have developed a high-temperature stable broadband plasmonic absorber. Their creation, using titanium nitride, achieves a remarkable average absorption of 95% within a total thickness of 240 nm. This absorber combines plasmonic resonances with dielectric-like loss, offering opportunities for diverse applications like solar thermophotovoltaics and optical circuits.<sup>318</sup> These TiN nanostructures were tested against Au under high-intensity pulsed laser exposure at 550 nm, a wavelength where both exhibit high absorbance. Post-test scanning electron microscope images confirm TiN nanostructures' resilience to intense pulses, unlike the failure observed in Au nanostructures. This durability under high-intensity laser illumination underscores TiN's potential for nonlinear plasmonics, emphasizing its promising role in advanced applications.

Further, M. Chirumamilla & S. Bozhevlyni, along with their team explored the application of 3D TiN nanopillars for ultra-broadband absorption in the visible and near-infrared spectral bands. They reported an average absorptivity value of 0.94 across a broad range of oblique angles (0°–75°). After a 24-hour annealing process at 1473 K, their nanopillars show remarkable thermal and spectral stability, indicating that they can be utilized in high-temperature applications, particularly solar thermophotovoltaics.<sup>319</sup> Recently, Akhtary and Zubair investigated TiN's potential as a substitute for noble metals like Ag and Au in solar cell plasmonic applications.<sup>320</sup> Their theoretical simulations highlighted TiN-based nanostructures' tunability for scattering light into the substrate by altering shape, size, and dielectric properties. Bowtie-shaped TiN nanostructures exhibited remarkable light absorption, reaching a maximum scattering cross-section of 4.58 W m<sup>-2</sup> on a 30 nm Si<sub>3</sub>N<sub>4</sub> substrate. With a peak absorption efficiency of ~30% across visible and infrared wavelengths, TiN nanostructures show promise for enhancing solar cell efficiency *via* plasmonic light trapping.

**3.8.3. Sea water desalination.** Hundreds of millions of people lack access to freshwater for even the most fundamental activities, such as farming, drinking, and cleansing. This phenomenon has become a persistent global problem. Freshwater comprises approximately 2.5% of the Earth's total water volume, of which lakes and rivers comprise approximately 0.5%.<sup>321</sup> Numerous surface water resources are drying up as a result of climate change, placing numerous communities in peril around the world. Moreover, the contamination of lakes and rivers due to industrial effluent discharge and leaching of contaminants exacerbates the scarcity of potable water.<sup>322,323</sup> Utilizing the ample resources of saline aquifers and the ocean is an appealing strategy for addressing the escalating freshwater scarcity. However, prior purification is necessary before these water sources can be utilized directly.<sup>324</sup>

Considerable effort has been devoted to the development of techniques for producing potable water through research, with

particular emphasis on decontamination, desalination, and disinfection, all of which have undergone comprehensive evaluation.<sup>325,326</sup> Desalination is becoming increasingly prevalent, with the most prevalent processes being membrane reverse osmosis and thermal distillation.<sup>327</sup> High-energy inputs and infrastructure costs hinder the adoption of these technologies worldwide. The utilization of sunlight for water evaporation holds promise for water desalination and disinfection. Yet, direct solar exposure faces limitations due to water's poor optical absorption and significant heat loss, hindering efficient evaporation. Introducing a potent solar absorber can address these challenges, unlocking the full potential of solar-driven water evaporation.<sup>324</sup>

Various materials such as semiconductors, carbon-based nanostructures (like nanotubes, nanofibers, and graphene), polymers, and plasmonic materials exhibit promising solar absorption capabilities, efficiently converting solar energy into heat. These materials have been investigated for water evaporation due to their high solar spectrum absorption and effective light-to-heat conversion efficiencies.<sup>328,329</sup> Among these options, plasmonic materials emerge as appealing contenders due to their exceptional absorption capabilities and minimal material input requirements.<sup>330,331</sup> The majority of research on plasmonic materials for solar water evaporation has concentrated on well-established Au and Ag metals.<sup>331</sup> Nevertheless, efforts have shifted towards cost-effective alternatives to Au and Ag for large-scale solar water evaporation. This pursuit emphasizes non-noble metals, doped metal oxides, nitrides, carbides, and semiconductors for their affordability and earth abundance.<sup>281,332</sup> Among these, metal nitrides emerge as promising due to their predicted high chemical stability, minimal toxicity, and efficient conversion of light to heat, offering potential in freshwater generation.<sup>315,333</sup> Utilizing the same concept as we discussed above, M. Kaur and his team developed a novel technique for desalination and water purification by utilizing anodized aluminium oxide (AAO) that has been loaded with TiN NPs. By harnessing the photothermal properties of TiN NPs and the efficient water transport capabilities of AAO, they have achieved a steam generation efficiency of 92% under solar irradiation. Furthermore, the introduction of a simple yet effective thermal insulation technique enhances water evaporation speed, making this portable solar steam generation structure not only cost-effective but also highly efficient for sustainable water purification and desalination solutions.<sup>334</sup>

Working in the same directions, Zhang and his team developed a cost-effective and highly efficient photothermal membrane for solar membrane distillation (MD), incorporating TiN nanoparticles to enhance solar energy absorption. Their innovative design achieved a solar efficiency of 64.1% and an MD flux of 0.940 kg m<sup>-2</sup> h, outperforming bare PVDF membranes by producing 65.8% more pure water. The unique interfacial heating of the photothermal coating mitigated temperature polarization, ensuring stable, high-quality, potable water production, highlighting its potential for solar MD applications.<sup>335</sup> M. Farid's team also utilized plasmonic TiN NPs on a hydrophobic membrane for the same kind of application discussed above. In the presence of 1 sun of solar irradiance, their TiN photothermal membrane generated an



average vapour flux of  $1.01 \text{ L m}^{-2} \text{ h}^{-1}$  and an impressive solar-thermal efficiency of 66.7%. Due to the plasmonic TiN NP layer's broad optical absorption and excellent light-to-heat conversion properties, the photothermal MD process achieved its superior performance. This increased the net driving force for vapour transport and facilitated efficient interfacial water heating at the membrane surface. The study also emphasized the TiN photothermal membrane's mechanical stability and exceptional photothermal conversion efficiency, marking a significant progress toward cost-effective and stable solar-driven MD applications.<sup>336</sup>

Further, X. Cheng *et al.* synthesized sub micrometer titanium oxynitride spheres for solar-driven seawater desalination. Their study showcased the dual-mode resonance in titanium oxynitride spheres, used ingeniously in a solar-driven seawater desalination device. With hollow spheres displaying enhanced evaporation rates due to their unique morphology, the system achieved a remarkable water evaporation rate of  $\sim 1.49 \text{ kg m}^{-2} \text{ h}^{-1}$  and a solar-to-thermal conversion efficiency of  $\sim 89.1\%$ , setting a new benchmark among plasmon-based solar desalination systems.<sup>337</sup> Recently, X. Bai *et al.* synthesized TiN nanoparticles with diverse morphologies, showcasing strong broadband light absorption through plasmonic effects. These nanoparticles were integrated into porous poly(vinyl alcohol) films, which achieved a remarkable seawater evaporation rate of  $3.8 \text{ kg m}^{-2} \text{ h}^{-1}$ , setting a new performance benchmark among plasmonic solar seawater desalination systems. Additionally, the composite film exhibited a 98.3% phenol removal rate, attributed to its superb photocatalytic capability and superhydrophilicity which highlight its potential in addressing water purification challenges.<sup>338</sup>

Initial investigations have demonstrated that TiN with other plasmonic metal nitrides can accomplish some of the highest efficiencies for solar-driven water evaporation under one sun's illumination. Further advancements in solar-driven water evaporation face challenges related to the chemical stability of metal nitride nanostructures. Comprehensive long-term cycling measurements are imperative to assess their durability. Additionally, the expansion of metal nitrides' plasmonic response requires the development of innovative synthetic techniques to broaden their localized surface plasmon resonance (LSPR) range. The enthusiasm that surrounds plasmonic metal nitrides guarantees that their development will continue to advance at an accelerated pace in the future.

## 4. Conclusions and perspectives

In summary, titanium nitrides (TiNs) have emerged as highly promising materials with diverse applications owing to their exceptional properties, including superior hardness, wear resistance, corrosion resistance, biocompatibility, and electrical conductivity. This review provides a comprehensive overview of diverse synthesis techniques and the manifold applications of TiN while examining the factors that enhance their performance. The synthesis of TiN materials has been explored through various methods, including chemical vapor deposition,

solvothermal/hydrothermal, laser ablation, sol-gel, magnetron sputtering and electrochemical deposition. Each synthesis method offers its advantages and challenges, with factors such as control over morphology, composition, and scalability being key considerations.

The applications of TiN encompass diverse fields, including but not limited to protective coatings, energy storage devices, electrocatalysis, photocatalysis, and biomedical implants. TiN coatings have remarkably improved the durability, wear resistance, and aesthetic appeal of cutting tools, jewellery, automotive components, and electronic devices. TiN-based electrodes have shown promise in enhancing energy storage devices' efficiency and stability, such as supercapacitors and batteries. Moreover, TiN has shown great potential as a catalyst in various electrochemical and photocatalytic processes. Despite the significant progress made in the synthesis and applications of titanium nitrides, there are several challenges and avenues for future research that need to be addressed:

### (1) Enhanced synthesis techniques

Continued efforts are required to develop advanced synthesis techniques that offer better control over the morphology, composition, and size of TiN nanostructures. This includes exploring novel approaches such as bottom-up synthesis, template-assisted methods, and precise control of doping and alloying.

### (2) Scalability and cost-effectiveness

Scaling up the synthesis of TiN materials while maintaining their quality and performance is essential for practical applications. Addressing the challenges related to cost-effective synthesis methods and large-scale production is crucial to facilitate their widespread adoption.

### (3) Stability and durability

Further research is needed to improve the stability and durability of TiN coatings, especially in harsh and demanding environments. Exploring new strategies to enhance the adhesion and interfacial properties of TiN coatings can contribute to their long-term performance and reliability.

### (4) Biomedical applications

Although TiN has shown great potential in biomedical implants, further investigations are required to explore its long-term biocompatibility, tissue integration, and immune response. Additionally, exploring the potential of TiN for drug delivery and biofunctionalization can open new avenues in the field of biomedical engineering.

### (5) Multi-functionality and hybrid materials

Exploring the synergistic effects of TiN with other materials, such as incorporating TiN into composites or hybrid structures, can lead to enhanced properties and multi-functionality. This can further expand the range of applications, including sensors, catalysis, and energy conversion.

In summary, TiN have exhibited remarkable characteristics and significant prospects in diverse fields of application. The



widespread adoption of TiN-based materials can be facilitated by effectively addressing the challenges in synthesis and meeting the specific requirements of diverse applications. Ongoing research and development endeavours, in conjunction with interdisciplinary collaborations, will play a pivotal role in harnessing the complete capabilities of titanium nitrides and fostering advancements in the field of materials science and engineering.

## Data availability

Data sharing does not apply to this article as no new data were created or analyzed in this study.

## Conflicts of interest

The authors declare no conflict of interest.

## Acknowledgements

The authors extend their sincere gratitude to Medi-Caps University, Indore, for the provision of University Research Fellowship (MU/URF/001) and Seed Money Support (MU/SMPS/No. 21). Additionally, the authors express their acknowledgment for the unwavering backing from all participating institutions, highlighting their significant contributions and meaningful scholarly dialogues.

## References

- 1 R. S. Ningthoujam and N. S. Gajbhiye, Synthesis, electron transport properties of transition metal nitrides and applications, *Prog. Mater. Sci.*, 2015, **70**, 50–154, DOI: [10.1016/j.jpmatsci.2014.11.004](https://doi.org/10.1016/j.jpmatsci.2014.11.004).
- 2 X. Zhang, R. M. Kong, H. Du, L. Xia and F. Qu, Highly efficient electrochemical ammonia synthesis: Via nitrogen reduction reactions on a VN nanowire array under ambient conditions, *Chem. Commun.*, 2018, **54**, DOI: [10.1039/c8cc00459e](https://doi.org/10.1039/c8cc00459e).
- 3 Z. Sun, J. Zhang, L. Yin, G. Hu, R. Fang and H.-M. Cheng, *et al.*, Conductive porous vanadium nitride/graphene composite as chemical anchor of polysulfides for lithium-sulfur batteries, *Nat. Commun.*, 2017, **8**, 14627.
- 4 Z. Wen, S. Cui, H. Pu, S. Mao, K. Yu and X. Feng, *et al.*, Metal nitride/graphene nanohybrids: General synthesis and multifunctional titanium nitride/graphene electrocatalyst, *Adv. Mater.*, 2011, **23**, DOI: [10.1002/adma.201102772](https://doi.org/10.1002/adma.201102772).
- 5 S. Yang, J. Kim, Y. J. Tak, A. Soon and H. Lee, Single-atom catalyst of platinum supported on titanium nitride for selective electrochemical reactions, *Angew. Chem., Int. Ed.*, 2016, **55**, DOI: [10.1002/anie.201509241](https://doi.org/10.1002/anie.201509241).
- 6 M. Wu, X. Lin, Y. Wang, L. Wang, W. Guo and D. Qi, *et al.*, Economical Pt-free catalysts for counter electrodes of dye-sensitized solar cells, *J. Am. Chem. Soc.*, 2012, **134**, DOI: [10.1021/ja209657v](https://doi.org/10.1021/ja209657v).
- 7 J. Bendix, C. Anthon, M. Schau-Magnussen, T. Brock-Nannestad, J. Vibenholt and M. Rehman, *et al.*, Heterobimetallic nitride complexes from terminal chromium(v) nitride complexes: Hyperfine coupling increases with distance, *Angew. Chem., Int. Ed.*, 2011, **50**, DOI: [10.1002/anie.201008153](https://doi.org/10.1002/anie.201008153).
- 8 B. Gao, X. Li, K. Ding, C. Huang, Q. Li and P. K. Chu, *et al.*, Recent progress in nanostructured transition metal nitrides for advanced electrochemical energy storage, *J. Mater. Chem. A*, 2019, **7**, DOI: [10.1039/c8ta05760e](https://doi.org/10.1039/c8ta05760e).
- 9 H. Wang, J. Li, K. Li, Y. Lin, J. Chen and L. Gao, *et al.*, Transition metal nitrides for electrochemical energy applications, *Chem. Soc. Rev.*, 2021, **50**, 1354–1390, DOI: [10.1039/D0CS00415D](https://doi.org/10.1039/D0CS00415D).
- 10 Y. Zhang, B. Ouyang, J. Xu, S. Chen, R. S. Rawat and H. J. Fan, 3D porous hierarchical nickel–molybdenum nitrides synthesized by RF plasma as highly active and stable hydrogen-evolution-reaction electrocatalysts, *Adv. Energy Mater.*, 2016, **6**, 1600221.
- 11 J. G. Chen, Carbide and nitride overlayers on early transition metal surfaces: Preparation, characterization, and reactivities, *Chem. Rev.*, 1996, **96**, DOI: [10.1021/cr950232u](https://doi.org/10.1021/cr950232u).
- 12 M.-S. Balogun, W. Qiu, W. Wang, P. Fang, X. Lu and Y. Tong, Recent advances in metal nitrides as high-performance electrode materials for energy storage devices, *J. Mater. Chem. A*, 2015, **3**, 1364–1387.
- 13 S. Xi, G. Lin, L. Jin, H. Li and K. Xie, Metallic porous nitride single crystals at two-centimeter scale delivering enhanced pseudocapacitance, *Nat. Commun.*, 2019, **10**, DOI: [10.1038/s41467-019-12818-x](https://doi.org/10.1038/s41467-019-12818-x).
- 14 W. F. Chen, K. Sasaki, C. Ma, A. I. Frenkel, N. Marinkovic and J. T. Muckerman, *et al.*, Hydrogen-evolution catalysts based on non-noble metal nickel–molybdenum nitride nanosheets, *Angew. Chem., Int. Ed.*, 2012, **51**, DOI: [10.1002/anie.201200699](https://doi.org/10.1002/anie.201200699).
- 15 D. H. Youn, S. Han, J. Y. Kim, J. Y. Kim, H. Park and S. H. Choi, *et al.*, Highly active and stable hydrogen evolution electrocatalysts based on molybdenum compounds on carbon nanotube-graphene hybrid support, *ACS Nano*, 2014, **8**, DOI: [10.1021/nn5012144](https://doi.org/10.1021/nn5012144).
- 16 G. R. Li, J. Song, G. L. Pan and X. P. Gao, Highly Pt-like electrocatalytic activity of transition metal nitrides for dye-sensitized solar cells, *Energy Environ. Sci.*, 2011, **4**, DOI: [10.1039/c1ee01105g](https://doi.org/10.1039/c1ee01105g).
- 17 Q. Luo, C. Lu, L. Liu and M. Zhu, A review on the synthesis of transition metal nitride nanostructures and their energy related applications, *Green Energy Environ.*, 2023, **8**, 406–437, DOI: [10.1016/j.gee.2022.07.002](https://doi.org/10.1016/j.gee.2022.07.002).
- 18 N. C. Saha and H. G. Tompkins, Titanium nitride oxidation chemistry: An x-ray photoelectron spectroscopy study, *J. Appl. Phys.*, 1992, **72**, DOI: [10.1063/1.351465](https://doi.org/10.1063/1.351465).
- 19 Q. W. Jiang, G. R. Li and X. P. Gao, Highly ordered TiN nanotube arrays as counter electrodes for dye-sensitized solar cells, *Chem. Commun.*, 2009, 6720–6722.
- 20 H. Holleck, Material selection for hard coatings, *J. Vac. Sci. Technol., A*, 1986, **4**, DOI: [10.1116/1.573700](https://doi.org/10.1116/1.573700).
- 21 S. W. Choi, Y. C. Kim, S. H. Chang, I. H. Oh and C. S. Kang, Corrosion performance of TiN and TiAlN films prepared by Arc Ion Plating Technique, 9th International Conference on Technology of Plasticity, ICTP 2008, 2008.

22 X. Liu, P. K. Chu and C. Ding, Surface modification of titanium, titanium alloys, and related materials for biomedical applications, *Mater. Sci. Eng., R*, 2004, **47**, DOI: [10.1016/j.mser.2004.11.001](https://doi.org/10.1016/j.mser.2004.11.001).

23 T. Polcar, T. Kubart, R. Novák, L. Kopecký and P. Široký, Comparison of tribological behaviour of TiN, TiCN and CrN at elevated temperatures, *Surf. Coat. Technol.*, 2005, **193**, DOI: [10.1016/j.surcoat.2004.07.098](https://doi.org/10.1016/j.surcoat.2004.07.098).

24 D. E. Wolfe and J. Singh, Microstructural evolution of titanium nitride (TiN) coatings produced by reactive ion beam-assisted, electron beam physical vapor deposition (RIBA, EB-PVD), *J. Mater. Sci.*, 1999, **34**, DOI: [10.1023/A:1004668325924](https://doi.org/10.1023/A:1004668325924).

25 E. Santecchia, A. M. S. Hamouda, F. Musharavati, E. Zalnezhad, M. Cabibbo and S. Spigarelli, Wear resistance investigation of titanium nitride-based coatings, *Ceram. Int.*, 2015, **41**, 10349–10379, DOI: [10.1016/j.ceramint.2015.04.152](https://doi.org/10.1016/j.ceramint.2015.04.152).

26 Y. L. Chin, J. C. Chou, Z. C. Lei, T. P. Sun, W. Y. Chung and S. K. Hsiung, Titanium nitride membrane application to extended gate field effect transistor pH sensor using VLSI technology, *Jpn. J. Appl. Phys., Part 1*, 2002, **40**, DOI: [10.1143/jjap.40.6311](https://doi.org/10.1143/jjap.40.6311).

27 A. U. Chaudhry, B. Mansoor, T. Mungole, G. Ayoub and D. P. Field, Corrosion mechanism in PVD deposited nano-scale titanium nitride thin film with intercalated titanium for protecting the surface of silicon, *Electrochim. Acta*, 2018, **264**, DOI: [10.1016/j.electacta.2018.01.042](https://doi.org/10.1016/j.electacta.2018.01.042).

28 R. Gao, W. Yu, H. Deng, H. S. Ku, Z. Li and M. Wang, *et al.*, Epitaxial titanium nitride microwave resonators: Structural, chemical, electrical, and microwave properties, *Phys. Rev. Mater.*, 2022, **6**, 036202, DOI: [10.1103/PHYSREV MATERIALS.6.036202/FIGURES/7/MEDIUM](https://doi.org/10.1103/PHYSREV MATERIALS.6.036202/FIGURES/7/MEDIUM).

29 K. Lin, X. Qin, M. Liu, X. Xu, G. Liang and J. Wu, *et al.*, Ultrafine Titanium Nitride Sheath Decorated Carbon Nanofiber Network Enabling Stable Lithium Metal Anodes, *Adv. Funct. Mater.*, 2019, **29**, DOI: [10.1002/adfm.201903229](https://doi.org/10.1002/adfm.201903229).

30 S. Kaskel, K. Schlichte and T. Kratzke, Catalytic properties of high surface area titanium nitride materials, *J. Mol. Catal. A: Chem.*, 2004, **208**, DOI: [10.1016/S1381-1169\(03\)00545-4](https://doi.org/10.1016/S1381-1169(03)00545-4).

31 B. M. Biwer and S. L. Bernasek, Investigation of the electronic structure of an iron-titanium nitride ammonia synthesis catalyst, *Appl. Surf. Sci.*, 1986, **25**, 41–52, DOI: [10.1016/0169-4332\(86\)90024-3](https://doi.org/10.1016/0169-4332(86)90024-3).

32 M. Al-Dhaifallah, M. A. Abdelkareem, H. Rezk, H. Alhumade, A. M. Nassee and A. G. Olabi, Co-decorated reduced graphene/titanium nitride composite as an active oxygen reduction reaction catalyst with superior stability, *Int. J. Energy Res.*, 2021, **45**, 1587–1598.

33 J. A. DeWitt, E. V. Phillips, K. L. Hebisch, A. W. Tricker and C. Sievers, Structural evolution of TiN catalysts during mechanocatalytic ammonia synthesis, *Faraday Discuss.*, 2023, **243**, 65–76, DOI: [10.1039/d2fd00164k](https://doi.org/10.1039/d2fd00164k).

34 Z.-G. Yang, H.-M. Xu, T.-Y. Shuai, Q.-N. Zhan, Z.-J. Zhang and K. Huang, *et al.*, Recent progress in the synthesis of transition metal nitride catalysts and their applications in electrocatalysis, *Nanoscale*, 2023, **15**, 11777–11800, DOI: [10.1039/D3NR01607B](https://doi.org/10.1039/D3NR01607B).

35 S. Das, S. Guha, R. Ghadai and A. Sharma, Influence of nitrogen gas over microstructural, vibrational and mechanical properties of CVD Titanium nitride (TiN) thin film coating, *Ceram. Int.*, 2021, **47**, 16809–16819, DOI: [10.1016/J.CERAMINT.2021.02.254](https://doi.org/10.1016/J.CERAMINT.2021.02.254).

36 S. Grosso, L. Latu-Romain, G. Berthomé, G. Renou, T. Le Coz and M. Mantel, Titanium and titanium nitride thin films grown by dc reactive magnetron sputtering Physical Vapor Deposition in a continuous mode on stainless steel wires: Chemical, morphological and structural investigations, *Surf. Coat. Technol.*, 2017, **324**, DOI: [10.1016/j.surcoat.2017.05.089](https://doi.org/10.1016/j.surcoat.2017.05.089).

37 Q. Fu, D. Kokalj, D. Stangier, F. E. Kruis and W. Tillmann, Aerosol synthesis of titanium nitride nanoparticles by direct current arc discharge method, *Adv. Powder Technol.*, 2020, **31**, DOI: [10.1016/j.apt.2020.08.012](https://doi.org/10.1016/j.apt.2020.08.012).

38 S. Dong, X. Chen, X. Zhang and G. Cui, Nanostructured transition metal nitrides for energy storage and fuel cells, *Coord. Chem. Rev.*, 2013, **257**, 1946–1956, DOI: [10.1016/J.CCR.2012.12.012](https://doi.org/10.1016/J.CCR.2012.12.012).

39 H. Sun, Z. Yan, F. Liu, W. Xu, F. Cheng and J. Chen, Self-Supported Transition-Metal-Based Electrocatalysts for Hydrogen and Oxygen Evolution, *Adv. Mater.*, 2020, **32**, DOI: [10.1002/adma.201806326](https://doi.org/10.1002/adma.201806326).

40 R. Peri, M. Bhagavathiachari and S. Balasubramanian, A detailed study on the electrochemical properties of transition metal-based carbide/nitride thin films in energy conversion and storage devices, *Electrochim. Acta*, 2022, **427**, DOI: [10.1016/j.electacta.2022.140860](https://doi.org/10.1016/j.electacta.2022.140860).

41 Z. Meng, S. Zheng, R. Luo, H. Tang, R. Wang and R. Zhang, *et al.*, Transition Metal Nitrides for Electrocatalytic Application: Progress and Rational Design, *Nanomaterials*, 2022, **12**, 2660, DOI: [10.3390/NANO12152660](https://doi.org/10.3390/NANO12152660).

42 L. Lin, S. Piao, Y. Choi, L. Lyu, H. Hong and D. Kim, *et al.*, Nanostructured Transition Metal Nitrides as Emerging Electrocatalysts for Water Electrolysis: Status and Challenges, *Energy-Chem.*, 2022, **4**, 100072, DOI: [10.1016/J.ENCHEM.2022.100072](https://doi.org/10.1016/J.ENCHEM.2022.100072).

43 S. Mahadik, S. Surendran, J. Y. Kim, G. Janani, D. K. Lee and T. H. Kim, *et al.*, Syntheses and electronic structure engineering of transition metal nitrides for supercapacitor applications, *J. Mater. Chem. A*, 2022, **10**, 14655–14673, DOI: [10.1039/D2TA02584A](https://doi.org/10.1039/D2TA02584A).

44 X. Yang, B. Xu, J. G. Chen and X. Yang, Recent Progress in Electrochemical Nitrogen Reduction on Transition Metal Nitrides, *ChemSusChem*, 2023, **16**, e202201715, DOI: [10.1002/CSSC.202201715](https://doi.org/10.1002/CSSC.202201715).

45 P. Zhang, L. Yue, Q. Liang, H. Gao, Q. Yan and L. Wang, A Review of Transition Metal Compounds as Functional Separators for Lithium–Sulfur Batteries, *ChemistrySelect*, 2023, **8**, e202203352, DOI: [10.1002/SLCT.202203352](https://doi.org/10.1002/SLCT.202203352).

46 M. Batool, A. Hameed and M. A. Nadeem, Recent developments on iron and nickel-based transition metal nitrides for overall water splitting: A critical review, *Coord. Chem. Rev.*, 2023, **480**, 215029, DOI: [10.1016/J.CCR.2023.215029](https://doi.org/10.1016/J.CCR.2023.215029).

47 Y. Zhou, W. Guo and T. Li, A review on transition metal nitrides as electrode materials for supercapacitors, *Ceram. Int.*, 2019, **45**, 21062–21076.



48 H. Wu, M. Qin, Z. Cao, X. Li, B. Jia and X. Qu, Highly efficient synthesis of 2D VN nanoparticles/carbon sheet nanocomposites and their application as supercapacitor electrodes, *Appl. Surf. Sci.*, 2019, 466, DOI: [10.1016/j.apsusc.2018.10.102](https://doi.org/10.1016/j.apsusc.2018.10.102).

49 S. Ahangarani, A. R. Sabour Rouhaghadam and M. Azadi, A Review on Titanium Nitride and Titanium Carbide Single and Multilayer Coatings Deposited by Plasma Assisted Chemical Vapor Deposition, *Int. J. Eng.*, 2016, 29, DOI: [10.5829/idosi.ije.2016.29.05b.12](https://doi.org/10.5829/idosi.ije.2016.29.05b.12).

50 N. Ramanuja, R. A. Levy, S. N. Dharmadhikari, E. Ramos, C. W. Pearce and S. C. Menasian, *et al.*, Synthesis and characterization of low pressure chemically vapor deposited titanium nitride films using  $TiCl_4$  and  $NH_3$ , *Mater. Lett.*, 2002, 57, 261–269, DOI: [10.1016/S0167-577X\(02\)00776-0](https://doi.org/10.1016/S0167-577X(02)00776-0).

51 L. von Fieandt, T. Larsson, E. Lindahl, O. Bäcke and M. Boman, Chemical vapor deposition of TiN on transition metal substrates, *Surf. Coat. Technol.*, 2018, 334, 373–383, DOI: [10.1016/J.SURFCOAT.2017.11.063](https://doi.org/10.1016/J.SURFCOAT.2017.11.063).

52 A. Kafizas, C. J. Carmalt and I. P. Parkin, CVD and precursor chemistry of transition metal nitrides, *Coord. Chem. Rev.*, 2013, 257, DOI: [10.1016/j.ccr.2012.12.004](https://doi.org/10.1016/j.ccr.2012.12.004).

53 I. H. Ifijen and M. Maliki, A comprehensive review on the synthesis and photothermal cancer therapy of titanium nitride nanostructures, *Inorg. Nano-Met. Chem.*, 2023, 53, 366–387, DOI: [10.1080/24701556.2022.2068596](https://doi.org/10.1080/24701556.2022.2068596).

54 J. Su, R. Boichot, E. Blanquet, F. Mercier and M. Pons, Chemical vapor deposition of titanium nitride thin films: kinetics and experiments, *CrystEngComm*, 2019, 21, 3974–3981, DOI: [10.1039/C9CE00488B](https://doi.org/10.1039/C9CE00488B).

55 F. Li-li, H. Yu-xing, T. Si-yao, L. Shuan, Z. Jie and L. Xing-guo, *et al.*, Evaluating the performances of surface-modified titanium bipolar plates using in situ nitriding by plasma-enhanced chemical vapor deposition, *Chin. J. Eng.*, 2023, 45(4), 602–610, DOI: [10.13374/J.ISSN2095-9389.2022.05.25.002](https://doi.org/10.13374/J.ISSN2095-9389.2022.05.25.002).

56 L. Niinistö, J. Päävääsäri, J. Niinistö, M. Putkonen and M. Nieminen, Advanced electronic and optoelectronic materials by atomic layer deposition: An overview with special emphasis on recent progress in processing of high- $k$  dielectrics and other oxide materials, *Phys. Status Solidi A*, 2004, 201, DOI: [10.1002/pssa.200406798](https://doi.org/10.1002/pssa.200406798).

57 P. Nanni, M. Viviani and V. Buscaglia, *Handbook of Low and High Dielectric Constant Materials and Their Applications*, 1999, p. 1, DOI: [10.1016/B978-012513905-2/50011-X](https://doi.org/10.1016/B978-012513905-2/50011-X).

58 B. A. McCool and W. J. Desisto, Self-limited pore size reduction of mesoporous silica membranes via pyridine-catalyzed silicon dioxide ALD, *Chem. Vap. Deposition*, 2004, 10, DOI: [10.1002/cvde.200304172](https://doi.org/10.1002/cvde.200304172).

59 A. Gervasini, P. Carniti, J. Keränen, L. Niinistö and A. Auroux, Surface characteristics and activity in selective oxidation of oxylene of supported  $V_2O_5$  catalysts prepared by standard impregnation and atomic layer deposition, *Catal. Today*, 2004, 96, 187–194, DOI: [10.1016/j.cattod.2004.06.142](https://doi.org/10.1016/j.cattod.2004.06.142).

60 H. Jensen, U. M. Jensen and G. Sorensen, Reactively sputtered Cr nitride coatings studied using the acoustic emission scratch test technique, *Surf. Coat. Technol.*, 1995, 74–75, DOI: [10.1016/0257-8972\(95\)08358-8](https://doi.org/10.1016/0257-8972(95)08358-8).

61 M. Schumacher, P. K. Baumann and T. A. V. D. Seidel, and ALD as two complementary technology solutions for next generation dielectric and conductive thin-film processing, *Chem. Vap. Deposition*, 2006, 12, DOI: [10.1002/cvde.200500027](https://doi.org/10.1002/cvde.200500027).

62 L. Mascaretti, C. Mancarella, M. Afshar, Š. Kment, A. L. Bassi and A. Naldoni, Plasmonic titanium nitride nanomaterials prepared by physical vapor deposition methods, *Nanotechnology*, 2023, 34, 502003, DOI: [10.1088/1361-6528/acfc4f](https://doi.org/10.1088/1361-6528/acfc4f).

63 H. Tiznado, M. Bouman, B. C. Kang, I. Lee and F. Zaera, Mechanistic details of atomic layer deposition (ALD) processes for metal nitride film growth, *J. Mol. Catal. A: Chem.*, 2008, 281, DOI: [10.1016/j.molcata.2007.06.010](https://doi.org/10.1016/j.molcata.2007.06.010).

64 J. Musschoot, Q. Xie, D. Deduystsche, S. Van den Berghe, R. L. Van Meirhaeghe and C. Detavernier, Atomic layer deposition of titanium nitride from TDMAT precursor, *Microelectron. Eng.*, 2009, 86, DOI: [10.1016/j.mee.2008.09.036](https://doi.org/10.1016/j.mee.2008.09.036).

65 H. J. Lee, J. H. Hwang, J. Y. Park and S. W. Lee, Alternative Surface Reaction Route in the Atomic Layer Deposition of Titanium Nitride Thin Films for Electrode Applications, *ACS Appl. Electron. Mater.*, 2021, 3, 999–1005, DOI: [10.1021/acsaelm.0c01079](https://doi.org/10.1021/acsaelm.0c01079).

66 J. W. Shin, J. Lee, K. Kim, C. Kwon, Y. B. Park and H. Park, *et al.*, Effect of nitrogen plasma on the mechanical and electrical properties of plasma-enhanced atomic layer deposited TiN films, *Ceram. Int.*, 2022, 48, DOI: [10.1016/j.ceramint.2022.05.273](https://doi.org/10.1016/j.ceramint.2022.05.273).

67 B. J. Lee, Y. S. Kim, D. W. Seo and J. W. Choi, The Effect of Deposition Temperature of TiN Thin Film Deposition Using Thermal Atomic Layer Deposition, *Coatings*, 2023, 13, DOI: [10.3390/coatings13010104](https://doi.org/10.3390/coatings13010104).

68 L. Zhang, J. Feng, K. C. Chou, L. Su and X. Hou, Simultaneously electrochemical detection of uric acid and ascorbic acid using glassy carbon electrode modified with chrysanthemum-like titanium nitride, *J. Electroanal. Chem.*, 2017, 803, DOI: [10.1016/j.jelechem.2017.09.006](https://doi.org/10.1016/j.jelechem.2017.09.006).

69 M. S. Balogun, C. Li, Y. Zeng, M. Yu, Q. Wu and M. Wu, *et al.*, Titanium dioxide@titanium nitride nanowires on carbon cloth with remarkable rate capability for flexible lithium-ion batteries, *J. Power Sources*, 2014, 272, DOI: [10.1016/j.jpowsour.2014.09.034](https://doi.org/10.1016/j.jpowsour.2014.09.034).

70 Y. T. Yang, H. W. Wu, Y. Zou, X. Y. Fang, S. Li and Y. F. Song, *et al.*, Facile Synthesis of Monodispersed Titanium Nitride Quantum Dots for Harmonic Mode-Locking Generation in an Ultrafast Fiber Laser, *Nanomaterials*, 2022, 12, DOI: [10.3390/nano12132280](https://doi.org/10.3390/nano12132280).

71 M. S. Balogun, M. Yu, C. Li, T. Zhai, Y. Liu and X. Lu, *et al.*, Facile synthesis of titanium nitride nanowires on carbon fabric for flexible and high-rate lithium ion batteries, *J. Mater. Chem. A*, 2014, 2, 10825–10829, DOI: [10.1039/C4TA00987H](https://doi.org/10.1039/C4TA00987H).

72 P. Qin, X. Li, B. Gao, J. Fu, L. Xia and X. Zhang, *et al.*, Hierarchical TiN nanoparticles-assembled nanopillars for flexible supercapacitors with high volumetric capacitance, *Nanoscale*, 2018, 10, 8728–8734, DOI: [10.1039/C8NR01485J](https://doi.org/10.1039/C8NR01485J).

73 X. Lu, T. Liu, T. Zhai, G. Wang, M. Yu and S. Xie, *et al.*, Improving the Cycling Stability of Metal-Nitride



Supercapacitor Electrodes with a Thin Carbon Shell, *Adv. Energy Mater.*, 2014, **4**, 1300994, DOI: [10.1002/AENM.201300994](https://doi.org/10.1002/AENM.201300994).

74 B. Wei, C. Shang, L. Shui, X. Wang and G. Zhou, TiVN composite hollow mesospheres for high-performance supercapacitors, *Mater. Res. Express*, 2018, **6**, 025801, DOI: [10.1088/2053-1591/AAED08](https://doi.org/10.1088/2053-1591/AAED08).

75 X. Bai, L. Xu, X. Shi, J. Ren, L. Xu and Q. Wang, *et al.*, Hydrothermal oxidation improves corrosion and wear properties of multi-arc ion plated titanium nitride coating for biological application, *Vacuum*, 2022, **198**, 110871, DOI: [10.1016/J.VACUUM.2022.110871](https://doi.org/10.1016/J.VACUUM.2022.110871).

76 Y. Yang, D. Wu, R. Li, P. Rao, J. Li and P. Deng, *et al.*, Engineering the strong metal support interaction of titanium nitride and ruthenium nanorods for effective hydrogen evolution reaction, *Appl. Catal., B*, 2022, **317**, 121796, DOI: [10.1016/J.APCATB.2022.121796](https://doi.org/10.1016/J.APCATB.2022.121796).

77 N. S. Lawand, P. J. French, J. J. Briaire and J. H. M. Frijns, Thin Titanium Nitride Films Deposited using DC Magnetron Sputtering used for Neural Stimulation and Sensing Purposes, *Procedia Eng.*, 2012, **47**, 726–729, DOI: [10.1016/J.PROENG.2012.09.250](https://doi.org/10.1016/J.PROENG.2012.09.250).

78 J. Shi, B. Jiang, C. Li, Z. Liu and F. Yan, Sputtered titanium nitride films as pseudocapacitive electrode for on chip micro-supercapacitors, *J. Mater. Sci.*, 2023, **58**, 337–354, DOI: [10.1007/S10853-022-07417-Z](https://doi.org/10.1007/S10853-022-07417-Z)/**METRICS**.

79 Y. L. Jeyachandran, S. K. Narayandass, D. Mangalaraj, S. Areva and J. A. Mielczarski, Properties of titanium nitride films prepared by direct current magnetron sputtering, *Mater. Sci. Eng., A*, 2007, **445–446**, 223–236, DOI: [10.1016/J.MSEA.2006.09.021](https://doi.org/10.1016/J.MSEA.2006.09.021).

80 M. Arif, A. Sanger and A. Singh, One-step sputtered titanium nitride nano-pyramid thin electrodes for symmetric super-capacitor device, *Mater. Lett.*, 2019, **245**, 142–146, DOI: [10.1016/J.MATLET.2019.02.082](https://doi.org/10.1016/J.MATLET.2019.02.082).

81 A. Achour, R. L. Porto, M. A. Soussou, M. Islam, M. Boujtita and K. A. Aissa, *et al.*, Titanium nitride films for micro-supercapacitors: Effect of surface chemistry and film morphology on the capacitance, *J. Power Sources*, 2015, **300**, 525–532, DOI: [10.1016/J.JPOWSOUR.2015.09.012](https://doi.org/10.1016/J.JPOWSOUR.2015.09.012).

82 A. Achour, R. Lucio-Porto, M. Chaker, A. Arman, A. Ahmadpourian and M. A. Soussou, *et al.*, Titanium vanadium nitride electrode for micro-supercapacitors, *Electrochem. Commun.*, 2017, **77**, 40–43, DOI: [10.1016/J.ELECOM.2017.02.011](https://doi.org/10.1016/J.ELECOM.2017.02.011).

83 X. Zhang, C. Jiang, J. Liang and W. Wu, Electrode materials and device architecture strategies for flexible supercapacitors in wearable energy storage, *J. Mater. Chem. A*, 2021, **9**, 8099–8128, DOI: [10.1039/D0TA12299H](https://doi.org/10.1039/D0TA12299H).

84 Q. Akbar Sial, L. Thai Duy, R. Singh, S. Iqbal, R. Yeasmin and Y. J. Lee, *et al.*, A multifunctional TiN/Ni electrode for wearable supercapacitor and sensor with an insight into charge storage mechanism, *Appl. Surf. Sci.*, 2021, **555**, 149718, DOI: [10.1016/J.APSUSC.2021.149718](https://doi.org/10.1016/J.APSUSC.2021.149718).

85 Q. Xie, Z. Fu, Z. Liu, W. Yue, J. Kang and L. Zhu, *et al.*, Improvement of microstructure and tribological properties of titanium nitride films by optimization of substrate bias current, *Thin Solid Films*, 2022, **749**, 139181, DOI: [10.1016/J.TSF.2022.139181](https://doi.org/10.1016/J.TSF.2022.139181).

86 A. Ghailane, A. O. Oluwatosin, H. Larhlimi, C. Hejjaj, M. Makha and H. Busch, *et al.*, Titanium nitride, Ti<sub>1-X</sub>N, coatings deposited by HiPIMS for corrosion resistance and wear protection properties, *Appl. Surf. Sci.*, 2022, **574**, 151635, DOI: [10.1016/J.APSUSC.2021.151635](https://doi.org/10.1016/J.APSUSC.2021.151635).

87 A. Rodríguez, M. C. Morant-Miñana, A. Dias-Ponte, M. Martínez-Calderón, M. Gómez-Aranzadi and S. M. Olaizola, Femtosecond laser-induced periodic surface nanostructuring of sputtered platinum thin films, *Appl. Surf. Sci.*, 2015, **351**, 135–139, DOI: [10.1016/j.apsusc.2015.05.117](https://doi.org/10.1016/j.apsusc.2015.05.117).

88 M. Arif, A. Sanger and A. Singh, One-step sputtered titanium nitride nano-pyramid thin electrodes for symmetric super-capacitor device, *Mater. Lett.*, 2019, **245**, 142–146, DOI: [10.1016/J.MATLET.2019.02.082](https://doi.org/10.1016/J.MATLET.2019.02.082).

89 J. Zhao and A. F. Burke, Electrochemical capacitors: Materials, technologies and performance, *Energy Storage Mater.*, 2021, **36**, 31–55, DOI: [10.1016/J.ENS.2020.12.013](https://doi.org/10.1016/J.ENS.2020.12.013).

90 B. M. Gray, A. L. Hector, M. Jura, J. R. Owen and J. Whittam, Effect of oxidative surface treatments on charge storage at titanium nitride surfaces for supercapacitor applications, *J. Mater. Chem. A*, 2017, **5**, 4550–4559, DOI: [10.1039/C6TA08308K](https://doi.org/10.1039/C6TA08308K).

91 J. Zhao, Y. Zeng, J. Wang, Q. Xu, R. Chen and H. Ni, *et al.*, Ultrahigh electrocatalytic activity with trace amounts of platinum loadings on free-standing mesoporous titanium nitride nanotube arrays for hydrogen evolution reactions, *Nanoscale*, 2020, **12**, 15393–15401, DOI: [10.1039/D0NR01316A](https://doi.org/10.1039/D0NR01316A).

92 Y. H. Mao, C. Y. Chen, J. X. Fu, T. Y. Lai, F. H. Lu and Y. C. Tsai, Electrodeposition of nickel copper on titanium nitride for methanol electrooxidation, *Surf. Coat. Technol.*, 2018, **350**, 949–953, DOI: [10.1016/J.SURFCOAT.2018.03.048](https://doi.org/10.1016/J.SURFCOAT.2018.03.048).

93 Y. Xie and F. Tian, Capacitive performance of molybdenum nitride/titanium nitride nanotube array for supercapacitor, *Mater. Sci. Eng., B*, 2017, **215**, 64–70, DOI: [10.1016/J.MSEB.2016.11.005](https://doi.org/10.1016/J.MSEB.2016.11.005).

94 J. He, J. M. Pringle and Y. B. Cheng, Titanium carbide and titanium nitride-based nanocomposites as efficient catalysts for the Co<sup>2+</sup>/Co<sup>3+</sup> redox couple in dye-sensitized solar cells, *J. Phys. Chem. C*, 2014, **118**, 16818–16824, DOI: [10.1021/JP4127418/SUPPL\\_FILE/JP4127418\\_SI\\_001.PDF](https://doi.org/10.1021/JP4127418/SUPPL_FILE/JP4127418_SI_001.PDF).

95 J. Zhang, A. Reda Woldu, X. Zhao, X. Peng, Y. Song and H. Xia, *et al.*, Plasmon-enhanced hydrogen evolution on Pt-anchored titanium nitride nanowire arrays, *Appl. Surf. Sci.*, 2022, **598**, 153745, DOI: [10.1016/J.APSUSC.2022.153745](https://doi.org/10.1016/J.APSUSC.2022.153745).

96 Y. Xie, Y. Wang and H. Du, Electrochemical capacitance performance of titanium nitride nanoarray, *Mater. Sci. Eng., B*, 2013, **178**, 1443–1451, DOI: [10.1016/j.mseb.2013.09.005](https://doi.org/10.1016/j.mseb.2013.09.005).

97 J. Zhao, B. Liu, S. Xu, J. Yang and Y. Lu, Fabrication and electrochemical properties of porous VN hollow nanofibers, *J. Alloys Compd.*, 2015, **651**, 785–792.

98 H. Du, Y. Xie, C. Xia, W. Wang and F. Tian, Electrochemical capacitance of polypyrrole–titanium nitride and polypyrrole–titania nanotube hybrids, *New J. Chem.*, 2014, **38**, 1284–1293, DOI: [10.1039/C3NJ01286G](https://doi.org/10.1039/C3NJ01286G).



99 D. Bokov, A. Turki Jalil, S. Chupradit, W. Suksatan, M. Javed Ansari and I. H. Shewael, *et al.*, Nanomaterial by Sol-Gel Method: Synthesis and Application, *Adv. Mater. Sci. Eng.*, 2021, 2021, DOI: [10.1155/2021/5102014](https://doi.org/10.1155/2021/5102014).

100 M. Parashar, V. K. Shukla and R. Singh, Metal oxides nanoparticles via sol-gel method: a review on synthesis, characterization and applications, *J. Mater. Sci.: Mater. Electron.*, 2020, 31, DOI: [10.1007/s10854-020-02994-8](https://doi.org/10.1007/s10854-020-02994-8).

101 B. Huang, C. Li, Y. Zhang, W. Ding, M. Yang and Y. Yang, *et al.*, Advances in fabrication of ceramic corundum abrasives based on sol-gel process, *Chin. J. Aeronaut.*, 2021, 34, 1–17, DOI: [10.1016/J.CJA.2020.07.004](https://doi.org/10.1016/J.CJA.2020.07.004).

102 A. Dehghanhadikolaei, J. Ansary and R. Ghoreishi, undefined. Sol-gel process applications, *Proc. Nat. Res. Soc.*, 2008, 2, 02008–02029, DOI: [10.11605/j.pnrs.201802008](https://doi.org/10.11605/j.pnrs.201802008).

103 J. D. Mackenzie, Applications of the sol-gel process, *J. Non-Cryst. Solids*, 1988, 100, DOI: [10.1016/0022-3093\(88\)90013-0](https://doi.org/10.1016/0022-3093(88)90013-0).

104 H. Zhang, F. Li and Q. Jia, Preparation of titanium nitride ultrafine powders by sol-gel and microwave carbothermal reduction nitridation methods, *Ceram. Int.*, 2009, 35, 1071–1075, DOI: [10.1016/J.CERAMINT.2008.04.027](https://doi.org/10.1016/J.CERAMINT.2008.04.027).

105 I. S. Kim and P. N. Kumta, Hydrazide sol-gel synthesis of nanostructured titanium nitride: precursor chemistry and phase evolution, *J. Mater. Chem.*, 2003, 13, 2028–2035, DOI: [10.1039/B301964K](https://doi.org/10.1039/B301964K).

106 M. Zhang, N. Garcia-Araez, A. L. Hector and J. R. Owen, A sol-gel route to titanium nitride conductive coatings on battery materials and performance of TiN-coated LiFePO<sub>4</sub>, *J. Mater. Chem. A*, 2017, 5, 2251–2260, DOI: [10.1039/C6TA09572K](https://doi.org/10.1039/C6TA09572K).

107 H. Wei, M. Wu, Z. Dong, Y. Chen, J. Bu and J. Lin, *et al.*, Composition, microstructure and SERS properties of titanium nitride thin film prepared via nitridation of sol-gel derived titania thin films, *J. Raman Spectrosc.*, 2017, 48, 578–585, DOI: [10.1002/JRS.5080](https://doi.org/10.1002/JRS.5080).

108 Y. M. Chi, M. Mishra, T. K. Chin, W. S. Liu and T. P. Perng, Fabrication of macroporous/mesoporous titanium nitride structure and its application as catalyst support for proton exchange membrane fuel cell, *ACS Appl. Energy Mater.*, 2019, 2, 398–405, DOI: [10.1021/ACSAEM.8B01426/SUPPL\\_FILE/AE8B01426\\_SI\\_001.PDF](https://doi.org/10.1021/ACSAEM.8B01426/SUPPL_FILE/AE8B01426_SI_001.PDF).

109 N. Crespo-Monteiro, Y. Jourlin, A. Valour, M. A. Usuga Higuita, S. Reynaud and M. Hochedel, *et al.*, Micro-nanostructured TiN thin film: Synthesis from a photo-patternable TiO<sub>2</sub> sol-gel coating and rapid thermal nitridation, *J. Phys. Chem. C*, 2020, 124, 25480–25488, DOI: [10.1021/ACS.JPCC.0C07157/SUPPL\\_FILE/JP0C07157\\_SI\\_001.PDF](https://doi.org/10.1021/ACS.JPCC.0C07157/SUPPL_FILE/JP0C07157_SI_001.PDF).

110 X. Qin, J. Zhang, C. Ke, H. Chen and L. Zhao, Preparation of TiN ultrafine powders from sol-gel by Fe-catalyzed carbothermal reduction nitridation, *Inorg. Chem. Commun.*, 2023, 148, 110278, DOI: [10.1016/J.INOCHE.2022.110278](https://doi.org/10.1016/J.INOCHE.2022.110278).

111 J. Theerthagiri, K. Karuppasamy, S. J. Lee, R. Shwetharani, H. S. Kim and S. K. K. Pasha, *et al.*, Fundamentals and comprehensive insights on pulsed laser synthesis of advanced materials for diverse photo- and electrocatalytic applications, *Light: Sci. Appl.*, 2022, 11, DOI: [10.1038/s41377-022-00904-7](https://doi.org/10.1038/s41377-022-00904-7).

112 J. Theerthagiri, K. Karuppasamy, A. Min, D. Govindarajan, M. L. A. Kumari and G. Muthusamy, *et al.*, Unraveling the fundamentals of pulsed laser-assisted synthesis of nanomaterials in liquids: Applications in energy and the environment, *Appl. Phys. Rev.*, 2022, 9, DOI: [10.1063/5.0104740/2835452](https://doi.org/10.1063/5.0104740/2835452).

113 J. A. Faust, PFAS on atmospheric aerosol particles: a review, *Environ. Sci.: Processes Impacts*, 2023, 25, 133–150, DOI: [10.1039/D2EM00002D](https://doi.org/10.1039/D2EM00002D).

114 G. W. Yang, Laser ablation in liquids: Applications in the synthesis of nanocrystals, *Prog. Mater. Sci.*, 2007, 52, DOI: [10.1016/j.pmatsci.2006.10.016](https://doi.org/10.1016/j.pmatsci.2006.10.016).

115 J. D. Yao, Z. Q. Zheng and G. W. Yang, Production of large-area 2D materials for high-performance photodetectors by pulsed-laser deposition, *Prog. Mater. Sci.*, 2019, 106, DOI: [10.1016/j.pmatsci.2019.100573](https://doi.org/10.1016/j.pmatsci.2019.100573).

116 H. Guo, W. Chen, Y. Shan, W. Wang, Z. Zhang and J. Jia, Microstructures and properties of titanium nitride films prepared by pulsed laser deposition at different substrate temperatures, *Appl. Surf. Sci.*, 2015, 357, 473–478, DOI: [10.1016/J.APSUSC.2015.09.061](https://doi.org/10.1016/J.APSUSC.2015.09.061).

117 M. Escalona, H. Bhuyan, S. Ibacache, M. J. Retamal, P. Saikia and C. Borgohain, *et al.*, Study of titanium nitride film growth by plasma enhanced pulsed laser deposition at different experimental conditions, *Surf. Coat. Technol.*, 2021, 405, 126492, DOI: [10.1016/J.SURFCOAT.2020.126492](https://doi.org/10.1016/J.SURFCOAT.2020.126492).

118 A. A. Popov, G. Tselikov, N. Dumas, C. Berard, K. Metwally and N. Jones, *et al.*, Laser-synthesized TiN nanoparticles as promising plasmonic alternative for biomedical applications, *Sci. Rep.*, 2019, 9, 1194.

119 J. Bonse, S. V. Kirner, R. Koter, S. Pentzien, D. Spaltmann and J. Krüger, Femtosecond laser-induced periodic surface structures on titanium nitride coatings for tribological applications, *Appl. Surf. Sci.*, 2017, 418, 572–579, DOI: [10.1016/J.APSUSC.2016.10.132](https://doi.org/10.1016/J.APSUSC.2016.10.132).

120 R. Fedorov, F. Lederle, M. Li, V. Olszok, K. Wöbbeking and W. Schade, *et al.*, Formation of Titanium Nitride, Titanium Carbide, and Silicon Carbide Surfaces by High Power Femtosecond Laser Treatment, *ChemPlusChem*, 2021, 86, 1231–1242, DOI: [10.1002/CPLU.202100118](https://doi.org/10.1002/CPLU.202100118).

121 M. Esmailzadeh, H. Dizajghorbani-Aghdam and R. Malekfar, Surface-Enhanced Raman scattering of methylene blue on titanium nitride nanoparticles synthesized by laser ablation in organic solvents, *Environ. Sci.: Processes Impacts*, 2021, 257, 119721, DOI: [10.1016/J.SAA.2021.119721](https://doi.org/10.1016/J.SAA.2021.119721).

122 J. Radhakrishnan, M. Diaz, F. Cordovilla and J. L. Ocaña, Tunable superhydrophobic titanium nitride surface by ultrafast laser processing, *Ceram. Int.*, 2022, 48, 37264–37274, DOI: [10.1016/j.ceramint.2022.08.304](https://doi.org/10.1016/j.ceramint.2022.08.304).

123 S. Farooq, C. V. P. Vital, G. Tikhonowski, A. A. Popov, S. M. Klimentov and L. Malagon, *et al.*, Thermo-optical performance of bare laser-synthesized TiN nanofluids for direct absorption solar collector applications, *Sol. Energy Mater. Sol. Cells*, 2023, 252, 112203, DOI: [10.1016/J.SOLMAT.2023.112203](https://doi.org/10.1016/J.SOLMAT.2023.112203).



124 Z. C. Chen, T. L. Chang, Q. X. Wu, C. C. Liu, H. C. Chen and C. H. Huang, Surface modification of bio-orderly CrTiN thin films with periodic corrugated nanopod structures by picosecond laser ablation, *J. Alloys Compd.*, 2023, **938**, 168193, DOI: [10.1016/J.JALLOCOM.2022.168193](https://doi.org/10.1016/J.JALLOCOM.2022.168193).

125 A. A. Popov, G. V. Tikhonowski, P. V. Shakhov, E. A. Popova-Kuznetsova, G. I. Tselikov and R. I. Romanov, *et al.*, Synthesis of Titanium Nitride Nanoparticles by Pulsed Laser Ablation in Different Aqueous and Organic Solutions, *Nanomaterials*, 2022, **12**, DOI: [10.3390/nano12101672](https://doi.org/10.3390/nano12101672).

126 F. Martins, C. Felgueiras, M. Smitkova and N. Caetano, Analysis of fossil fuel energy consumption and environmental impacts in european countries, *Energiespectrum*, 2019, **12**, DOI: [10.3390/en12060964](https://doi.org/10.3390/en12060964).

127 A. I. Osman, L. Chen, M. Yang, G. Msigwa, M. Farghali and S. Fawzy, *et al.*, Cost, environmental impact, and resilience of renewable energy under a changing climate: a review, *Environ. Chem. Lett.*, 2023, **21**, DOI: [10.1007/s10311-022-01532-8](https://doi.org/10.1007/s10311-022-01532-8).

128 U. K. Pata, A. E. Caglar, M. T. Kartal and S. Kılıç Depren, Evaluation of the role of clean energy technologies, human capital, urbanization, and income on the environmental quality in the United States, *J. Cleaner Prod.*, 2023, **402**, DOI: [10.1016/j.jclepro.2023.136802](https://doi.org/10.1016/j.jclepro.2023.136802).

129 J. Feng, Q. Li, J. Cai, T. Yang, J. Chen and X. Hou, Electrochemical detection mechanism of dopamine and uric acid on titanium nitride-reduced graphene oxide composite with and without ascorbic acid, *Sens. Actuators, B*, 2019, **298**, 126872.

130 E. Ramasamy, C. Jo, A. Anthony, I. Jeong, J. K. Kim and J. Lee, Soft-template simple synthesis of ordered mesoporous titanium nitride-carbon nanocomposite for high performance dye-sensitized solar cell counter electrodes, *Chem. Mater.*, 2012, **24**, 1575–1582.

131 S. P. Shylendra, M. Wajrak, K. Alameh and J. J. Kang, Nafion Modified Titanium Nitride pH Sensor for Future Biomedical Applications, *Sensors*, 2023, **23**, 699.

132 B. P. Cumming, G. E. Schröder-Turk, S. Debbarma and M. Gu, Bragg-mirror-like circular dichroism in bio-inspired quadruple-gyroid 4srs nanostructures, *Light: Sci. Appl.*, 2017, **6**, DOI: [10.1038/lsa.2016.192](https://doi.org/10.1038/lsa.2016.192).

133 W. Xu, Y. Zhang, X. Yin, L. Zhang, Y. Cao and X. Ni, *et al.*, Highly sensitive electrochemical BPA sensor based on titanium nitride-reduced graphene oxide composite and core-shell molecular imprinting particles, *Anal. Bioanal. Chem.*, 2021, **413**, 1081–1090.

134 C. Wang, W. Li and Y. Long, Molten salt-assisted synthesis of C-TiN nanocomposites for sensitive dopamine determination, *Mater. Lett.*, 2022, **329**, 133234.

135 M. Naveed Ur Rehman, T. Munawar, M. S. Nadeem, F. Mukhtar, A. Maqbool and M. Riaz, *et al.*, Facile synthesis and characterization of conducting polymer-metal oxide based core-shell PANI-Pr<sub>2</sub>O-NiO-Co<sub>3</sub>O<sub>4</sub> nanocomposite: As electrode material for supercapacitor, *Ceram. Int.*, 2021, **47**, 18497–18509, DOI: [10.1016/j.ceramint.2021.03.173](https://doi.org/10.1016/j.ceramint.2021.03.173).

136 S. Sardana, A. Gupta, K. Singh, A. S. Maan and A. Ohlan, Conducting polymer hydrogel based electrode materials for supercapacitor applications, *J. Energy Storage*, 2022, **45**, 103510.

137 J. Cui, F.-F. Xing, H. Luo, J.-Q. Qin, Y. Li and Y. Zhong, *et al.*, General synthesis of hollow mesoporous conducting polymers by dual-colloid interface co-assembly for high-energy-density micro-supercapacitors, *J. Energy Chem.*, 2021, **62**, 145–152, DOI: [10.1016/j.jechem.2021.03.016](https://doi.org/10.1016/j.jechem.2021.03.016).

138 Q. Meng, K. Cai, Y. Chen and L. Chen, Research progress on conducting polymer based supercapacitor electrode materials, *Nano Energy*, 2017, **36**, 268–285.

139 J. Chmiola, C. Largeot, P.-L. Taberna, P. Simon and Y. Gogotsi, Monolithic carbide-derived carbon films for micro-supercapacitors, *Science*, 1979, **2010**(328), 480–483.

140 R. Raccichini, A. Varzi, S. Passerini and B. Scrosati, The role of graphene for electrochemical energy storage, *Nat. Mater.*, 2015, **14**, 271–279.

141 M. Ghaemmaghami and R. Mohammadi, Carbon nitride as a new way to facilitate the next generation of carbon-based supercapacitors, *Sustainable Energy Fuels*, 2019, **3**, 2176–2204, DOI: [10.1039/C9SE00313D](https://doi.org/10.1039/C9SE00313D).

142 R. Zhao, K. Li, R. Liu, M. Sarfraz, I. Shakir and Y. Xu, Reversible 3D self-assembly of graphene oxide and stimuli-responsive polymers for high-performance graphene-based supercapacitors, *J. Mater. Chem. A*, 2017, **5**, 19098–19106, DOI: [10.1039/C7TA05908F](https://doi.org/10.1039/C7TA05908F).

143 M. Abdah, N. Azman, S. Kulandaivalu and Y. Sulaiman, Review of the use of transition-metal-oxide and conducting polymer-based fibres for high-performance supercapacitors, *Mater. Des.*, 2020, **186**, 108199.

144 K. P. Annamalai, S. Gokulnath, T. Boobalan and M. Sathish, Construction of indigenous tin incorporated nickel dichalcogenide nanosheets for high energy all solid-state hybrid supercapacitor, *Composites, Part B*, 2023, **260**, 110747, DOI: [10.1016/j.compositesb.2023.110747](https://doi.org/10.1016/j.compositesb.2023.110747).

145 Q. Yun, L. Li, Z. Hu, Q. Lu, B. Chen and H. Zhang, Layered transition metal dichalcogenide-based nanomaterials for electrochemical energy storage, *Adv. Mater.*, 2020, **32**, 1903826.

146 L. Lin, W. Lei, S. Zhang, Y. Liu, G. G. Wallace and J. Chen, Two-dimensional transition metal dichalcogenides in supercapacitors and secondary batteries, *Energy Storage Mater.*, 2019, **19**, 408–423.

147 J. Cherusseri, N. Choudhary, K. S. Kumar, Y. Jung and J. Thomas, Recent trends in transition metal dichalcogenide based supercapacitor electrodes, *Nanoscale Horiz.*, 2019, **4**, 840–858.

148 J. Shi, B. Jiang, C. Li, F. Yan, D. Wang and C. Yang, *et al.*, Review of Transition Metal Nitrides and Transition Metal Nitrides/Carbon nanocomposites for supercapacitor electrodes, *Mater. Chem. Phys.*, 2020, **245**, DOI: [10.1016/j.matchemphys.2019.122533](https://doi.org/10.1016/j.matchemphys.2019.122533).

149 Y. Zhong, X. Xia, F. Shi, J. Zhan, J. Tu and H. J. Fan, Transition metal carbides and nitrides in energy storage and conversion, *Adv. Sci.*, 2016, **3**, 1500286.

150 Y. Zheng, X. Li, C. Pi, H. Song, B. Gao and P. K. Chu, *et al.*, Recent advances of two-dimensional transition metal nitrides for energy storage and conversion applications, *FlatChem*, 2020, **19**, 100149.

151 A. Achour, J. B. Ducros, R. L. Porto, M. Boujtita, E. Gautron and L. Le Brizoual, *et al.*, Hierarchical nanocomposite electrodes based on titanium nitride and carbon nanotubes for micro-supercapacitors, *Nano Energy*, 2014, **7**, 104–113, DOI: [10.1016/j.nanoen.2014.04.008](https://doi.org/10.1016/j.nanoen.2014.04.008).

152 X. Hou, Q. Li, L. Zhang, T. Yang, J. Chen and L. Su, Tunable preparation of chrysanthemum-like titanium nitride as flexible electrode materials for ultrafast-charging/discharging and excellent stable supercapacitors, *J. Power Sources*, 2018, **396**, 319–326.

153 P. Yang, D. Chao, C. Zhu, X. Xia, Y. Zhang and X. Wang, *et al.*, Ultrafast-charging supercapacitors based on corn-like titanium nitride nanostructures, *Adv. Sci.*, 2016, **3**, 1500299.

154 N. Parveen, M. O. Ansari, S. A. Ansari and P. Kumar, Nanostructured Titanium Nitride and Its Composites as High-Performance Supercapacitor Electrode Material, *Nanomaterials*, 2023, **13**, 105, DOI: [10.3390/NANO13010105](https://doi.org/10.3390/NANO13010105).

155 A. Achour, M. Chaker, H. Achour, A. Arman, M. Islam and M. Mardani, *et al.*, Role of nitrogen doping at the surface of titanium nitride thin films towards capacitive charge storage enhancement, *J. Power Sources*, 2017, **359**, 349–354, DOI: [10.1016/j.jpowsour.2017.05.074](https://doi.org/10.1016/j.jpowsour.2017.05.074).

156 D. Choi and P. N. Kumta, Nanocrystalline TiN Derived by a Two-Step Halide Approach for Electrochemical Capacitors, *J. Electrochem. Soc.*, 2006, **153**, A2298, DOI: [10.1149/1.2359692](https://doi.org/10.1149/1.2359692).

157 Y. Haldorai, D. Arreaga-Salas, C. S. Rak, Y. S. Huh, Y.-K. Han and W. Voit, Platinized titanium nitride/graphene ternary hybrids for direct methanol fuel cells and titanium nitride/graphene composites for high performance supercapacitors, *Electrochim. Acta*, 2016, **220**, 465–474, DOI: [10.1016/j.electacta.2016.10.130](https://doi.org/10.1016/j.electacta.2016.10.130).

158 X. Lu, G. Wang, T. Zhai, M. Yu, S. Xie and Y. Ling, *et al.*, Stabilized TiN Nanowire Arrays for High-Performance and Flexible Supercapacitors, *Nano Lett.*, 2012, **12**, 5376–5381, DOI: [10.1021/nl302761z](https://doi.org/10.1021/nl302761z).

159 E. Kao, C. Yang, R. Warren, A. Kozinda and L. Lin, ALD titanium nitride coated carbon nanotube electrodes for electrochemical supercapacitors. 2015 Transducers-2015 18th International Conference on Solid-State Sensors, Actuators and Microsystems (TRANSDUCERS), IEEE; 2015, p. 498–501.

160 W. Liu, J. L. Cheong, M.-F. Ng and J. Y. Ying, Carbon nitride mediated synthesis of titanium-based electrodes for high-performance asymmetric supercapacitors, *Nano Energy*, 2023, **112**, 108489.

161 M. Chen, H. Fan, Y. Zhang, X. Liang, Q. Chen and X. Xia, Coupling PEDOT on Mesoporous Vanadium Nitride Arrays for Advanced Flexible All-Solid-State Supercapacitors, *Small*, 2020, **16**, 2003434.

162 L. Fu, Q. Qu, R. Holze, V. V. Kondratiev and Y. Wu, Composites of metal oxides and intrinsically conducting polymers as supercapacitor electrode materials: the best of both worlds?, *J. Mater. Chem. A*, 2019, **7**, 14937–14970, DOI: [10.1039/C8TA10587A](https://doi.org/10.1039/C8TA10587A).

163 Z. Xu, Z. Zhang, H. Yin, S. Hou, H. Lin and J. Zhou, *et al.*, Investigation on the role of different conductive polymers in supercapacitors based on a zinc sulfide/reduced graphene oxide/conductive polymer ternary composite electrode, *RSC Adv.*, 2020, **10**, 3122–3129, DOI: [10.1039/C9RA07842H](https://doi.org/10.1039/C9RA07842H).

164 Z. Wang, M. Zhu, Z. Pei, Q. Xue, H. Li and Y. Huang, *et al.*, Polymers for supercapacitors: Boosting the development of the flexible and wearable energy storage, *Mater. Sci. Eng., R*, 2020, **139**, 100520.

165 Z. Wang, M. Zhu, Z. Pei, Q. Xue, H. Li and Y. Huang, *et al.*, Polymers for supercapacitors: Boosting the development of the flexible and wearable energy storage, *Mater. Sci. Eng., R*, 2020, **139**, 100520.

166 L. Lu and Y. Xie, Fabrication and supercapacitor behavior of phosphomolybdic acid/polyaniline/titanium nitride core-shell nanowire array, *New J. Chem.*, 2017, **41**, 335–346, DOI: [10.1039/C6NJ02368A](https://doi.org/10.1039/C6NJ02368A).

167 C. Xia, Y. Xie, H. Du and W. Wang, Ternary nanocomposite of polyaniline/manganese dioxide/titanium nitride nanowire array for supercapacitor electrode, *J. Nanopart. Res.*, 2015, **17**, 30, DOI: [10.1007/s11051-014-2855-7](https://doi.org/10.1007/s11051-014-2855-7).

168 N. Parveen, M. O. Ansari, S. A. Ansari and P. Kumar, Nanostructured Titanium Nitride and Its Composites as High-Performance Supercapacitor Electrode Material, *Nanomaterials*, 2022, **13**, 105.

169 Y. Xie and D. Wang, Supercapacitance performance of polypyrrole/titanium nitride/polyaniline coaxial nanotube hybrid, *J. Alloys Compd.*, 2016, **665**, 323–332.

170 D. J. Kim, J. K. Kim, J. H. Lee, H. H. Cho, Y.-S. Bae and J. H. Kim, Scalable and bendable organized mesoporous TiN films templated by using a dual-functional amphiphilic graft copolymer for solid supercapacitors, *J. Mater. Chem. A*, 2016, **4**, 12497–12503, DOI: [10.1039/C6TA03475F](https://doi.org/10.1039/C6TA03475F).

171 J. Shi, B. Jiang, Z. Liu, C. Li, F. Yan and X. Liu, *et al.*, Sputtered titanium nitride films on nanowires Si substrate as pseudo-capacitive electrode for supercapacitors, *Ceram. Int.*, 2021, **47**, 26758–26767, DOI: [10.1016/j.ceramint.2021.06.084](https://doi.org/10.1016/j.ceramint.2021.06.084).

172 S. Yadav, A. S. Ghrera, A. Devi and A. Rana, Crystalline flower-like nickel cobaltite nanosheets coated with amorphous titanium nitride layer as binder-free electrodes for supercapacitor application, *Electrochim. Acta*, 2023, **437**, 141526, DOI: [10.1016/j.electacta.2022.141526](https://doi.org/10.1016/j.electacta.2022.141526).

173 X. Peng, K. Huo, J. Fu, B. Gao, L. Wang and L. Hu, *et al.*, Porous Dual-Layered MoO<sub>x</sub> Nanotube Arrays with Highly Conductive TiN Cores for Supercapacitors, *ChemElectroChem*, 2015, **2**, 512–517, DOI: [10.1002/celec.201402349](https://doi.org/10.1002/celec.201402349).

174 X. Zhou, C. Shang, L. Gu, S. Dong, X. Chen and P. Han, *et al.*, Mesoporous coaxial titanium nitride-vanadium nitride fibers of core-shell structures for high-performance supercapacitors, *ACS Appl. Mater. Interfaces*, 2011, **3**, 3058–3063.

175 B. Wei, F. Ming, H. Liang, Z. Qi, W. Hu and Z. Wang, All nitride asymmetric supercapacitors of niobium titanium nitride-vanadium nitride, *J. Power Sources*, 2021, **481**, 228842, DOI: [10.1016/j.jpowsour.2020.228842](https://doi.org/10.1016/j.jpowsour.2020.228842).

176 M. Ding, P. Wang, Z. Zhang and L. Yin, Metal-organic framework-derived porous NiCo-layered double hydroxide@ MnO<sub>2</sub> hierarchical nanostructures as catalytic



cathodes for long-life Li–O<sub>2</sub> Batteries, *ACS Appl. Energy Mater.*, 2020, **4**, 61–71.

177 X. Ma, L. Huang, F. Wu, S. Xiong and B. Xi, Formation of C@ Fe<sub>3</sub>O<sub>4</sub>@ C Hollow Sandwiched Structures with Enhanced Lithium-Storage Properties, *Eur. J. Inorg. Chem.*, 2016, 3722–3727.

178 M. Ma, S. Zhang, Y. Yao, H. Wang, H. Huang and R. Xu, *et al.*, Heterostructures of 2D molybdenum dichalcogenide on 2D nitrogen-doped carbon: superior potassium-ion storage and insight into potassium storage mechanism, *Adv. Mater.*, 2020, **32**, 2000958.

179 S. T. Oyama, Introduction to the chemistry of transition metal carbides and nitrides, *The chemistry of transition metal carbides and nitrides*, Springer; 1996, p. 1–27.

180 Z. Cui, C. Zu, W. Zhou, A. Manthiram and J. B. Goodenough, Mesoporous titanium nitride-enabled highly stable lithium–sulfur batteries, *Adv. Mater.*, 2016, **28**, 6926–6931.

181 Y. Wang, R. Zhang, Y. Pang, X. Chen, J. Lang and J. Xu, *et al.*, Carbon@ titanium nitride dual shell nanospheres as multi-functional hosts for lithium sulfur batteries, *Energy Storage Mater.*, 2019, **16**, 228–235.

182 Y. Wang, R. Zhang, Z. Sun, H. Wu, S. Lu and J. Wang, *et al.*, Spontaneously Formed Mott–Schottky Electrocatalyst for Lithium–Sulfur Batteries, *Adv. Mater. Interfaces*, 2020, **7**, 1902092.

183 C. Wang, R. Liu, Y. Fang, W. Yang, F. Jin and M. Gu, *et al.*, Free-Standing Titanium Nitride Films as Carbon-Free Sulfur Hosts for Flexible Lithium–Sulfur Batteries, *ACS Appl. Nano Mater.*, 2022, **5**, 3531–3540.

184 W. Zeng, M. M. Cheng and K. Y. S. Ng, Cathode Framework of Nanostructured Titanium Nitride/Graphene for Advanced Lithium–Sulfur Batteries, *ChemElectroChem*, 2019, **6**, 2796–2804.

185 W. Chen, H. Jin, S. Xie, H. Xie, J. Zhu and H. Ji, *et al.*, TiN nanocrystal anchored on N-doped graphene as effective sulfur hosts for high-performance lithium–sulfur batteries, *J. Energy Chem.*, 2021, **54**, 16–22.

186 Y. Cao, C. Wang, X. Wang, H. Zhang, X. Jiang and C. Xiong, *et al.*, Two-dimensional mesoporous B, N co-doped carbon nanosheets decorated with TiN nanostructures for enhanced performance lithium–sulfur batteries, *Appl. Phys.*, 2021, **127**, 1–9.

187 M. Liu, Z. Zhang, Y. Xie, Z. Guo, H. Feng and W. Liu, *et al.*, Titanium nitride as a promising sodium-ion battery anode: interface-confined preparation and electrochemical investigation, *Dalton Trans.*, 2022, **51**, 12855–12865.

188 T. Zhang, C. Chen, X. Bian, B. Jin, Z. Li and H. Xu, *et al.*, Yolk-shell-structured Si@ TiN nanoparticles for high-performance lithium-ion batteries, *RSC Adv.*, 2022, **12**, 19678–19685.

189 Y. Liu, J. Xu, S. Lu and Y. Xiang, Titanium Nitride Nanorods Array-Decorated Graphite Felt as Highly Efficient Negative Electrode for Iron–Chromium Redox Flow Battery, *Small*, 2023, 2300943.

190 L. Sun, X. Meng, J. Zhang, Y. Meng, M. Wang and X. Zhou, *et al.*, Oxygen-doped TiN entrapped in N-doped porous graphitic carbon promotes sulfur cathode kinetics, *J. Power Sources*, 2023, **575**, 233173.

191 Q. Luo, C. Lu, L. Liu and M. Zhu, A review on the synthesis of transition metal nitride nanostructures and their energy related applications, *Green Energy Environ.*, 2023, **8**, 406–437, DOI: [10.1016/j.gee.2022.07.002](https://doi.org/10.1016/j.gee.2022.07.002).

192 Y. Men, P. Li, J. Zhou, G. Cheng, S. Chen and W. Luo, Tailoring the electronic structure of Co<sub>2</sub>P by N doping for boosting hydrogen evolution reaction at all pH values, *ACS Catal.*, 2019, **9**, 3744–3752.

193 Y. Han, X. Yue, Y. Jin, X. Huang and P. K. Shen, Hydrogen evolution reaction in acidic media on single-crystalline titanium nitride nanowires as an efficient non-noble metal electrocatalyst, *J. Mater. Chem. A*, 2016, **4**, 3673–3677.

194 M. Yu, S. Zhao, H. Feng, L. Hu, X. Zhang and Y. Zeng, *et al.*, Engineering thin MoS<sub>2</sub> nanosheets on TiN nanorods: advanced electrochemical capacitor electrode and hydrogen evolution electrocatalyst, *ACS Energy Lett.*, 2017, **2**, 1862–1868.

195 C. Wang, H. Shi, H. Liu, J. Fu, D. Wei and W. Zeng, *et al.*, Quasi-atomic-scale platinum anchored on porous titanium nitride nanorod arrays for highly efficient hydrogen evolution, *Electrochim. Acta*, 2018, **292**, 727–735.

196 X. Peng, A. M. Qasim, W. Jin, L. Wang, L. Hu and Y. Miao, *et al.*, Ni-doped amorphous iron phosphide nanoparticles on TiN nanowire arrays: an advanced alkaline hydrogen evolution electrocatalyst, *Nano Energy*, 2018, **53**, 66–73.

197 G. S. Shanker, G. B. Markad, M. Jagadeeswararao, U. Bansode and A. Nag, Colloidal nanocomposite of TiN and N-doped few-layer graphene for plasmonics and electrocatalysis, *ACS Energy Lett.*, 2017, **2**, 2251–2256.

198 H. Zhang, X. Chen, Z. Lin, L. Zhang, H. Cao and L. Yu, *et al.*, Hybrid niobium and titanium nitride nanotube arrays implanted with nanosized amorphous rhenium–nickel: An advanced catalyst electrode for hydrogen evolution reactions, *Int. J. Hydrogen Energy*, 2020, **45**, 6461–6475.

199 S. Chandrasekaran, R. Sukanya, E. Arumugam, S. M. Chen and S. Vignesh, Effective sonochemical synthesis of titanium nitride nanoflakes decorated graphitic carbon nitride as an efficient bifunctional electrocatalyst for HER and OER performance, *Colloids Surf. A*, 2023, **665**, 131190.

200 J. Qiao, L. Kong, S. Xu, K. Lin, W. He and M. Ni, *et al.*, Research progress of MXene-based catalysts for electrochemical water-splitting and metal-air batteries, *Energy Storage Mater.*, 2021, **43**, DOI: [10.1016/j.ensm.2021.09.034](https://doi.org/10.1016/j.ensm.2021.09.034).

201 T. W. Chen, G. Anushya, S. M. Chen, P. Kalimuthu, V. Mariyappan and P. Gajendran, *et al.*, Recent Advances in Nanoscale Based Electrocatalysts for Metal-Air Battery, Fuel Cell and Water-Splitting Applications: An Overview, *Materials*, 2022, **15**, 458, DOI: [10.3390/MA15020458/S1](https://doi.org/10.3390/MA15020458/S1).

202 F. Liu, X. Yang, D. Dang and X. Tian, Engineering of Hierarchical and Three-Dimensional Architectures Constructed by Titanium Nitride Nanowire Assemblies for Efficient Electrocatalysis, *ChemElectroChem*, 2019, **6**, DOI: [10.1002/celc.201900252](https://doi.org/10.1002/celc.201900252).

203 Q. Zhang, Y. Wang, Y. Wang, A. M. Al-Enizi, A. A. Elzatahry and G. Zheng, Myriophyllum-like hierarchical TiN@ Ni 3 N



nanowire arrays for bifunctional water splitting catalysts, *J. Mater. Chem. A*, 2016, **4**, 5713–5718.

204 D. Guo, Z. Wan, Y. Li, B. Xi and C. Wang, TiN@Co<sub>5</sub>.47N composite material constructed by atomic layer deposition as reliable electrocatalyst for oxygen evolution reaction, *Adv. Funct. Mater.*, 2021, **31**, 2008511.

205 K. Zhang, W. Mai, J. Li, H. Wang, G. Li and W. Hu, Highly scattered Ir oxides on TiN as an efficient oxygen evolution reaction electrocatalyst in acidic media, *J. Mater. Sci.*, 2020, **55**, 3507–3520.

206 M. Bele, P. Jovanović, Z. Marinko, S. Drev, V. S. Šelih and J. Kovač, *et al.*, Increasing the oxygen-evolution reaction performance of nanotubular titanium oxynitride-supported Ir nanoparticles by a strong metal–support interaction, *ACS Catal.*, 2020, **10**, 13688–13700.

207 H. Pan and C. J. Barile, Titanium nitride-supported Cu–Ni bifunctional electrocatalysts for CO<sub>2</sub> reduction and the oxygen evolution reaction, *Sustainable Energy Fuels*, 2020, **4**, 5654–5664.

208 Q. Zhang and J. Guan, Applications of Atomically Dispersed Oxygen Reduction Catalysts in Fuel Cells and Zinc–Air Batteries, *Energy Environ. Mater.*, 2021, **4**, DOI: [10.1002/eem2.12128](https://doi.org/10.1002/eem2.12128).

209 J. Chen, X. Wei, J. Zhang, Y. Luo, Y. Chen and G. Wang, *et al.*, Titanium nitride hollow spheres consisting of TiN nanosheets and their controllable carbon–nitrogen active sites as efficient electrocatalyst for oxygen reduction reaction, *Ind. Eng. Chem. Res.*, 2019, **58**, 2741–2748.

210 Y. Liu, Y. Shen, S. Zhu and D. Li, TiN nanoparticles hybridized with Fe, N co-doped carbon nanosheets composites as highly efficient electrocatalyst for oxygen reduction reaction, *Chem. Eng. J.*, 2020, **400**, 125968.

211 Z. Pan, Y. Xiao, Z. Fu, G. Zhan, S. Wu and C. Xiao, *et al.*, Hollow and porous titanium nitride nanotubes as high-performance catalyst supports for oxygen reduction reaction, *J. Mater. Chem. A*, 2014, **2**, 13966–13975.

212 B. Avasarala, T. Murray, W. Li and P. Haldar, Titanium nitride nanoparticles based electrocatalysts for proton exchange membrane fuel cells, *J. Mater. Chem.*, 2009, **19**, 1803–1805.

213 Z. Pan, Y. Xiao, Z. Fu, G. Zhan, S. Wu and C. Xiao, *et al.*, Hollow and porous titanium nitride nanotubes as high-performance catalyst supports for oxygen reduction reaction, *J. Mater. Chem. A*, 2014, **2**, 13966–13975.

214 E. Yousefi, M. Ghorbani, A. Dolati, H. Yashiro and M. Outokeesh, Preparation of new titanium nitride–carbon nanocomposites in supercritical benzene and their oxygen reduction activity in alkaline medium, *Electrochim. Acta*, 2015, **164**, 114–124.

215 Y. Zheng, J. Zhang, H. Zhan, D. Sun, D. Dang and X. L. Tian, Porous and three dimensional titanium nitride supported platinum as an electrocatalyst for oxygen reduction reaction, *Electrochim. Commun.*, 2018, **91**, 31–35.

216 X. L. Tian, L. Wang, B. Chi, Y. Xu, S. Zaman and K. Qi, *et al.*, Formation of a tubular assembly by ultrathin TiO<sub>2</sub>–8Co<sub>0.2</sub>N nanosheets as efficient oxygen reduction electrocatalysts for hydrogen–metal–air fuel cells, *ACS Catal.*, 2018, **8**, 8970–8975.

217 J. Chen, X. Wei, J. Zhang, Y. Luo, Y. Chen and G. Wang, *et al.*, Titanium nitride hollow spheres consisting of TiN nanosheets and their controllable carbon–nitrogen active sites as efficient electrocatalyst for oxygen reduction reaction, *Ind. Eng. Chem. Res.*, 2019, **58**, 2741–2748.

218 Z. Yuan, Y. Cao, Z. Zhang, Y. Fang, Q. Liu and D. Dang, *et al.*, Dandelion-like titanium nitride supported platinum as an efficient oxygen reduction catalyst in acidic media, *Int. J. Hydrogen Energy*, 2022, **47**, 15035–15043.

219 P. Zheng, S. Hu, L. Han, Y. Fu, X. Zeng and M. Li, *et al.*, Modulating the structure of iron-doped titanium nitride deposited on a nitrogen-doped carbon catalyst for the oxygen reduction reaction in Zn-air batteries, *Catal. Sci. Technol.*, 2022, **12**, 7408–7416.

220 S. Kumar, S. Kumar, R. N. Rai, Y. Lee, T. Hong Chuong Nguyen and S. Young Kim, *et al.*, Recent development in two-dimensional material-based advanced photoanodes for high-performance dye-sensitized solar cells, *Sol. Energy*, 2023, **249**, 606–623, DOI: [10.1016/J.SOLENER.2022.12.013](https://doi.org/10.1016/J.SOLENER.2022.12.013).

221 A. Ebenezer Anitha and M. Dotter, A Review on Liquid Electrolyte Stability Issues for Commercialization of Dye-Sensitized Solar Cells (DSSC), *Energies*, 2023, **16**, 5129, DOI: [10.3390/EN16135129](https://doi.org/10.3390/EN16135129).

222 Y. Zhang, M. Li, D. Li, Y. Tian, J. Guo and C. Li, *et al.*, TiN-Based Materials for Multispectral Electromagnetic Wave Absorption, *J. Electron. Mater.*, 2023, **52**, DOI: [10.1007/S11664-023-10280-6](https://doi.org/10.1007/S11664-023-10280-6).

223 N. Venugopal, V. S. Gerasimov, A. E. Ershov, S. V. Karpov and S. P. Polyutov, Titanium nitride as light trapping plasmonic material in silicon solar cell, *Opt. Mater.*, 2017, **72**, 397–402.

224 Z. Khezripour, F. F. Mahani and A. Mokhtari, Performance improvement of ultrathin organic solar cells utilizing light-trapping aluminum-titanium nitride nanosquare arrays, *Opt. Mater.*, 2018, **84**, 651–657.

225 E. Ramasamy, C. Jo, A. Anthony, I. Jeong, J. K. Kim and J. Lee, Soft-template simple synthesis of ordered mesoporous titanium nitride–carbon nanocomposite for high performance dye-sensitized solar cell counter electrodes, *Chem. Mater.*, 2012, **24**, 1575–1582.

226 G. Wang and S. Liu, Porous titanium nitride microspheres on Ti substrate as a novel counter electrode for dye-sensitized solar cells, *Mater. Lett.*, 2015, **161**, 294–296.

227 S. Magdi, Q. Gan and M. A. Swillam, Organic photovoltaic with various plasmonic nanostructures using titanium nitride. *Physics, Simulation, and Photonic Engineering of Photovoltaic Devices V*, SPIE, 9743, 2016, 247–252.

228 W. Li, X. Yan, A. G. Aberle and S. Venkataraj, Effect of a TiN alkali diffusion barrier layer on the physical properties of Mo back electrodes for CIGS solar cell applications, *Curr. Appl. Phys.*, 2017, **17**, 1747–1753.

229 S. Gnanasekar and A. N. Grace, Titanium nitride nanoflower buds as Pt-free counter electrodes for dye-sensitized solar cells, *ACS Appl. Nano Mater.*, 2021, **4**, 8251–8261.

230 T. Sun, T. Chen, J. Chen, Q. Lou, Z. Liang and G. Li, *et al.*, High-performance p-i-n perovskite photodetectors and image sensors with long-term operational stability enabled by a corrosion-resistant titanium nitride back electrode, *Nanoscale*, 2023, **15**, 7803–7811.

231 Z. Khezripour, F. F. Mahani and A. Mokhtari, Performance improvement of ultrathin organic solar cells utilizing light-trapping aluminum-titanium nitride nanosquare arrays, *Opt. Mater.*, 2018, **84**, 651–657.

232 L. Wang, G. Zhu, M. Wang, W. Yu, J. Zeng and X. Yu, *et al.*, Dual plasmonic Au/TiN nanofluids for efficient solar photothermal conversion, *Sol. Energy*, 2019, **184**, 240–248.

233 Y. Di and T. Qin, Efficient wide-spectrum dye-sensitized solar cell by plasmonic TiN@ Ni-MXene as electrocatalyst, *Ceram. Int.*, 2022, **48**, 12635–12640.

234 S. H. Mohamed and A. A. Alhazime, Suppressing photoluminescence and enhancing light absorption of TiO<sub>2</sub> via using TiO<sub>2</sub>/TiN/TiO<sub>2</sub> plasmonic multilayers for better solar harvesting, *J. Mater. Res. Technol.*, 2022, **18**, 4470–4478.

235 M. Dhonde, K. Sahu and V. V. S. Murty, The application of solar-driven technologies for the sustainable development of agriculture farming: a comprehensive review, *Rev. Environ. Sci. Bio/Technol.*, 2022, (21), 139–167, DOI: [10.1007/S11157-022-09611-6](https://doi.org/10.1007/S11157-022-09611-6).

236 A. Kurup, P. Dhatrak and N. Khasnis, Surface modification techniques of titanium and titanium alloys for biomedical dental applications: A review, *Mater. Today: Proc.*, 2020, **39**, 84–90, DOI: [10.1016/j.matpr.2020.06.163](https://doi.org/10.1016/j.matpr.2020.06.163).

237 R. del Castillo, K. Chochlidakis, P. Galindo-Moreno and C. Ercoli, Titanium Nitride Coated Implant Abutments: From Technical Aspects And Soft tissue Biocompatibility to Clinical Applications. A Literature Review, *J. Prosthodontics*, 2022, **31**, DOI: [10.1111/jopr.13446](https://doi.org/10.1111/jopr.13446).

238 R. Zhang, B. Han and X. Liu, Functional Surface Coatings on Orthodontic Appliances: Reviews of Friction Reduction, Antibacterial Properties, and Corrosion Resistance, *Int. J. Mol. Sci.*, 2023, **24**, 6919, DOI: [10.3390/IJMS24086919](https://doi.org/10.3390/IJMS24086919).

239 J. Yang, C. Liu, H. Sun, Y. Liu, Z. Liu and D. Zhang, *et al.*, The progress in titanium alloys used as biomedical implants: From the view of reactive oxygen species, *Front. Bioeng. Biotechnol.*, 2022, **10**, DOI: [10.3389/fbioe.2022.1092916](https://doi.org/10.3389/fbioe.2022.1092916).

240 B. Subramanian, C. V. Muraleedharan, R. Ananthakumar and M. Jayachandran, A comparative study of titanium nitride (TiN), titanium oxy nitride (TiON) and titanium aluminum nitride (TiAlN), as surface coatings for bio implants, *Surf. Coat. Technol.*, 2011, **205**, 5014–5020.

241 G. Brunello, P. Brun, C. Gardin, L. Ferroni, E. Bressan and R. Meneghelli, *et al.*, Biocompatibility and antibacterial properties of zirconium nitride coating on titanium abutments: An in vitro study, *PLoS One*, 2018, **13**, e0199591.

242 R. P. van Hove, I. N. Sierevelt, B. J. van Royen and P. A. Nolte, Titanium-nitride coating of orthopaedic implants: a review of the literature, *BioMed Res. Int.*, 2015, 2015.

243 N. S. Lawand, H. van Zeijl, P. J. French, J. J. Briaire and J. H. M. Frijns, Titanium nitride (TiN) as a gate material in BiCMOS devices for biomedical implants, *Sensors*, 2013, 1–4.

244 R. Rojas-Roblero, L. Melo-Máximo, D. V. Melo-Máximo and E. Uribe-Lam, Thin films of Titanium Nitride deposite on substrates used for biomedical applications, *J. Sci. Technol.*, 2022, **8**, 9–15.

245 Y. Mao, Y. Bao, D. X. Han and B. Zhao, Research Progress on Nitrite Electrochemical Sensor, *Chin. J. Anal. Chem.*, 2018, **46**, 147–155, DOI: [10.1016/S1872-2040\(17\)61066-1](https://doi.org/10.1016/S1872-2040(17)61066-1).

246 S. Boher, R. Ullah, M. Tuzen and T. A. Saleh, Metal doped nanocomposites for detection of pesticides and phenolic compounds by colorimetry: Trends and challenges, *Open-Nano*, 2023, **13**, 100168, DOI: [10.1016/J.ONANO.2023.100168](https://doi.org/10.1016/J.ONANO.2023.100168).

247 C. L. Lien and C. J. Yuan, The development of CMOS amperometric sensing chip with a novel 3-dimensional TiN nanoelectrode array, *Sensors*, 2019, **19**, DOI: [10.3390/s19050994](https://doi.org/10.3390/s19050994).

248 G. K. Hyde, S. D. McCullen, S. Jeon, S. M. Stewart, H. Jeon and E. G. Loba, *et al.*, Atomic layer deposition and biocompatibility of titanium nitride nano-coatings on cellulose fiber substrates, *Biomed. Mater.*, 2009, **4**, 025001, DOI: [10.1088/1748-6041/4/2/025001](https://doi.org/10.1088/1748-6041/4/2/025001).

249 A. C. Agudelo, J. R. Gancedo, J. F. Marco and D. Hanžel, Corrosion resistance of titanium nitride and mixed titanium/titanium nitride coatings on iron in humid SO<sub>2</sub>-containing atmospheres, *J. Vac. Sci. Technol., A*, 1997, **15**, DOI: [10.1116/1.580862](https://doi.org/10.1116/1.580862).

250 S. A. Shafiee, S. C. Perry, H. H. Hamzah, M. M. Mahat, F. A. Al-lolage and M. Z. Ramli, Recent advances on metal nitride materials as emerging electrochemical sensors: A mini review, *Electrochem. Commun.*, 2020, **120**, 106828, DOI: [10.1016/J.ELECOM.2020.106828](https://doi.org/10.1016/J.ELECOM.2020.106828).

251 M. A. Ali, K. Mondal, Y. Wang, H. Jiang, N. K. Mahal and M. J. Castellano, *et al.*, In situ integration of graphene foam-titanium nitride based bio-scaffolds and microfluidic structures for soil nutrient sensors, *Lab Chip*, 2017, **17**, 274–285.

252 Y. Haldorai, S.-K. Hwang, A.-I. Gopalan, Y. S. Huh, Y.-K. Han and W. Voit, *et al.*, Direct electrochemistry of cytochrome c immobilized on titanium nitride/multi-walled carbon nanotube composite for amperometric nitrite biosensor, *Biosens. Bioelectron.*, 2016, **79**, 543–552.

253 F.-Y. Kong, S.-X. Gu, J.-Y. Wang, H.-L. Fang and W. Wang, Facile green synthesis of graphene–titanium nitride hybrid nanostructure for the simultaneous determination of acetaminophen and 4-aminophenol, *Sens. Actuators, B*, 2015, **213**, 397–403.

254 J. Feng, Q. Li, J. Cai, T. Yang, J. Chen and X. Hou, Electrochemical detection mechanism of dopamine and uric acid on titanium nitride-reduced graphene oxide composite with and without ascorbic acid, *Sens. Actuators, B*, 2019, **298**, 126872.

255 Y. Chu, H. Zhang, H. Zhou, T. Xu, H. Yan and Z. Huang, *et al.*, L-tyrosine-assisted synthesis of nanosilver/titanium nitride with hollow microsphere structure for electrochemical detection of hydrogen peroxide, *J. Solid State Electrochem.*, 2023, **27**, 753–761.

256 S. P. Shylendra, M. Wajrak, K. Alameh and J. J. Kang, Nafion Modified Titanium Nitride pH Sensor for Future Biomedical Applications, *Sensors*, 2023, **23**, 699.



257 C. Wang, W. Li and Y. Long, Molten salt-assisted synthesis of C-TiN nanocomposites for sensitive dopamine determination, *Mater. Lett.*, 2022, **329**, 133234.

258 M. Annalakshmi, P. Balasubramanian, S.-M. Chen and T.-W. Chen, Amperometric sensing of nitrite at nanomolar concentrations by using carboxylated multiwalled carbon nanotubes modified with titanium nitride nanoparticles, *Microchim. Acta*, 2019, **186**, 1–9.

259 Z. Wei, Y. Wang and J. Zhang, Electrochemical detection of NGF using a reduced graphene oxide-titanium nitride nanocomposite, *Sci. Rep.*, 2018, **8**, 6929.

260 W. Xu, Y. Zhang, X. Yin, L. Zhang, Y. Cao and X. Ni, *et al.*, Highly sensitive electrochemical BPA sensor based on titanium nitride-reduced graphene oxide composite and core-shell molecular imprinting particles, *Anal. Bioanal. Chem.*, 2021, **413**, 1081–1090.

261 H. E. Rebenne and D. G. Bhat, Review of CVD TiN coatings for wear-resistant applications: deposition processes, properties and performance, *Surf. Coat. Technol.*, 1994, **63**, DOI: [10.1016/S0257-8972\(05\)80002-7](https://doi.org/10.1016/S0257-8972(05)80002-7).

262 P. Roquiny, F. Bodart and G. Terwagne, Colour control of titanium nitride coatings produced by reactive magnetron sputtering at temperature less than 100 °C, *Surf. Coat. Technol.*, 1999, **116**, 278–283, DOI: [10.1016/S0257-8972\(99\)00076-6](https://doi.org/10.1016/S0257-8972(99)00076-6).

263 A. Hodroj and J. F. Pierson, Development of novel titanium nitride-based decorative coatings by calcium addition, *Appl. Surf. Sci.*, 2011, **257**, DOI: [10.1016/j.apsusc.2011.04.144](https://doi.org/10.1016/j.apsusc.2011.04.144).

264 G. Venkatesan, P. R. Jithin, T. V. Rajan, M. K. Pitchan, S. Bhowmik and R. Rane, *et al.*, Effect of titanium nitride coating for improvement of fire resistivity of polymer composites for aerospace application, *Proc. Inst. Mech. Eng., Part G*, 2018, **232**, DOI: [10.1177/0954410017703147](https://doi.org/10.1177/0954410017703147).

265 A. Saurabh, C. M. Meghana, P. K. Singh and P. C. Verma, Titanium-based materials: synthesis, properties, and applications, *Mater. Today: Proc.*, 2022, **56**, 412–419, DOI: [10.1016/J.MATPR.2022.01.268](https://doi.org/10.1016/J.MATPR.2022.01.268).

266 R. Rejith, D. Kesavan, P. Chakravarthy and S. V. S. Narayana Murty, Bearings for aerospace applications, *Tribol. Int.*, 2023, **181**, DOI: [10.1016/j.triboint.2023.108312](https://doi.org/10.1016/j.triboint.2023.108312).

267 P. Patsalas, C. Charitidis and S. Logothetidis, In situ and real-time ellipsometry monitoring of submicron titanium nitride/titanium silicide electronic devices, *Appl. Surf. Sci.*, 2000, **154**, DOI: [10.1016/S0169-4332\(99\)00444-4](https://doi.org/10.1016/S0169-4332(99)00444-4).

268 A. Khan, M. Puttegowda, P. Jagadeesh, H. M. Marwani, A. M. Asiri and A. Manikandan, *et al.*, Review on nitride compounds and its polymer composites: a multifunctional material, *J. Mater. Res. Technol.*, 2022, **18**, DOI: [10.1016/j.jmrt.2022.03.032](https://doi.org/10.1016/j.jmrt.2022.03.032).

269 C. Liang, S. Wang, S. Sha, S. Lv, G. Wang and B. Wang, *et al.*, Novel semiconductor materials for advanced supercapacitors, *J. Mater. Chem. C*, 2023, **11**, DOI: [10.1039/d2tc04816g](https://doi.org/10.1039/d2tc04816g).

270 W. H. Kao, Y. L. Su and Y. T. Hsieh, Effects of Duplex Nitriding and TiN Coating Treatment on Wear Resistance, Corrosion Resistance and Biocompatibility of Ti6Al4V Alloy, *J. Mater. Eng. Perform.*, 2017, **26**, 3686–3697, DOI: [10.1007/S11665-017-2815-3/FIGURES/12](https://doi.org/10.1007/S11665-017-2815-3/FIGURES/12).

271 F. Xia, W. Jia, C. Ma and J. Wang, Synthesis of Ni-TiN composites through ultrasonic pulse electrodeposition with excellent corrosion and wear resistance, *Ceram. Int.*, 2018, **44**, 766–773, DOI: [10.1016/J.CERAMINT.2017.09.245](https://doi.org/10.1016/J.CERAMINT.2017.09.245).

272 E. J. Herrera-Jimenez, A. Raveh, T. Schmitt, E. Bousser, J. E. Klemberg-Sapieha and L. Martinu, Solid solution hardening in nanolaminate ZrN-TiN coatings with enhanced wear resistance, *Thin Solid Films*, 2019, **688**, 137431, DOI: [10.1016/J.TSF.2019.137431](https://doi.org/10.1016/J.TSF.2019.137431).

273 N. A. Richter, B. Yang, J. P. Barnard, T. Niu, X. Sheng and D. Shaw, *et al.*, Significant texture and wear resistance improvement of TiN coatings using pulsed DC magnetron sputtering, *Appl. Surf. Sci.*, 2023, **635**, 157709, DOI: [10.1016/J.APSUSC.2023.157709](https://doi.org/10.1016/J.APSUSC.2023.157709).

274 J. Liu, D. Liu, S. Li, Z. Deng, Z. Pan and C. Li, *et al.*, The effects of graphene oxide doping on the friction and wear properties of TiN bioinert ceramic coatings prepared using wide-band laser cladding, *Surf. Coat. Technol.*, 2023, **458**, 129354, DOI: [10.1016/j.surfcoat.2023.129354](https://doi.org/10.1016/j.surfcoat.2023.129354).

275 L. Dal Negro and S. V. Boriskina, Deterministic aperiodic nanostructures for photonics and plasmonics applications, *Laser Photonics Rev.*, 2012, **6**, DOI: [10.1002/lpor.201000046](https://doi.org/10.1002/lpor.201000046).

276 S. Gwo, H. Y. Chen, M. H. Lin, L. Sun and X. Li, Nanomanipulation and controlled self-assembly of metal nanoparticles and nanocrystals for plasmonics, *Chem. Soc. Rev.*, 2016, **45**, DOI: [10.1039/c6cs00450d](https://doi.org/10.1039/c6cs00450d).

277 M. Dasog, Transition Metal Nitrides Are Heating Up the Field of Plasmonics, *Chem. Mater.*, 2022, **34**, 4249–4258, DOI: [10.1021/acs.chemmater.2c00305](https://doi.org/10.1021/acs.chemmater.2c00305).

278 M. L. Tseng, H. H. Hsiao, C. H. Chu, M. K. Chen, G. Sun and A. Q. Liu, *et al.*, Metalenses: Advances and Applications, *Adv. Opt. Mater.*, 2018, **6**, DOI: [10.1002/adom.201800554](https://doi.org/10.1002/adom.201800554).

279 V.-C. Su, C. H. Chu, G. Sun and D. P. Tsai, Advances in optical metasurfaces: fabrication and applications [Invited], *Opt. Express*, 2018, **26**, DOI: [10.1364/oe.26.013148](https://doi.org/10.1364/oe.26.013148).

280 P. Cheben, R. Halir, J. H. Schmid, H. A. Atwater and D. R. Smith, Subwavelength integrated photonics, *Nature*, 2018, **560**, DOI: [10.1038/s41586-018-0421-7](https://doi.org/10.1038/s41586-018-0421-7).

281 G. V. Naik, V. M. Shalaev and A. Boltasseva, Alternative Plasmonic Materials: Alternative Plasmonic Materials: Beyond Gold and Silver, *Adv. Mater.*, 2013, **25**, 3264–3294, DOI: [10.1002/adma.201370156](https://doi.org/10.1002/adma.201370156).

282 B. Gerislioglu, G. Bakan, R. Ahuja, J. Adam, Y. K. Mishra and A. Ahmadivand, The role of Ge2Sb2Te5 in enhancing the performance of functional plasmonic devices, *Mater. Today Phys.*, 2020, **12**, DOI: [10.1016/j.mtphys.2020.100178](https://doi.org/10.1016/j.mtphys.2020.100178).

283 D. D. Awschalom, L. C. Bassett, A. S. Dzurak, E. L. Hu and J. R. Petta, Quantum spintronics: Engineering and manipulating atom-like spins in semiconductors, *Science*, 1979, **2013**, 339, DOI: [10.1126/science.1231364](https://doi.org/10.1126/science.1231364).

284 G. V. Naik, J. Kim and A. Boltasseva, Oxides and nitrides as alternative plasmonic materials in the optical range, *Opt. Mater. Express*, 2011, **1**, 1090–1099.



285 U. Guler, A. V. Kildishev, A. Boltasseva and V. M. Shalaev, Plasmonics on the slope of enlightenment: The role of transition metal nitrides, *Faraday Discuss.*, 2015, 178, DOI: [10.1039/c4fd00208c](https://doi.org/10.1039/c4fd00208c).

286 G. V. Naik, J. L. Schroeder, X. Ni, A. V. Kildishev, T. D. Sands and A. Boltasseva, Titanium nitride as a plasmonic material for visible and near-infrared wavelengths, *Opt. Mater. Express*, 2012, 2, DOI: [10.1364/ome.2.000478](https://doi.org/10.1364/ome.2.000478).

287 P. Patsalas, Zirconium nitride: A viable candidate for photonics and plasmonics, *Thin Solid Films*, 2019, 688, DOI: [10.1016/j.tsf.2019.137438](https://doi.org/10.1016/j.tsf.2019.137438).

288 M. Wittmer Properties and Microelectronic Applications of Thin Films of Refractory Metal Nitrides. Proceedings – The Electrochemical Society, 1986, vol. 86-2, DOI: [10.1116/1.573382](https://doi.org/10.1116/1.573382).

289 H. O. Pierson, *Handbook of Refractory Carbides and Nitrides*, 1996.

290 N. Kinsey, M. Ferrera, G. V. Naik, V. E. Babicheva, V. M. Shalaev and A. Boltasseva, Experimental demonstration of titanium nitride plasmonic interconnects, *Opt. Express*, 2014, 22, DOI: [10.1364/oe.22.012238](https://doi.org/10.1364/oe.22.012238).

291 P. Patsalas, N. Kalfagiannis and S. Kassavetis, Optical properties and plasmonic performance of titanium nitride, *Materials*, 2015, 8, DOI: [10.3390/ma8063128](https://doi.org/10.3390/ma8063128).

292 S. Ishii, R. P. Sugavaneshwar and T. Nagao, Titanium nitride nanoparticles as plasmonic solar heat transducers, *J. Phys. Chem. C*, 2016, **120**, 2343–2348.

293 A. Catellani and A. Calzolari, Tailoring the plasmonic properties of ultrathin TiN films at metal-dielectric interfaces [Invited], *Opt. Mater. Express*, 2019, 9, DOI: [10.1364/ome.9.001459](https://doi.org/10.1364/ome.9.001459).

294 A. Catellani and A. Calzolari, Plasmonic properties of refractory titanium nitride, *Phys Rev B*, 2017, 95, DOI: [10.1103/PhysRevB.95.115145](https://doi.org/10.1103/PhysRevB.95.115145).

295 W. P. Guo, R. Mishra, C. W. Cheng, B. H. Wu, L. J. Chen and M. T. Lin, *et al.*, Titanium Nitride Epitaxial Films as a Plasmonic Material Platform: Alternative to Gold, *ACS Photonics*, 2019, 6, DOI: [10.1021/acspophotonics.9b00617](https://doi.org/10.1021/acspophotonics.9b00617).

296 M. P. Wells, G. Gobalakrishnan, R. Bower, B. Zou, R. Kilmurray, A. P. Mihai, *et al.* Stability of Thin Film Refractory Plasmonic Materials Taken to High Temperatures in Air, *arXiv*, 2017, arxiv.1711.08923, DOI: [10.48550/arxiv.1711.08923](https://doi.org/10.48550/arxiv.1711.08923).

297 M. N. Gadalla, A. S. Greenspon, M. Tamagnone, F. Capasso and E. L. Hu, Excitation of Strong Localized Surface Plasmon Resonances in Highly Metallic Titanium Nitride Nano-Antennas for Stable Performance at Elevated Temperatures, *ACS Appl. Nano Mater.*, 2019, 2, DOI: [10.1021/acsanm.9b00370](https://doi.org/10.1021/acsanm.9b00370).

298 T. Krekeler, S. S. Rout, G. V. Krishnamurthy, M. Störmer, M. Arya and A. Ganguly, *et al.*, Unprecedented Thermal Stability of Plasmonic Titanium Nitride Films up to 1400 °C, *Adv. Opt. Mater.*, 2021, 9, DOI: [10.1002/adom.202100323](https://doi.org/10.1002/adom.202100323).

299 T. Reese, A. N. Reed, A. D. Sample, F. Freire-Fernández, R. D. Schaller and A. M. Urbas, *et al.*, Ultrafast Spectroscopy of Plasmonic Titanium Nitride Nanoparticle Lattices, *ACS Photonics*, 2021, 8, DOI: [10.1021/acspophotonics.1c00297](https://doi.org/10.1021/acspophotonics.1c00297).

300 J. Judek, P. Wróbel, P. P. Michałowski, M. Ożga, B. Witkowski and A. Seweryn, *et al.*, Titanium nitride as a plasmonic material from near-ultraviolet to very-long-wavelength infrared range, *Materials*, 2021, 14, DOI: [10.3390/ma14227095](https://doi.org/10.3390/ma14227095).

301 P. Mishra, A. K. Debnath and S. Dutta Choudhury, Titanium nitride as an alternative and reusable plasmonic substrate for fluorescence coupling, *Phys. Chem. Chem. Phys.*, 2022, 24, DOI: [10.1039/d1cp05822c](https://doi.org/10.1039/d1cp05822c).

302 C. C. Chang, J. Nogan, Z. P. Yang, W. J. M. Kort-Kamp, W. Ross and T. S. Luk, *et al.*, Highly Plasmonic Titanium Nitride by Room-Temperature Sputtering, *Sci. Rep.*, 2019, 9, DOI: [10.1038/s41598-019-51236-3](https://doi.org/10.1038/s41598-019-51236-3).

303 D. Fomra, R. Secondo, K. Ding, V. Avrutin, N. Izyumskaya and Ü. Özgür, *et al.*, Plasmonic titanium nitride via atomic layer deposition: A low-temperature route, *J. Appl. Phys.*, 2020, 127, DOI: [10.1063/1.5130889](https://doi.org/10.1063/1.5130889).

304 L. Mascaretti, T. Barman, B. R. Bricchi, F. Münz, A. Li Bassi and Š. Kment, *et al.*, Controlling the plasmonic properties of titanium nitride thin films by radiofrequency substrate biasing in magnetron sputtering, *Appl. Surf. Sci.*, 2021, 554, DOI: [10.1016/j.apsusc.2021.149543](https://doi.org/10.1016/j.apsusc.2021.149543).

305 S. Reiter, W. Han, C. Mai, D. Spirito, J. Jose and M. Zöllner, *et al.*, Titanium Nitride Plasmonic Nanohole Arrays for CMOS-Compatible Integrated Refractive Index Sensing: Influence of Layer Thickness on Optical Properties, *Plasmonics*, 2023, 18, DOI: [10.1007/s11468-023-01810-3](https://doi.org/10.1007/s11468-023-01810-3).

306 G. V. Naik, B. Saha, J. Liu, S. M. Saber, E. A. Stach and J. M. K. Irudayaraj, *et al.*, Epitaxial superlattices with titanium nitride as a plasmonic component for optical hyperbolic metamaterials, *Proc. Natl. Acad. Sci. U. S. A.*, 2014, 111, DOI: [10.1073/pnas.1319446111](https://doi.org/10.1073/pnas.1319446111).

307 A. O. Govorov and H. H. Richardson, Generating heat with metal nanoparticles, *Nano Today*, 2007, 2, DOI: [10.1016/S1748-0132\(07\)70017-8](https://doi.org/10.1016/S1748-0132(07)70017-8).

308 C. Ayala-Orozco, C. Urban, M. W. Knight, A. S. Urban, O. Neumann and S. W. Bishnoi, *et al.*, Au nanomatrixyoshikas as efficient near-infrared photothermal transducers for cancer treatment: Benchmarking against nanoshells, *ACS Nano*, 2014, 8, DOI: [10.1021/mn501871d](https://doi.org/10.1021/mn501871d).

309 U. Guler, J. C. Ndukaife, G. V. Naik, A. G. A. Nnanna, A. V. Kildishev and V. M. Shalaev, *et al.*, Local heating with lithographically fabricated plasmonic titanium nitride nanoparticles, *Nano Lett.*, 2013, 13, DOI: [10.1021/nl4033457](https://doi.org/10.1021/nl4033457).

310 U. Guler, S. Suslov, A. V. Kildishev, A. Boltasseva and V. M. Shalaev, Colloidal Plasmonic Titanium Nitride Nanoparticles: Properties and Applications, *Nanophotonics*, 2015, 4, DOI: [10.1515/nanoph-2015-0017](https://doi.org/10.1515/nanoph-2015-0017).

311 L. Gui, S. Bagheri, N. Strohfeldt, M. Hentschel, C. M. Zgrabik and B. Metzger, *et al.*, Nonlinear Refractory Plasmonics with Titanium Nitride Nanoantennas, *Nano Lett.*, 2016, 16, DOI: [10.1021/acs.nanolett.6b02376](https://doi.org/10.1021/acs.nanolett.6b02376).

312 A. Polman and H. A. Atwater, Photonic design principles for ultrahigh-efficiency photovoltaics, *Nat. Mater.*, 2012, 11, DOI: [10.1038/nmat3263](https://doi.org/10.1038/nmat3263).

313 E. Rephaeli and S. Fan, Absorber and emitter for solar thermo-photovoltaic systems to achieve efficiency exceeding



the Shockley-Queisser limit, *Opt. Express*, 2009, 17, DOI: [10.1364/oe.17.015145](https://doi.org/10.1364/oe.17.015145).

314 M. Planck, *The Theory of Heat Radiation*, 1914, p. 30.

315 U. Guler, V. M. Shalaev and A. Boltasseva, Nanoparticle plasmonics: Going practical with transition metal nitrides, *Mater. Today*, 2015, 18, DOI: [10.1016/j.mattod.2014.10.039](https://doi.org/10.1016/j.mattod.2014.10.039).

316 A. Lenert, D. M. Bierman, Y. Nam, W. R. Chan, I. Celanović and M. Soljačić, *et al.*, A nanophotonic solar thermophotovoltaic device, *Nat. Nanotechnol.*, 2014, 9, DOI: [10.1038/nnano.2013.286](https://doi.org/10.1038/nnano.2013.286).

317 S. Molesky and Z. Jacob, High temperature epsilon-near-zero and epsilon-near-pole metamaterial emitters for thermophotovoltaics, *Opt. Express*, 2013, 21, A96–A110, DOI: [10.1364/oe.21.000a96](https://doi.org/10.1364/oe.21.000a96).

318 W. Li, U. Guler, N. Kinsey, G. V. Naik, A. Boltasseva and J. Guan, *et al.*, Plasmonics: Refractory Plasmonics with Titanium Nitride: Broadband Metamaterial Absorber, *Adv. Mater.*, 2014, 26, 7921, DOI: [10.1002/adma.201470316](https://doi.org/10.1002/adma.201470316).

319 M. Chirumamilla, A. Chirumamilla, Y. Yang, A. S. Roberts, P. K. Kristensen and K. Chaudhuri, *et al.*, Large-Area Ultrabroadband Absorber for Solar Thermophotovoltaics Based on 3D Titanium Nitride Nanopillars, *Adv. Opt. Mater.*, 2017, 5, DOI: [10.1002/adom.201700552](https://doi.org/10.1002/adom.201700552).

320 N. Akhtary and A. Zubair, Titanium nitride based plasmonic nanoparticles for photovoltaic application, *Opt. Continuum*, 2023, 2, DOI: [10.1364/optcon.493184](https://doi.org/10.1364/optcon.493184).

321 M. M. Mekonnen and A. Y. Hoekstra, Sustainability: Four billion people facing severe water scarcity, *Sci. Adv.*, 2016, 2, DOI: [10.1126/sciadv.1500323](https://doi.org/10.1126/sciadv.1500323).

322 S. Suthar, J. Sharma, M. Chabukdhara and A. K. Nema, Water quality assessment of river Hindon at Ghaziabad, India: Impact of industrial and urban wastewater, *Environ. Monit. Assess.*, 2010, 165, DOI: [10.1007/s10661-009-0930-9](https://doi.org/10.1007/s10661-009-0930-9).

323 J. Odige, Harmful effects of wastewater disposal into water bodies: a case review of the Ikpoba river, Benin city, Nigeria, *Tropical Freshwater Biology*, 2015, 23, DOI: [10.4314/tfb.v23i1.5](https://doi.org/10.4314/tfb.v23i1.5).

324 M. J. Margeson and M. Dasog, Plasmonic metal nitrides for solar-driven water evaporation, *Environ. Sci.*, 2020, 6, DOI: [10.1039/d0ew00534g](https://doi.org/10.1039/d0ew00534g).

325 S. Bolisetty, M. Peydayesh and R. Mezzenga, Sustainable technologies for water purification from heavy metals: review and analysis, *Chem. Soc. Rev.*, 2019, 48, DOI: [10.1039/c8cs00493e](https://doi.org/10.1039/c8cs00493e).

326 J. Szabo and S. Minamyer, Decontamination of chemical agents from drinking water infrastructure: A literature review and summary, *Environ. Int.*, 2014, 72, DOI: [10.1016/j.envint.2014.01.025](https://doi.org/10.1016/j.envint.2014.01.025).

327 M. Elimelech and W. A. Phillip, The future of seawater desalination: Energy, technology, and the environment, *Science*, 1979, 2011, 333, DOI: [10.1126/science.1200488](https://doi.org/10.1126/science.1200488).

328 X. Jin, Y. Li, W. Li, Y. Zheng, Z. Fan and X. Han, *et al.*, Nanomaterial Design for Efficient Solar-Driven Steam Generation, *ACS Appl. Energy Mater.*, 2019, 2, DOI: [10.1021/acsae.9b00934](https://doi.org/10.1021/acsae.9b00934).

329 Z. Deng, J. Zhou, L. Miao, C. Liu, Y. Peng and L. Sun, *et al.*, The emergence of solar thermal utilization: Solar-driven steam generation, *J. Mater. Chem. A*, 2017, 5, DOI: [10.1039/c7ta01361b](https://doi.org/10.1039/c7ta01361b).

330 H. Yu, Y. Peng, Y. Yang and Z. Y. Li, Plasmon-enhanced light-matter interactions and applications, *npj Comput. Mater.*, 2019, 5, DOI: [10.1038/s41524-019-0184-1](https://doi.org/10.1038/s41524-019-0184-1).

331 J. Liang, H. Liu, J. Yu, L. Zhou and J. Zhu, Plasmon-enhanced solar vapor generation, *Nanophotonics*, 2019, 8, DOI: [10.1515/nanoph-2019-0039](https://doi.org/10.1515/nanoph-2019-0039).

332 X. Liu and M. T. Swihart, Heavily-doped colloidal semiconductor and metal oxide nanocrystals: An emerging new class of plasmonic nanomaterials, *Chem. Soc. Rev.*, 2014, 43, DOI: [10.1039/c3cs60417a](https://doi.org/10.1039/c3cs60417a).

333 R. A. Karaballi, Y. E. Monfared and M. Dasog, Overview of Synthetic Methods to Prepare Plasmonic Transition-Metal Nitride Nanoparticles, *Chem. – Eur. J.*, 2020, 26, DOI: [10.1002/chem.201905217](https://doi.org/10.1002/chem.201905217).

334 M. Kaur, S. Ishii, S. L. Shinde and T. Nagao, All-ceramic solar-driven water purifier based on anodized aluminum oxide and plasmonic titanium nitride. Optics InfoBase Conference Papers, vol. Part F125-JSAP 2018, 2018, DOI: [10.1364/jsap.2018.19a\\_211b\\_3](https://doi.org/10.1364/jsap.2018.19a_211b_3).

335 Y. Zhang, K. Li, L. Liu, K. Wang, J. Xiang and D. Hou, *et al.*, Titanium nitride nanoparticle embedded membrane for photothermal membrane distillation, *Chemosphere*, 2020, 256, DOI: [10.1016/j.chemosphere.2020.127053](https://doi.org/10.1016/j.chemosphere.2020.127053).

336 M. U. Farid, J. A. Kharraz and A. K. An, Plasmonic Titanium Nitride Nano-enabled Membranes with High Structural Stability for Efficient Photothermal Desalination, *ACS Appl. Mater. Interfaces*, 2021, 13, 3805–3815, DOI: [10.1021/acsami.0c17154](https://doi.org/10.1021/acsami.0c17154).

337 X. Cheng, X. Bai, J. Yang, X. M. Zhu and J. Wang, Titanium Oxynitride Spheres with Broad Plasmon Resonance for Solar Seawater Desalination, *ACS Appl. Mater. Interfaces*, 2022, 14, 28769–28780, DOI: [10.1021/acsami.2c03845](https://doi.org/10.1021/acsami.2c03845).

338 X. Bai, S. H. Lam, J. Hu, K. K. Chui, X. M. Zhu and L. Shao, *et al.*, Colloidal Plasmonic TiN Nanoparticles for Efficient Solar Seawater Desalination, *ACS Appl. Mater. Interfaces*, 2023, 15, 55856–55869, DOI: [10.1021/acsami.3c13479](https://doi.org/10.1021/acsami.3c13479).

